SETTLEMENT OF STRUCTURES ON SHALLOW FOUNDATIONS: A PROBABILISTIC ANALYSIS

by

JORGE DIAZ PADILLA GUERRERO

Ingeniero Civil, Universidad Nacional Autónoma de México
(1968)

Maestro en Ingeniería, Universidad Nacional Autónoma de México
(1970)

Submitted in partial fulfillment
of the requirements for the degree of
Doctor of Philosophy

at the

Massachusetts Institute of Technology
February, 1974

Signature of Author . . . . . .
Department of Civil Engineering, January 16, 1973

Certified by . . . . . .
Thesis Supervisor

Accepted by . . . . . .
Chairman, Departmental Committee on Graduate Students
of the Department of Civil Engineering

Archives
MASS. INST. TECH.
APR 22 1974
LIBRARIES

To Patricia

ABSTRACT

SETTLEMENT OF STRUCTURES ON SHALLOW FOUNDATIONS:
A PROBABILISTIC ANALYSIS

by

JORGE DIAZ PADILLA GUERRERO

Submitted to the Department of Civil Engineering on January 16, 1973, in partial fulfillment of the requirements for the degree of Doctor of Philosophy.

In this work, a probabilistic model is developed to predict the settlements and differential settlements of a structure in terms of prescribed probabilistic input about loads and soil properties. The model accounts for the interaction between the structure and the foundation through the redistribution of forces generated by uneven movements of the supports. Only structures on shallow foundations are treated, but no other restrictions are placed upon the configuration of the structure. A one-dimensional settlement model is employed in which the total settlements are regarded as a summation of contributions in a number of sublayers. The model can accomodate most stress-strain characteristics commonly used to represent soil behavior.

Using probabilistic information about the settlements, the uncertainty of induced deformations and forces in the members of the superstructure can be calculated. The methodology is illustrated through several examples of structures supported on clay. Also, a case study is presented of a probabilistic analysis of soil exploration data at a site.

Thesis Supervisor: Erik H. Vanmarcke

Title: Associate Professor of Civil Engineering

ACKNOWLEDGEMENTS

The author wishes to express his gratitude to Prof. Erik H. Vanmarcke, his advisor and friend, for all his help, his kindness and his constant encouragement received not only during the preparation of this thesis but throughout many years spent as a student at MIT. Appreciation is also extended to Prof. C. Allin Cornell for many valuable ideas and suggestions used in this work and for his help in many matters, both academic and non-academic.

This research was supported by the National Science Foundation under grant No. GK-25510X and by the National Bureau of Standards under contract No. 2-36049. Dames and Moore Consulting Engineers provided financial support and the test data for the case study.

TABLE OF CONTENTS

		Page
TITLE PAGE		1
DEDICATION		2
ABSTRACT		3
ACKNOWLEDGEMENTS		4
TABLE OF CONTENTS		5
CHAPTER 1	INTRODUCTION	8
CHAPTER 2	ELEMENTS OF UNCERTAINTY ANALYSIS	10
2.1	Introduction	10
2.2	Random Variables and Probabilistic Models	11
2.3	Elementary Probabilistic Methodology	12
2.4	Elements of Stochastic Processes	14
CHAPTER 3	THE UNCERTAINTY OF SOIL PROPERTIES: DATA-BASED MODELS	25
3.1	Introduction	25
3.2	Modeling of Natural Soil Variability	27
3.3	Global Estimates of the Parameters	28
3.4	Experimental Variability and Testing Errors	32
3.5	Case Study	35
CHAPTER 4	SPATIAL AVERAGES OF SOIL PROPERTIES	49
4.1	Introduction	49
4.2	Means and Variances of Spatial Averages	51
4.3	Covariances Between Spatial Averages	55
4.4	Experimental Variability and Testing Errors	58

CHAPTER 5	THE PREDICTION OF SETTLEMENTS OF STRUCTURES: A DETERMINISTIC PROCEDURE	60
5.1	Introduction	60
5.2	The One-dimensional Settlement Model	61
5.3	Soil-structure Interaction	65
5.4	Settlements of Structures on Cohesive Soils	74
5.5	Illustrations	82
CHAPTER 6	THE PREDICTION OF SETTLEMENTS OF STRUCTURES: A PROBABILISTIC MODEL	90
6.1	Introduction	90
6.2	The One-dimensional Settlement Model	91
6.3	Methodology	96
6.4	Model Uncertainty	99
6.5	Settlements of Structures on Cohesive Soils	100
6.6	Illustrations	112
CHAPTER 7	SOME DECISION PROBLEMS IN SETTLEMENT-CONTROLLED DESIGN	120
7.1	Introduction	120
7.2	Cost Minimization Problem	121
7.3	The Uncertainty of Settlement-induced Displacements and Forces	123
7.4	Updating Information about Soil Properties Through Further Exploration	126
CHAPTER 8	COMMENTS AND CONCLUSIONS	136
REFERENCES		140
BIOGRAPHY		144
APPENDIX A	Some Properties of the Expected Value Operator	145
APPENDIX B	Additional Details About the Evaluation of Variance Functions	147

APPENDIX C	The Load Transfer Ceofficients and the A Matrix	149
APPENDIX D	A Multivariate Approximation for the Mean Value and the Covariance of Random Variables	151
APPENDIX E	Probabilistic Parameters of the Spatial Averages of Pseudo-flexibilities for a Cohesive Soil	153
APPENDIX F	List of Symbols	158
APPENDIX G	List of Figures	163
APPENDIX H	List of Tables	166

CHAPTER 1

INTRODUCTION

A rational approach to the problem of settlement-controlled design requires a systematic analysis of the many uncertainties involved. Foundation engineers have always dealt qualitatively with uncertainties while making decisions about soil exploration and foundation design (3,11). However, as new materials are used and new design concepts developed, and as the need for considering the interaction between the structure and the foundation is recognized, it becomes increasingly more important to substitute quantitative analysis of variability, risks and decisions for vague and judgemental assessments.

The engineer's ultimate objective is design optimization, i.e., the maximization of the expected utility or minimization of the expected losses derived from the design (36,37). This requires consideration of the initial costs of the foundation and the superstructure, the losses associated with possible future damage, as well as the cost of exploration and testing of the subsoil properties. It also requires a capability for assessing the reliability of settlement predictions and of settlement-induced damage estimates, and for reassessing this information in the light of additional measurements of the soil properties.

In this work, a probabilistic approach to the settlement-prediction problem is developed.

A deterministic settlement model which accounts for the interaction between the soil and the structure is presented in Chapter 5. Only structures on shallow foundations are dealt with, but the features of the shallow foundation, the configuration of the superstructure, or the stress-strain characteristics of the soil are not restricted.

The model presented in Chapter 5 is extended in Chapter 6 into a probabilistic framework. The model yields "first-order" probabilistic information (i.e., means, variances and coefficients of correlation) about the settlements of a structure in terms of a first-order description of loads and soil properties.

The uncertainty of soil properties is discussed in Chapter 3, where a case study is analyzed and the various components of this uncertainty are discussed. The soil parameters used as inputs to the probabilistic settlement-prediction model take the form of spatial averages over finite regions of the soil mass. These are discussed in Chapter 4 along with their probabilistic representation.

Chapter 7 deals with various topics related to settlement-controlled design. There, a simple foundation cost-minimization problem is developed. The uncertainty of settlement-induced forces in the superstructure is discussed as well as the question of updating the information about the soil parameters through additional sampling and testing.

In Chapter 2, some necessary elements of probability and stochastic processes are presented. Readers already familiar with this material can bypass this chapter without any loss of continuity.

CHAPTER 2

ELEMENTS OF UNCERTAINTY ANALYSIS

2.1 Introduction

In the analysis of soil and foundation engineering problems, a geotechnical engineer usually idealizes the actual soil profile at a site in terms of a number of homogeneous layers with constant soil properties (42). The choice of values for the layer properties must often be made in the face of uncertainty.

In fact, within any nominally homogeneous soil volume, the engineering soil properties exhibit a considerable amount of variability from one point to another. This is due to the basic heterogeneity or the natural variability of the soil, which is caused by variations in the mineral composition and in the characteristics of the strata during the soil formation. On the other hand, the properties assigned to each soil layer must be inferred from the field or laboratory results of a limited number of soil samples. Due to the natural variability of the soil, the information provided by a relatively small amount of test data is not sufficient to fully describe the soil characteristics. Therefore, another quite different component of uncertainty, i.e., statistical uncertainty, enters into the estimation of layer soil properties. Statistical uncertainty is, in a sense, not basic because it can be decreased at the expense of additional testing. However, in nearly all geotechnical projects,

the scope of the exploration and the amount of test data are limited by economic considerations. A third and major source of uncertainty is introduced in the measurement of actual soil properties. It is the variability due to sample disturbance, test imperfections and human errors.

These three components of uncertainty may be quantified using the methodology of probability and statistics. This chapter provides the necessary background information about this methodology.

2.2 Random Variables and Probabilistic Models

The initial step in formulating a probabilistic model is to identify the variables which may be treated as random (uncertain). In most problems, the choice of random variables is not difficult. For example, in a model employed to estimate the settlements of a structure, the soil compressibility characteristics and the values of the loads constitute a natural choice of random variables. On the other hand, the spacing of columns, for example, may be treated as deterministic. In reality, most phenomena are random to a certain degree. However, their variability and, more importantly, the effects of this variability may be quite different for each phenomenon. In engineering analysis, a variable should be treated as a random variable only if its contribution to the total variability of the output of the analysis is important and if the effects of this output variability are significant from a decision point of view.

2.3 Elementary Probabilistic Methodology

First-order probability distributions

Let $U(x,y,z)$ represent the uncertain value of a soil property at a point (x,y,z) below the ground surface. The random variable $U(x_i,y_i,z_i)$ will be denoted simply by U_i and is characterized by its probability density function $f_{U_i}(u_i)$[†] or by its cumulative distribution function

$$F_{U_i}(u_i) = \int_{-\infty}^{u_i} f_{U_i}(x)dx \qquad (2.3.1)$$

which increases monotonically from 0 to 1.

In many situations, it is not possible to determine the exact form of the function $f_{U_i}(u_i)$, or practical to include it in a probabilistic model, and one is restricted to work with a first-order description of U_i, i.e., with its mean and its variance.

The mean, average, or expected value of U_i is defined as:

$$m_{U_i} = E[U_i] = \int_{-\infty}^{\infty} u_i \, f_{U_i}(u_i)du_i \qquad (2.3.2)$$

It is a measure of the central tendency of the random variable. The expected scatter in U_i, or the dispersion of values around the mean is measured by the variance:

---

† Following Benjamin and Cornell (2), a capital letter is used to represent a random variable, and the same letter in lower case represents particular values which the random variable may take.

$$\sigma^2_{U_i} = \mathrm{Var}[U_i] = \int_{-\infty}^{\infty} (u_i - m_{U_i})^2 f_{U_i}(u_i)\,du_i \qquad (2.3.3)$$

As the definition suggests, $\sigma^2_{U_i}$ equals the average of the square of the deviations from the mean. The square root of the variance is called the standard deviation, σ_{U_i}, and the dimensionless ratio σ_{U_i}/m_{U_i} is referred to as the coefficient of variation V_{U_i}.

Joint probability distributions

As a first-order probability density function describes the probabilistic behavior of a single random variable, a joint probability density function may be specified to describe the behavior of two or more random variables. Again in this case, a number of averages prove extremely useful.

To fully describe a pair of random variables U_i and U_j (i.e., the values of a soil property at two points below the ground surface), the joint probability distribution, $f_{U_i,U_j}(u_i,u_j)$, is needed. An important average called the covariance is defined as:

$$\mathrm{cov}[U_i,U_j] = \int_{-\infty}^{\infty}\int (u_i - m_{U_i})(u_j - m_{U_j}) f_{U_i,U_j}(u_i,u_j)\,du_i\,du_j \qquad (2.3.4)$$

When the covariance is normalized by the product of the standard deviations of the random variables, the correlation coefficient between the two variables is obtained. That is,

$$\rho_{U_i,U_j} = \frac{\text{cov}[U_i,U_j]}{\sigma_{U_i}\,\sigma_{U_j}} \tag{2.3.5}$$

The correlation coefficient ρ_{U_i,U_j} measures the linear dependence between U_i and U_j. It always lies between -1 and +1, and an extreme value of this coefficient implies that the two random variables are perfectly linearly dependent. For example, if ρ_{U_i,U_j} is close to -1, an above average value of the variable U_i implies that U_j is very likely to have a value below the mean. A value of ρ_{U_i,U_j} close to zero does not necessarily imply a weak probabilistic dependence between the random variables. It merely suggests a weak linear trend in the relationship between the two variables. However, if the variables U_i and U_j are stochastically independent, then ρ_{U_i,U_j} will be equal to zero and the joint density function $f_{U_i,U_j}(u_i,u_j)$ can then be expressed as the product of probability distributions $f_{U_i}(u_i)f_{U_j}(u_j)$.

2.4 Elements of Stochastic Processes

One-dimensional processes

Consider a soil mass and a bore hole at a point of coordinates (x^*,y^*) on the soil surface, as illustrated in Fig. 2.4.1. To determine the values of a soil property $U(x^*,y^*,z)$, a number of measurements are made on soil samples taken from the bore hole. The set of points where observations are made is the index set Z, and U(z)

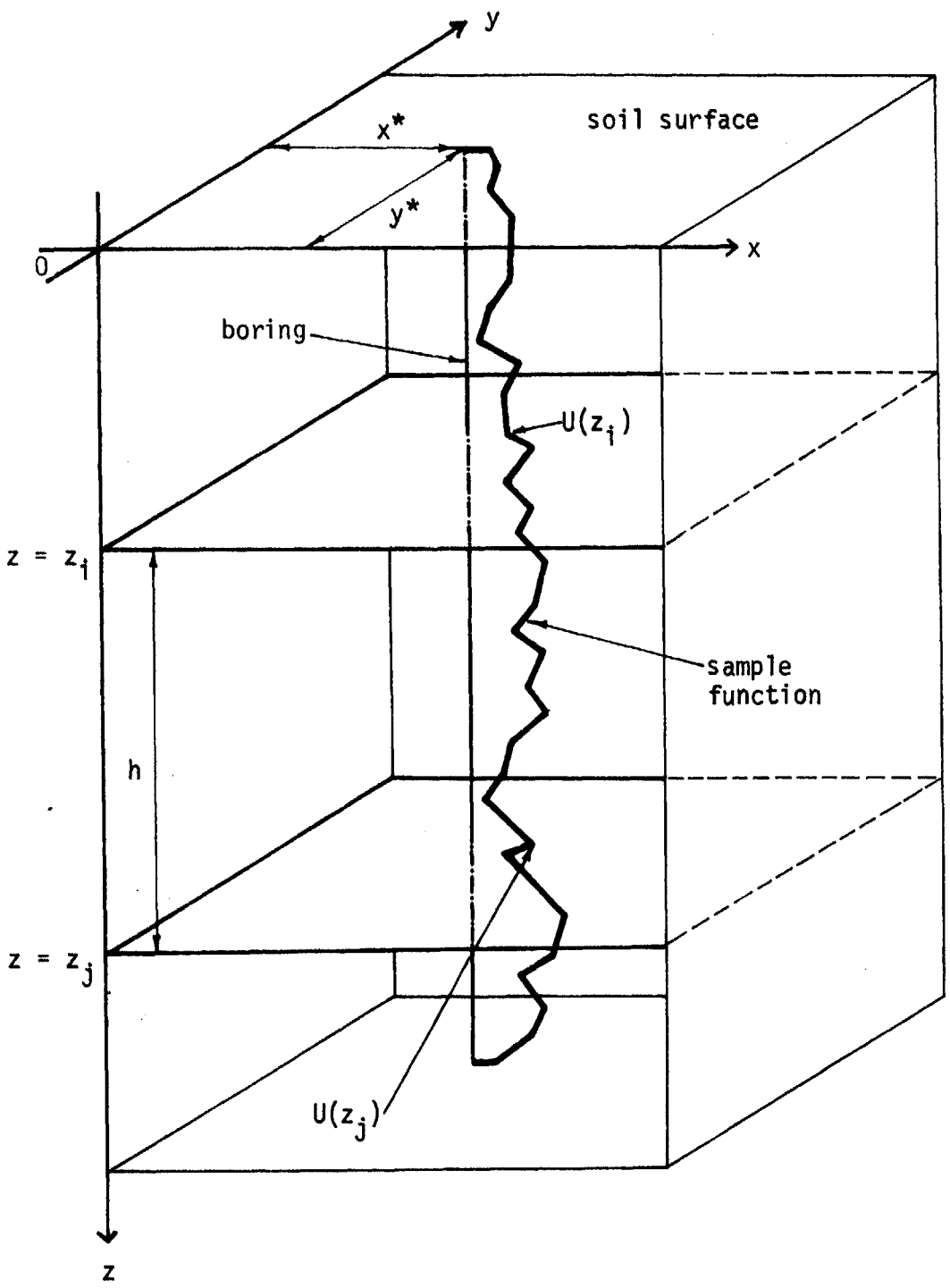


Figure 2.4.1 Schematic Representation of a One-dimensional Stochastic Process $\{U(z), z \in Z\}$

represents the measured value of the random soil property at a depth z. A family of random variables $\{U(Z), z\varepsilon Z\}$ is called a one-dimensional stochastic process (32). A boring log may be interpreted as a sample function of such a process.

Stationarity

The soil properties within a soil mass may be modeled (21,27) as a summation of a deterministic trend, $m_U(x,y,z)$, and a random component about this trend, $U'(x,y,z)$:

$$U(x,y,z) = m_U(x,y,z) + U'(x,y,z) \qquad (2.4.1)$$

For a fixed pair of surface coordinates, $x = x^*$ and $y = y^*$, Eq. 2.4.1 may be written as:

$$U(z) = m_U(z) + U'(z) \qquad (2.4.2)$$

in which $m_U(z)$ and $U'(z)$ represent the vertical trend function and the random fluctuations about this function, respectively. In this case, a different first-order probability distribution of the property U may be needed to represent the behavior of U at each value of the depth. Thus, the nth order joint probability distribution of the U values at n points along a vertical line may become a function of the n particular values of z.

In general, to describe completely the one-dimensional process $\{U(z), z\varepsilon Z\}$ mentioned above, an infinite number of joint probability distributions are necessary. However, if the process belongs to a

special class of processes known as covariance-stationary* (32), the first- and second-order moments (i.e., the means, variances and covariances) become independent of a shift in the origin of the z axis.

If it is assumed that the random components about the trend function define a covariance-stationary process, then the covariance between the values of the soil property U at two depths z_i and z_j (see Fig. 2.4.1) becomes a function only of the distance between z_i and z_j, not of z_i and z_j separately:

$$\text{cov}[U(z_i),U(z_j)] = \gamma_U(z_j - z_i) = \gamma_U(h) \qquad (2.4.3)$$

The function $\gamma_U(h)$ is referred to as the covariance function of the process and its argument $h = z_j - z_i$ is known as the "lag". In particular, $\gamma_U(0) = \sigma_U^2$ which is a constant independent of depth. The ratio $R_U(h) = \gamma_U(h)/\gamma_U(0)$ defines the autocorrelation function** which, for a particular value of h, is the correlation coefficient between values of the process separated by a distance h. Note that both $\gamma_U(h)$ and $R_U(h)$ are even functions.

For a class of stochastic processes known as first-order autoregressive processes (7), the autocorrelation function takes the following exponential form:

---

* These processes are also referred to as "weakly stationary" or "second-order stationary".

** Autocorrelation functions have been widely studied in connection with prediction problems in geology. See Ref. (1) for a good bibliography on this topic.

$$R_U(h) = \exp\left\{-\frac{|h|}{d_U}\right\} \qquad (2.4.4)$$

where d_U is an exponential decay parameter referred to as the "correlation distance" of the process. It is the value of h at which the autocorrelation function becomes equal to e^{-1}.

Another convenient form of the autocorrelation function is:

$$R_U(h) = \exp\left\{-\frac{h^2}{d_U^2}\right\} \qquad (2.4.5)$$

Both Eqns. 2.4.4 and 2.4.5 are illustrated in Fig. 2.4.2.

An equivalent representation of the correlation structure: variance functions

Define S(h) as the integral of a covariance-stationary process over a distance h. The variance of this integral is defined as the variance function:

$$\sigma_U^2(h) = \mathrm{Var}[S(h)] = \mathrm{Var}\left[\int_{z_i}^{z_i+h} U(z)dz\right] \qquad (2.4.6)$$

The variance functions corresponding to the simple autocorrelation functions considered in the previous section are given in Table 2.4.1. Fig. 2.4.3 shows these variance functions normalized by the product $\sigma_U^2 h^2$.

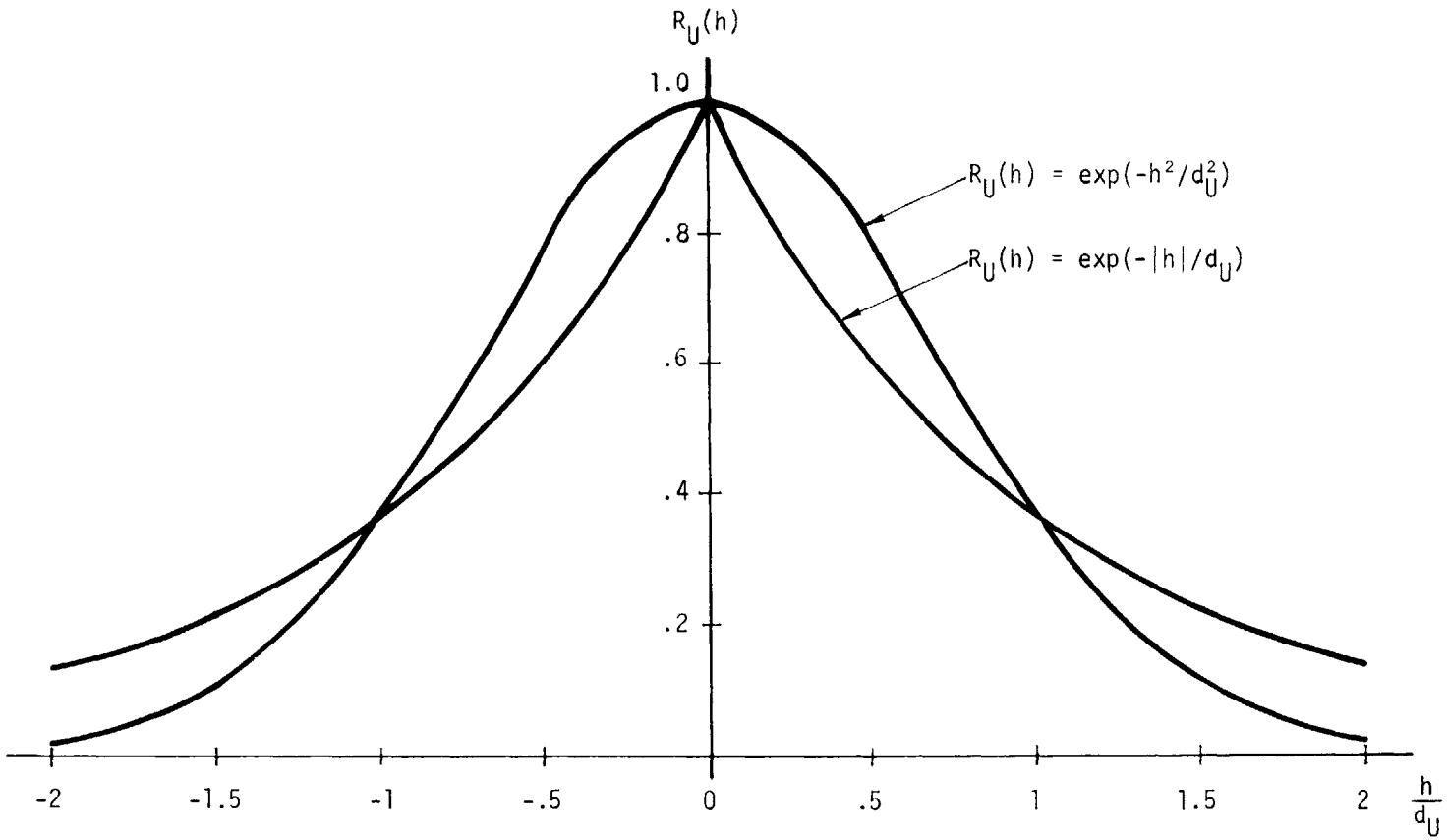


Figure 2.4.2 Autocorrelation Functions $R_U(h) = \exp(-|h|/d_U)$ and $R_U(h) = \exp(-h^2/d_U^2)$

autocorrelation function $R_U(h)$	variance function $\sigma_U^2(h)$	value of $\sigma_U^2(h)$ for large h
$\exp\left[-\frac{\lvert h\rvert}{d_U}\right]$	$2\sigma_U^2 d_U\left(h - d_U\{1 - \exp\left[-\frac{h}{d_U}\right]\}\right)$	$2\sigma_U^2 d_U h$
$\exp\left[-\frac{h^2}{d_U^2}\right]$	$\sigma_U^2 d_U^2\{(\frac{h}{d_U})\sqrt{\pi}\,\Phi^{\dagger}(\frac{h}{d_U}) + \exp\left[-\frac{h^2}{d_U^2}\right] - 1\}$	$\sigma_U^2 d_U h\sqrt{\pi}$

† $\Phi(v) = \frac{2}{\sqrt{\pi}} \int_0^v \exp(-x^2)dx$

Table 2.4.1 Variance Functions for Some Stochastic Processes with Well-known Autocorrelation Functions*

* From Vanmarcke (47)

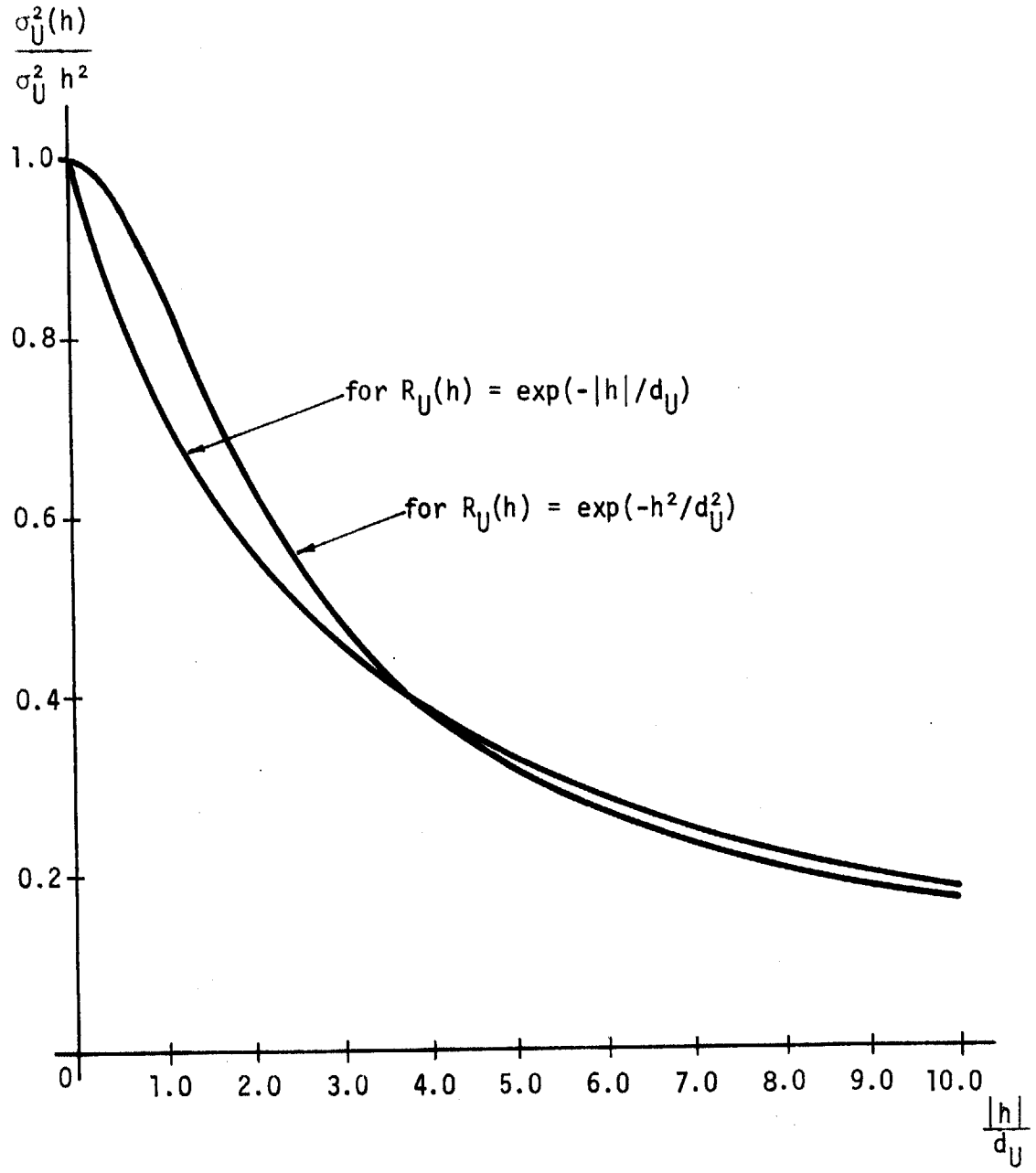


Figure 2.4.3 Normalized Variance Functions* for $R_U(h) = \exp(-|h|/d_U)$ and $R_U(h) = \exp(-h^2/d_U^2)$

---

* From Hauser (18)

Three-dimensional processes

So far, only one-dimensional processes have been discussed by viewing the soil property $U(x,y,z)$ as a function of the depth z for fixed values of the surface coordinates x and y. In general, of course, the property U will vary as a function of distance along the three coordinate axes. The values of U define a three-dimensional stochastic process, formally denoted by $\{U(x,y,z); x\epsilon X, y\epsilon Y, z\epsilon Z\}$, where X, Y and Z represent the three index sets.

The concepts presented above for a one-dimensional case may be extended to deal with this more general problem. For example, if it is assumed that the random components $U'(x,y,z)$ define a covariance-stationary process, then the covariance between the property values U_i and U_j at two points in the soil will be a function only of the difference of coordinates between the two points:

$$\text{cov}[U_i,U_j] = \gamma_U(x_j-x_i,y_j-y_i,z_j-z_i) = \gamma_U(h_x,h_y,h_z) \qquad (2.4.7)$$

where $\gamma_U(\cdot)$ is the covariance function and $h_x = x_j-x_i$, $h_y = y_j-y_i$ and $h_z = z_j-z_i$ are the lags in each direction.

The autocorrelation functions shown in Table 2.4.1 may be generalized as follows:

$$R_U(h_x,h_y,h_z) = \exp\left[-\left(\frac{|h_x|}{d_{U_x}} + \frac{|h_y|}{d_{U_y}} + \frac{|h_z|}{d_{U_z}}\right)\right] \qquad (2.4.8)$$

$$R_U(h_x,h_y,h_z) = \exp\left[-\left(\frac{h_x^2}{d_{U_x}^2} + \frac{h_y^2}{d_{U_y}^2} + \frac{h_z^2}{d_{U_z}^2}\right)\right] \qquad (2.4.9)$$

in which a correlation distance d_U is defined in each direction. Both of these forms have been used in multi-dimensional stochastic process analysis, primarily on the basis of analytical convenience.

If the process is homogeneous, then $d_{U_x} = d_{U_y} = d_{U_z} = d_U$ and the above equations become:

$$R_U(h_x,h_y,h_z) = \exp\{-\frac{1}{d_U}(|h_x| + |h_y| + |h_z|)\} \tag{2.4.10}$$

$$R_U(h_x,h_y,h_z) = \exp\{-\frac{1}{d_U^2}(h_x^2 + h_y^2 + h_z^2)\} \tag{2.4.11}$$

Note that $\sqrt{h_x^2 + h_y^2 + h_z^2}$ is the actual distance between the points of interest. Frequently, a (fully) spatially homogeneous process model will not be a good choice when modeling the correlation structure of soil properties. A more appropriate model may account for the effects of layering and overburden pressure by assuming homogeneity in the horizontal direction, i.e., $d_{U_x} = d_{U_y}$, and a different correlation structure in the vertical direction.

Non-stationarity

In studying the statistical behavior of soil properties such as water contents and void ratios, the stationary model may constitute a reasonable selection. However, in some other cases, such a model may be found deficient. For example, Lumb (27) has found that in some types of clays the standard deviation of the cohesion increases with depth. Another example may be the variability of the maximum

past pressure for a recompressed soil. In this case, as depth increases, the soil changes from a recompressed state to a normally consolidated one and the maximum past pressure approaches the overburden stress. Therefore, one expects the variability to decrease with depth (see Fig. 3.5.3).

If non-stationarity effects are important, the soil volume may be assumed as made up of a number of elementary layers within each of which the soil property at hand is treated as stationary. Alternately, one may choose to standardize the values of U by subtracting the layer trend and dividing the difference by the layer standard deviation of U and analyze the resulting standardized values as a stationary process.

CHAPTER 3

THE UNCERTAINTY OF SOIL PROPERTIES: DATA-BASED MODELS

3.1 Introduction

In recent years, there have been a number of efforts aimed at quantifying the variability of soil properties (14,27,38). Table 3.1.1, which is taken from Schultze (38), lists the coefficients of variation which have been obtained for some properties of various types of soils. Very little information is available, however, about the correlation structure of soil properties. The latter may be equal in importance to the variability when dealing with probabilistic models for quantifying the safety or the performance of geotechnical works (20,48).

In this chapter, a methodology is presented for modeling the covariance structure of soil properties. In contrast to the theoretical models of Chapter 2, those discussed in this chapter are developed in the context of boring logs and actual geotechnical data. After the models are presented, they are illustrated through an application to a real case. Of course, the conclusions based on this illustration cannot be generalized; they apply only to the particular site and subsoil studied here. Hopefully, however, this case study can be used as a guide in studying other sites. In this way, more general information about the correlation structures of soil properties will eventually become available.

material	property	number of samples	coefficient of variation
gravelly sand	porosity	81	0.104
	void ratio	81	0.133
	angle of internal friction	81	0.053
silt	porosity	327	0.133
	void ratio	327	0.216
	unit weight of solids	329	0.011
	natural water content	406	0.228
	modulus of compressibility	186	0.371
	uniformity coefficient	272	0.894
	degree of saturation	334	0.192
	activity	171	0.767
clay	water content	29	0.129
	liquid limit	75	0.221
	plastic limit	75	0.157
	plasticity index	75	0.283
	consistency index	69	0.092
	unconfined compression strength	123	0.391
	modulus of compressibility	11	0.284

Table 3.1.1 Coefficients of Variation for Some Properties of Various Types of Soils*

* From Schultze (38)

3.2 Modeling of Natural Soil Variability

Assume a homogeneous soil volume such as the one shown in Fig. 3.2.1 and a number of borings drilled through it. To measure a soil property, U, a number of samples are taken from the borings and tested in the field or in the laboratory. If one does not account for sampling or testing variability, the sample values may be viewed as observations of a multi-dimensional stochastic process $\{U(x,y,z); x\epsilon X, y\epsilon Y, z\epsilon Z\}$ where,

$$U(x,y,z) = m_U(x,y,z) + U'(x,y,z) \qquad (3.2.1)$$

in which $m_U(x,y,z)$ represents a deterministic trend which may be defined a priori (based on experience), by an eye-fitted relationship, or by more elaborate methods of regression analysis; $U'(x,y,z)$ denotes the random fluctuations about the trend function $m_U(x,y,z)$.

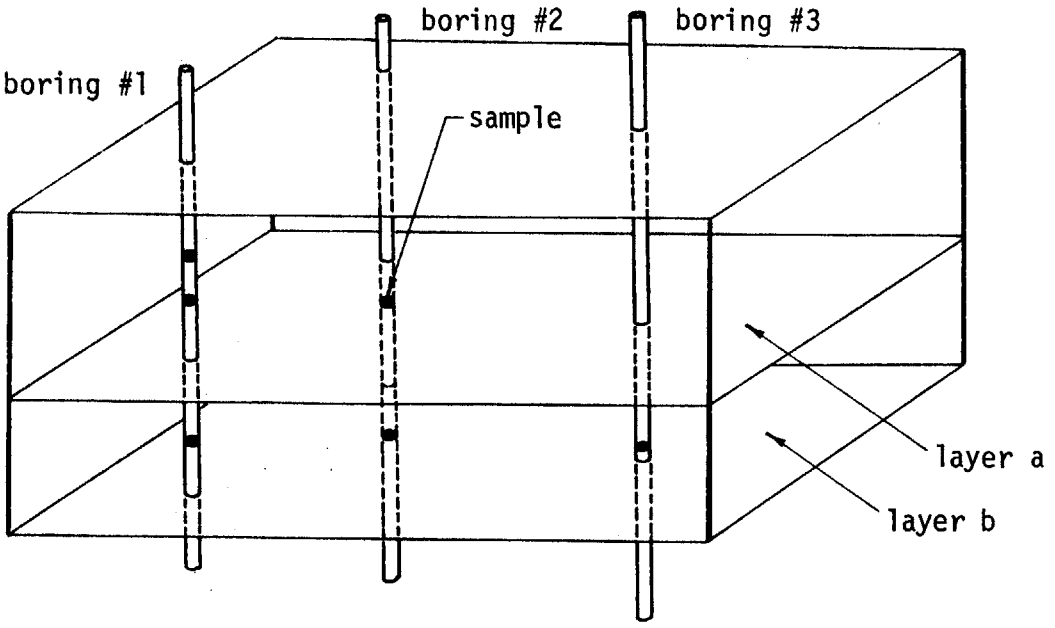


Figure 3.2.1 Soil Volume, Borings and Samples

Assume now that the soil mass is fictitiously divided into a number of smaller volumes and that within each volume the stochastic process $\{U'(x,y,z); x\varepsilon X, y\varepsilon Y, z\varepsilon Z\}$ can be regarded as covariance-stationary. In Fig. 3.2.1 two of these basic volumes are shown as layers a and b.

3.3 Global Estimates of the Parameters

Estimating the mean and the variance

The mean, the variance and the coefficient of variation of a soil property U in a "homogeneous" volume may be estimated from data sampled within this volume, through the sample mean, $\bar{u}$, the sample variance, s_u^2, and the sample coefficient of variation, v_u. If n_s measurements of the property U are available for the volume in question, the above estimators may be computed as:

$$\bar{u} = \frac{1}{n_s} \sum_{j=1}^{n_s} u_j \tag{3.3.1}$$

$$s_u^2 = \frac{1}{n_s} \sum_{j=1}^{n_s} (u_j - \bar{u})^2 = \frac{1}{n_s} \sum_{j=1}^{n_s} u_j^2 - \bar{u}^2 \tag{3.3.2}$$

$$v_u = \frac{s_u}{\bar{u}} \tag{3.3.3}$$

in which u_j represents the jth measurement and $s_u = \sqrt{s_u^2}$ is the sample standard deviation.

Estimating the vertical correlation

One way to model the vertical correlation structure of the soil stratum under consideration, is to estimate the variance function from the boring data and then compare it to those derived from theoretical models. To do this, the observations in each boring and within each layer must be reduced first to a single measurement (perhaps by taking an average). If $u'^{(i)}_j$ represents the transformed measurement for the ith layer and the jth boring ($u'^{(i)}_j = u^{(i)}_j$ - trend (i)), then the h-step variance function, starting at layer a, may be computed as follows:

$$s_u^2(h,a) = \frac{1}{m} \sum_{j=1}^{m} \left\{ \sum_{i=a}^{h+a-1} u'^{(i)}_j \right\}^2 - \left\{ \frac{1}{m} \sum_{j=1}^{m} \sum_{i=a}^{h+a-1} u'^{(i)}_j \right\}^2 \qquad (3.3.4)$$

in which m is the number of borings.

The ratio $s_u^2(h,a)/(s_u^2 h^2)$ for different values of h will define a curve similar to those shown in Fig. 2.4.3, from which a reasonable theoretical model for the autocorrelation function of the stratum may be inferred. The point variance s_u^2 is estimated with Eq. 3.3.2.

If for each layer it is assumed that the trend is equal to the sample mean and the values are normalized with respect to the sample standard deviation, Eq. 3.3.4 will yield directly the ratios $s_u^2(h,a)/s_u^2$ since the normalized values have a unit variance:

$$\frac{s_u^2(h,a)}{s_u^2} = \frac{1}{m} \sum_{j=1}^{m} \left\{ \sum_{i=a}^{h+a-1} u_j^*(i) \right\}^2 \qquad (3.3.5)$$

where $u_j^{*(i)}$ is the normalized value of $u_j^{'(i)}$.

More details about the computational procedures used to evaluate these variance functions are presented in Appendix B.

Estimating the horizontal correlation

In a similar way to the one-dimensional approach discussed above, two-dimensional variance functions may be employed to model the horizontal correlation structure of the stratum. However, the method requires (horizontally) regularly spaced boring data at sufficiently close distances. In many practical situations, such data is not available. Here, instead of calculating variance functions, sample correlation coefficients may be estimated for pairs of observations separated by distances lying in various ranges. Referring to Fig. 3.3.1 for the distance interval $d_1 \leq d \leq d_2$, the pairs of borings used to evaluate a point of the autocorrelation function are 1-2, 3-4, 3-5, and 4-5. The boring data are first transformed by eliminating vertical trends and averaging all layer values within each boring. Using all possible pairs of transformed observations u'_{j1} and u'_{j2}, the sample correlation coefficient for observations separated by a distance interval d, r_d, can now be computed in the standard way:

$$r_d = \frac{\sum_{j=1}^{n_p} u'_{j1}\, u'_{j2} - \left(\sum_{i=1}^{n_p} u'_{i1} \sum_{j=1}^{n_p} u'_{j2}\right) / n_p}{\sqrt{\left\{\sum_{i=1}^{n_p} (u'_{i1})^2 - \left(\sum_{i=1}^{n_p} u'_{i1}\right)^2 / n_p\right\} \left\{\sum_{j=1}^{n_p} (u'_{j2})^2 - \left(\sum_{j=1}^{n_p} u'_{j2}\right)^2 / n_p\right\}}} \qquad (3.3.6)$$

where n_p is the number of pairs of observations.

An easier way to do the above calculation is by first assuming that the layer trend is equal to the sample mean and then normalizing the results with respect to the sample standard deviation. In this case, the computation is reduced essentially to a summation of products of normalized values (only once each pair of values). For the

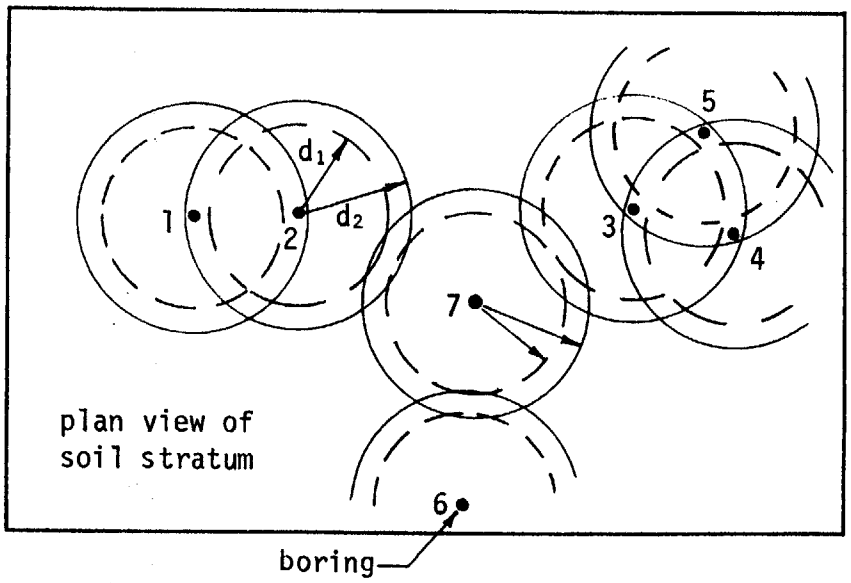


Figure 3.3.1 Pairs of Observations Separated by a Distance Interval d

example illustrated in Fig. 3.3.1, if u_i^* represents the normalized value for the ith boring, r_d will be given by:

$$r_d = \frac{u_1^* u_2^* + u_3^* u_4^* + u_3^* u_5^* + u_4^* u_5^*}{4} \qquad (3.3.7)$$

3.4 Experimental Variability and Testing Errors

In Section 3.2 the observed value of a soil property U at a point (x,y,z) was idealized as the sum of a trend m_U and a random deviation U'. This would be a reasonable model if the results produced by field or laboratory testing of soil samples reproduced exact in-situ values. Evidently, this is seldom (if ever) the case when measuring soil properties. The effects due to sample disturbance and testing variability will generally be present in the values of the observations. These additional sources of variability may be incorporated into the probabilistic model by adding "error" components, one due to sample disturbance, E_d, and one due to testing, E_t. Eq. 3.2.1 now becomes:

$$\hat{U}(x,y,z) = m_U(x,y,z) + U'(x,y,z) + E_d + E_t \qquad (3.4.1)$$

in which $\hat{U}(x,y,z)$ is a field- or laboratory-measured value.

The relative importance of the error terms will depend on which soil property is being measured, who performs the test, in which laboratory, etc. For example, compressibility tests of cohesive soils

are usually carefully done and thus E_t may be expected to be small. On the other hand, the term E_d will depend on the degree of disturbance of the soil sample, and it may be substantial.

The error component E_d will tend to be systematic. For equal levels of sample disturbance, the measurements tend to be in error (or biased) by a constant but unknown amount. In the spirit of a first-order Bayesian analysis, the "random variable" E_d may be characterized by a best estimate (a mean value), m_{E_d}, evaluated on the basis of experience, and a variance, $\sigma^2_{E_d}$, evaluated in terms of subjective or degree-of-belief considerations. The second error term, E_t, may be modeled as a zero mean random variable with a variance denoted by $\sigma^2_{E_t}$. This variance has been estimated (17,28,39) by testing "identical" specimens under similar conditions and measuring the variability of the results. Table 3.4.1, taken from Singh and Lee (39), lists some of the results. The component E_d is assumed to be perfectly correlated from sample to sample, and the component E_t is treated as statistically independent from sample to sample. Furthermore, it is reasonable to assume that the variables $U'(x,y,z)$, E_d and E_t are mutually independent. It then follows that:

$$E[\hat{U}] = m_U + m_{E_d} \tag{3.4.2}$$

$$Var[\hat{U}] = \sigma^2_U + \sigma^2_{E_d} + \sigma^2_{E_t} \tag{3.4.3}$$

$$cov[\hat{U}_i,\hat{U}_j] = \sigma^2_U \rho_{U_i,U_j} + \sigma^2_{E_d} \quad , i \neq j \tag{3.4.4}$$

It should be noted that in the presence of sampling or testing errors, the parameters $\bar{u}$ and s_u^2, as obtained from the raw data, are not estimators of m_U and σ_U^2 but of $m_U + m_{E_d}$ and $\sigma_U^2 + \sigma_{E_t}^2$, instead.

material	property		coefficient of variation
clay	liquid limit		0.10 - 0.11
	plastic limit		0.15 - 0.18
	plasticity index		0.05 - 0.18
clayey silt	liquid limit		0.06 - 0.07
	plastic limit		0.08 - 0.09
	plasticity index		0.35 - 0.40
	cohesion	direct shear	0.52 - 0.56
	angle of int. friction	direct shear	0.22 - 0.29
	shear strength	direct shear	0.19 - 0.20
	cohesion	triaxial	0.61
	angle of int. friction	triaxial	0.07
	shear strength	triaxial	0.34
sand	angle of int. friction	direct shear	0.13 - 0.14

Table 3.4.1 Coefficients of Variation for Some Soil Properties Due to Experimental Variability*

* From Singh and Lee (39).

3.5 Case Study

Description of site and available data

The site studied in this section is located in the San Francisco bay area in northern California. It was formerly a tidal marsh and in past years it has been affected by various periods of flooding and drying. The surface has almost a constant elevation and an area of nearly 550 acres. The subsurface may be modeled as a deep layer of soft compressible organic silty clay ("bay mud") between 30' and 50' thick, lying on top of layers of stiff sandy clays and dense clayey sands.

The field exploration program consisted of drilling 84 borings and extracting from them a number of soil samples. Of these, 790 were undisturbed samples of the bay mud for which the wet density, γ_{wet} (lb/ft^3), and the water content, w, were determined in the laboratory. In addition, consolidation tests were performed on 57 of these samples.

Specific gravity tests were done on 4 samples. Table 3.5.1 shows that the specific gravity, g, has a fairly constant value for the compressible layer. In the remainder of this analysis it is assumed that g is deterministic with a value equal to its mean, $\bar{g} = 2.66$.

For each pair of values of γ_{wet} and w, the dry density, γ_{dry} (lb/ft^3), was obtained by

$$\gamma_{dry} = \frac{\gamma_{wet}}{1+w} \qquad (3.5.1)$$

and the initial void ratio, e_o, was calculated:

$$e_o = \frac{\bar{g}\,\gamma_w}{\gamma_{dry}} - 1 \qquad (3.5.2)$$

where γ_w = 62.43 lb/ft^3, density of the water. With this information, the load-deformation results of the consolidation tests were transformed into load-void ratio plots. Maximum past pressures and compression indices were then obtained.

z (ft)	g	
1	2.65	$\bar{g}$ = 2.66
7	2.60	s_g = 0.05
15	2.72	v_g = 1.87%
30	2.67	

Table 3.5.1 Results of Specific Gravity Tests for Bay Mud Samples

Histograms and numerical summaries

The soil properties for which means, variances and correlation coefficients are evaluated are listed in Table 3.5.2.

A first step in assessing variability is to organize the raw data (some of it shown in Figs. 3.5.1 to 3.5.3) and to transform it into histograms which are shown in Figs. 3.5.4 to 3.5.8 for the soil properties mentioned above. Except in the case of $\bar{P}_m$, the complete set of data was used to plot the histograms. For the maximum past pressures, only observations taken between z = 15' and z = 20' were considered. Table 3.5.3 gives numerical summaries for all the soil properties considered.

soil property	notation
water content	W
initial void ratio	E_o
recompression ratio	$RR = \frac{C_r}{1 + E_o}$
compression ratio	$CR = \frac{C_c}{1 + E_o}$
maximum past pressure (ton/ft^2)	$\bar{P}_m$

Table 3.5.2 Soil Properties Analyzed in the Case Study

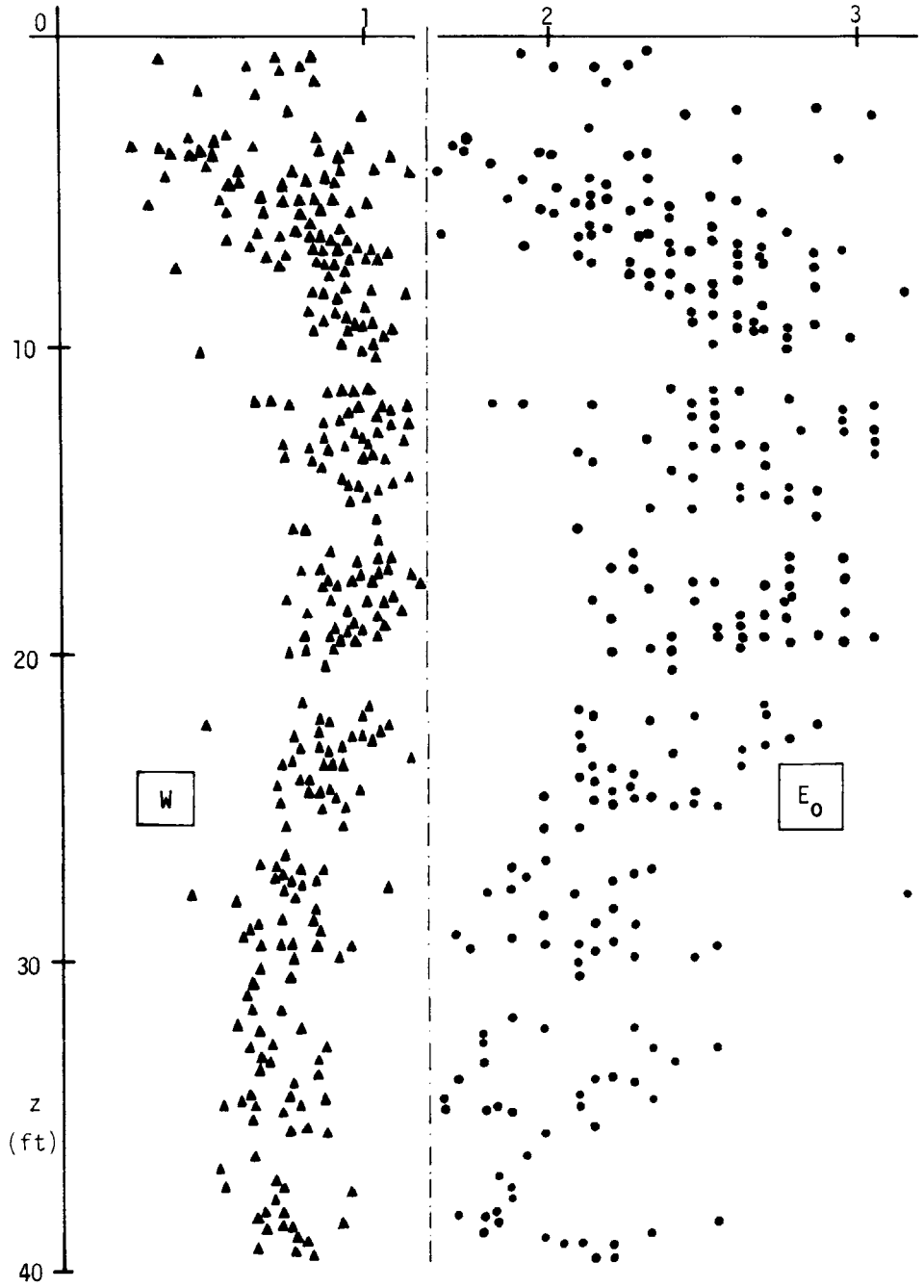


Figure 3.5.1 W and E_o Values as Functions of Depth

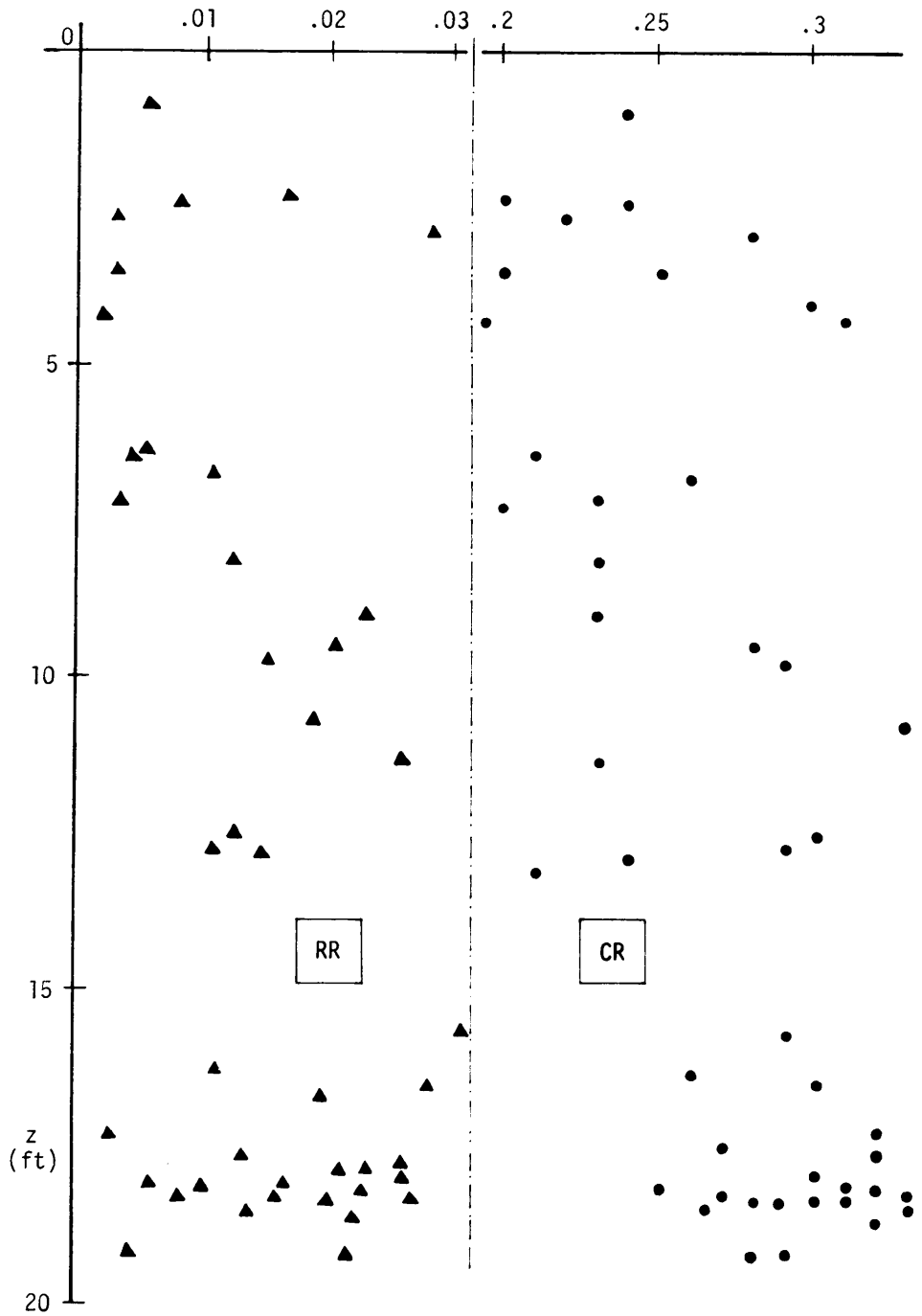


Figure 3.5.2 RR and CR Values as Functions of Depth

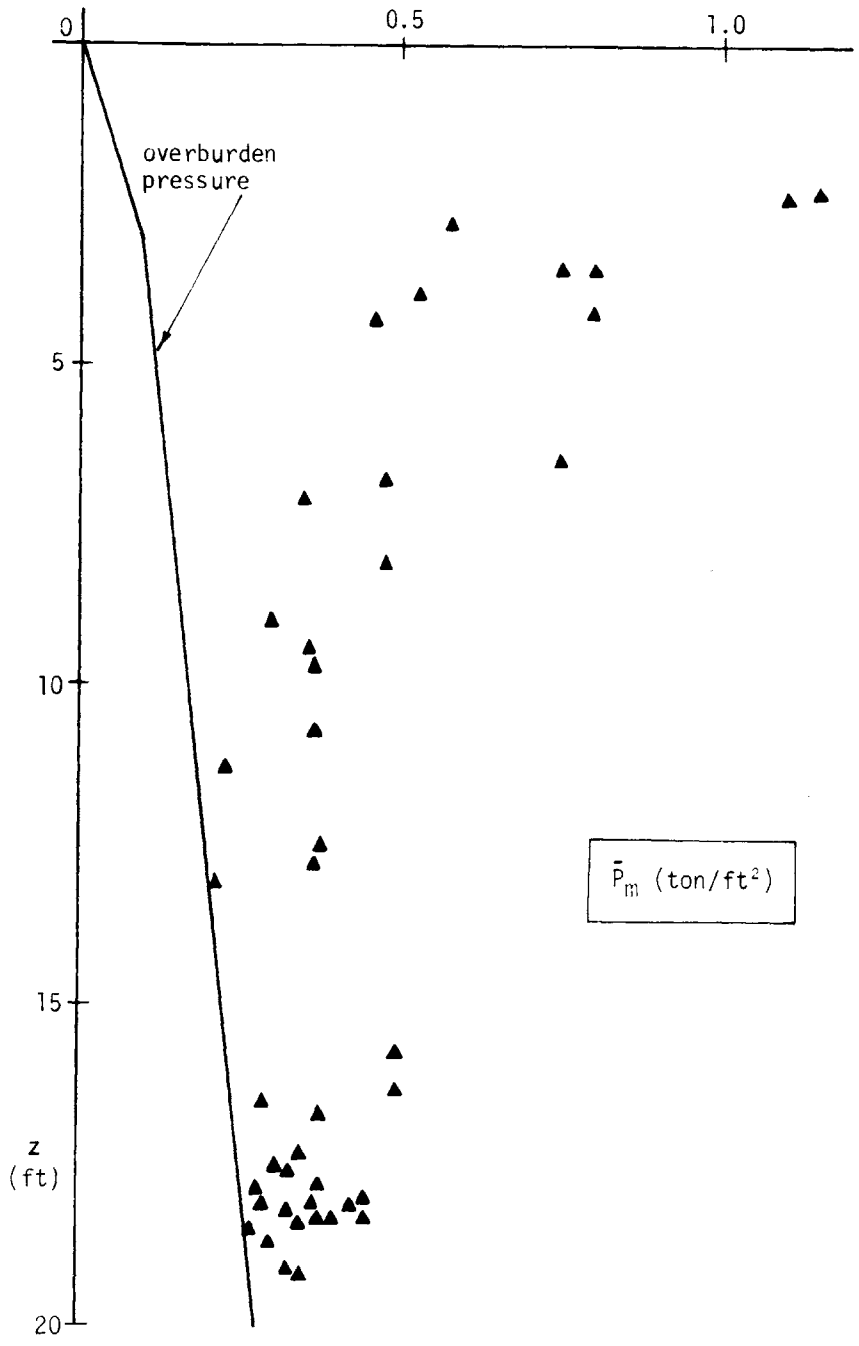


Figure 3.5.3 $\bar{P}_m$ Values as a Function of Depth

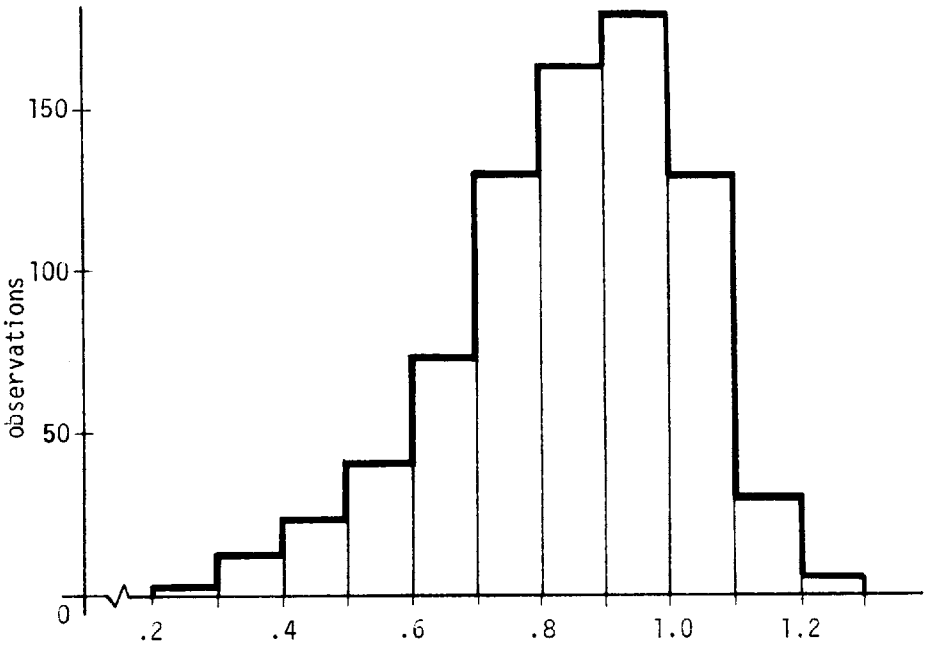


Figure 3.5.4 Histogram for W Values

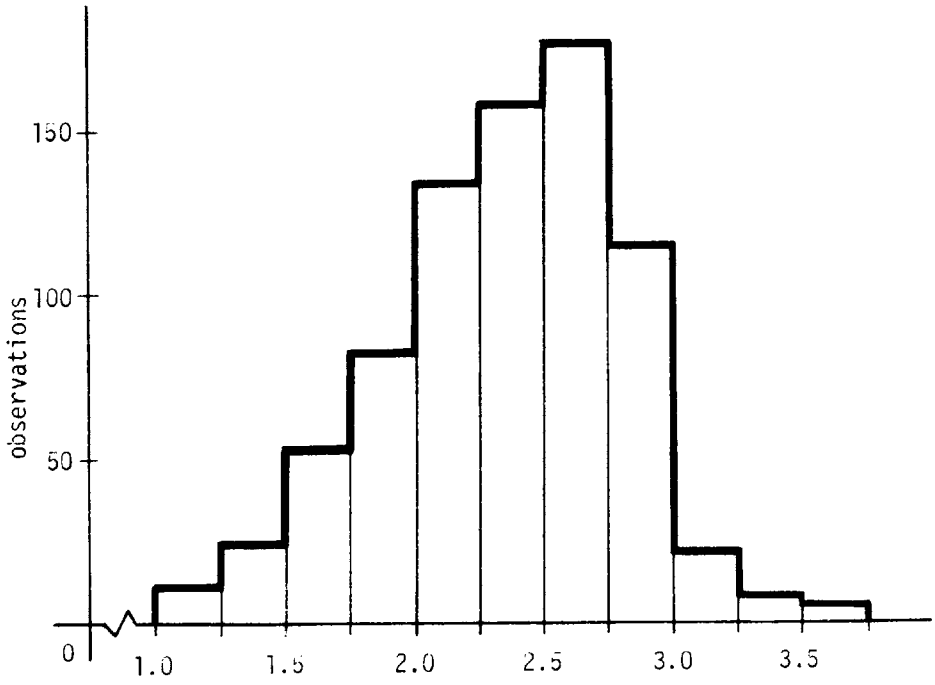


Figure 3.5.5 Histogram for E_0 Values

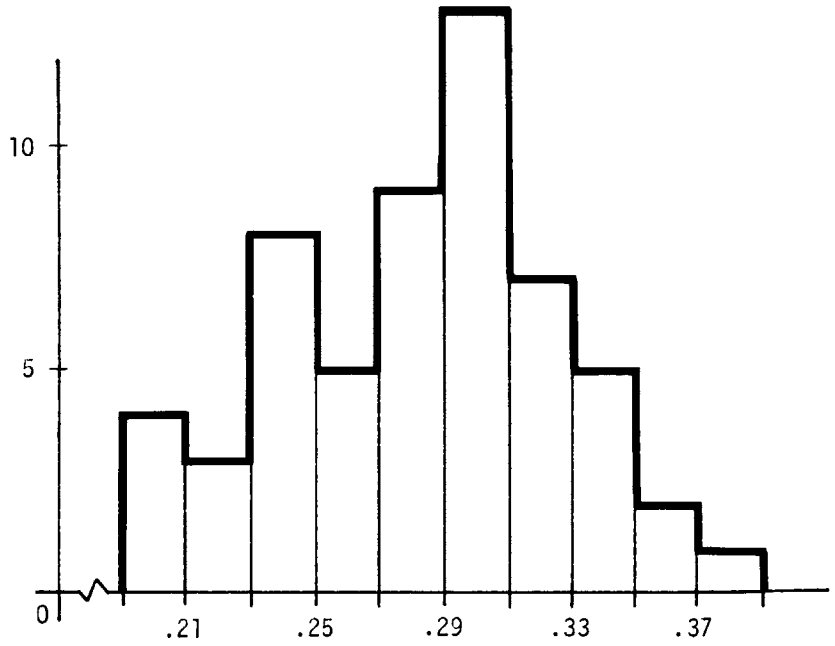


Figure 3.5.6 Histogram for CR Values

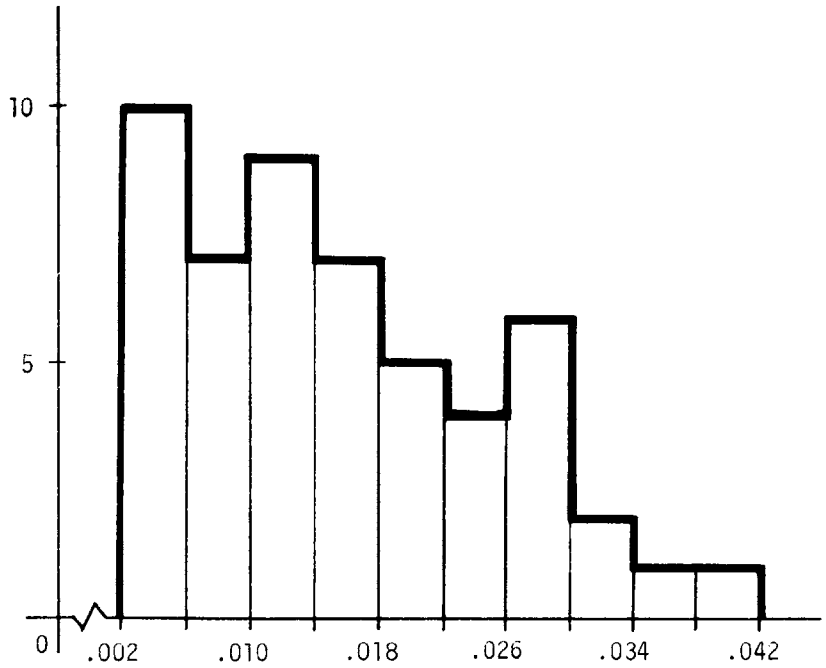


Figure 3.5.7 Histogram for RR Values

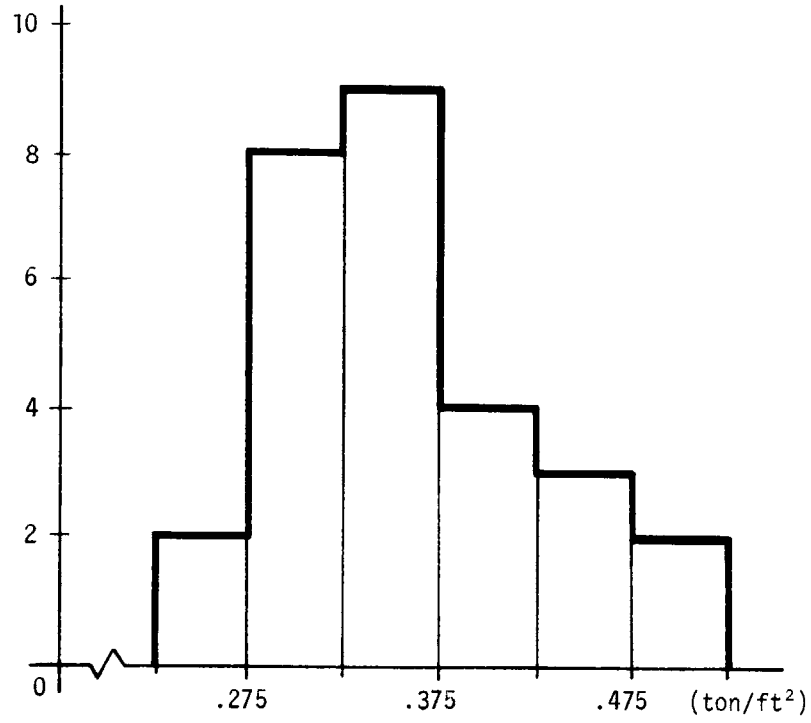


Figure 3.5.8 Histogram for $\bar{P}_m$ Values

soil property, U	$\bar{u}$	s_u	v_u
W	0.84	0.19	0.22
E_o	2.33	0.46	0.20
RR	0.019	0.015	0.79
CR	0.28	0.044	0.16
$\bar{P}_m$ (ton/ft²)	0.35	0.066	0.19
G	2.66	0.05	0.02

Table 3.5.3 Numerical Summaries for the Soil Properties

Vertical correlation

For the soil properties given in Table 3.5.2, the results of the vertical correlation analyses are shown in Figs. 3.5.9 to 3.5.12. The plots were obtained by assuming 5' thick layers of bay mud, subtracting the layer mean from each observation, using Eqns. 3.3.5 and B.1 with some minor corrections due to the lack of data and neglecting sampling and testing errors. The first two plots show that the vertical autocorrelation functions for the water contents and the void ratios may be assumed to be of the form $e^{-|h|/d_U}$ with a correlation distance, d_U, varying between 4' and 6'. Furthermore, the figures indicate that these properties may be assumed as globally homogeneous. For the other properties, although the amount of data is much smaller, some interesting trends may be observed. Both the maximum past pressures and the recompression ratios appear to be weakly correlated in the vertical direction. On the other hand, the compression ratios seem to have a strong vertical correlation. A possible fit may be to an autocorrelation function of the simple exponential form with a decay parameter value of 10'.

Horizontal correlation

Due to the limited amount of data, it was only possible to analyze for horizontal correlation effects the soil measurements taken between z = 15' and z = 20'. The results for the maximum past pressure and some possible fits are shown in Fig. 3.5.13. Note that in this case the correlation distance appears to be quite large

and of the order of 300' or 400'. The smallest inter-boring distance was 300', approximately, and hence short-distance correlation effects for modeling other properties could not be detected.

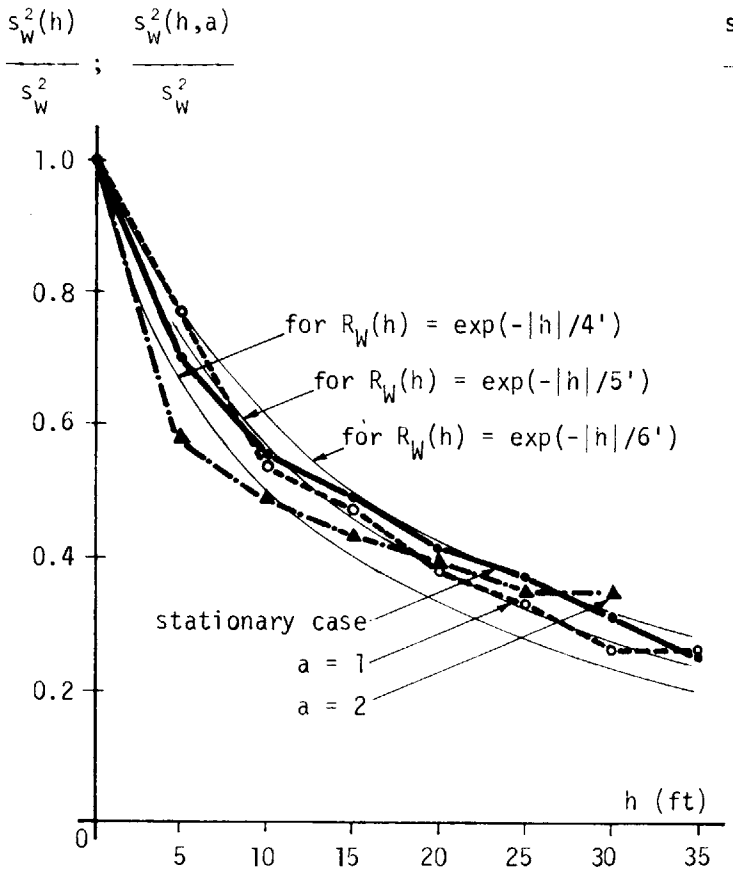


Figure 3.5.9 Normalized Variance Function for W Values

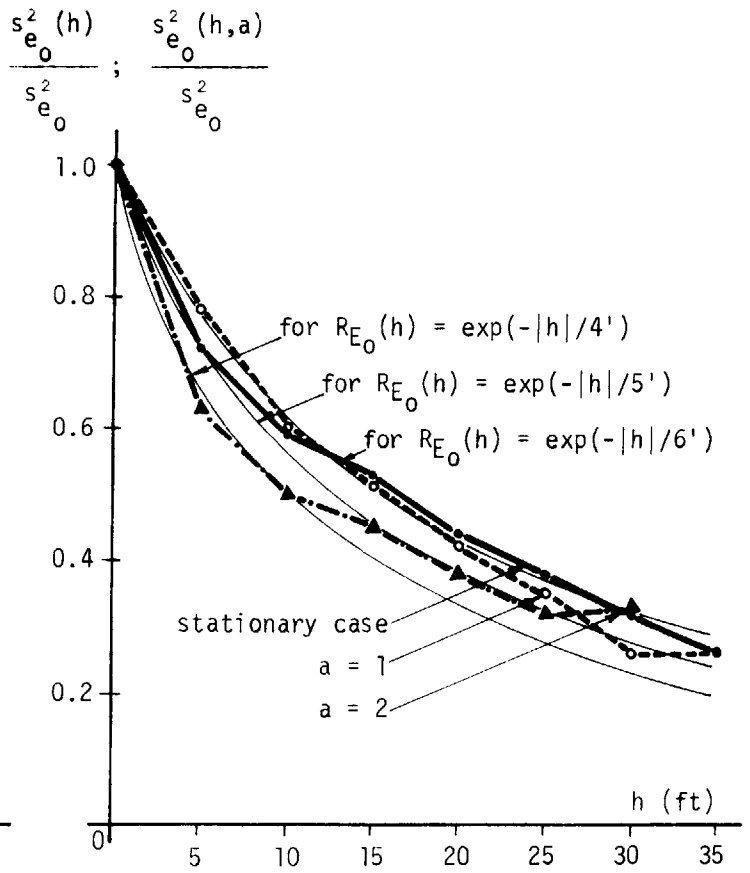


Figure 3.5.10 Normalized Variance Function for E_o Values

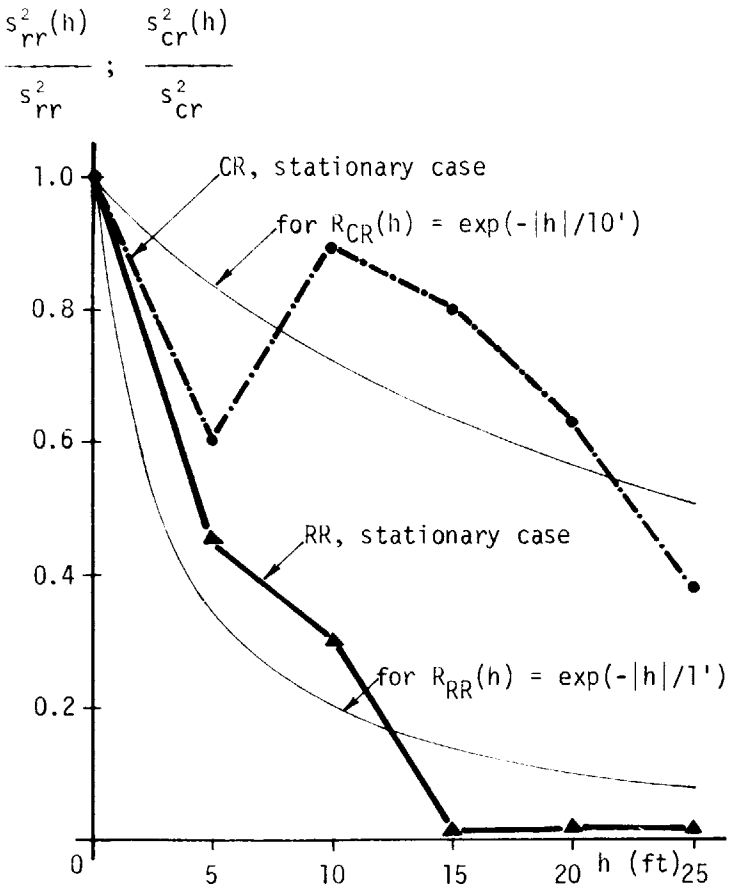


Figure 3.5.11 Normalized Variance Function for RR and CR Values

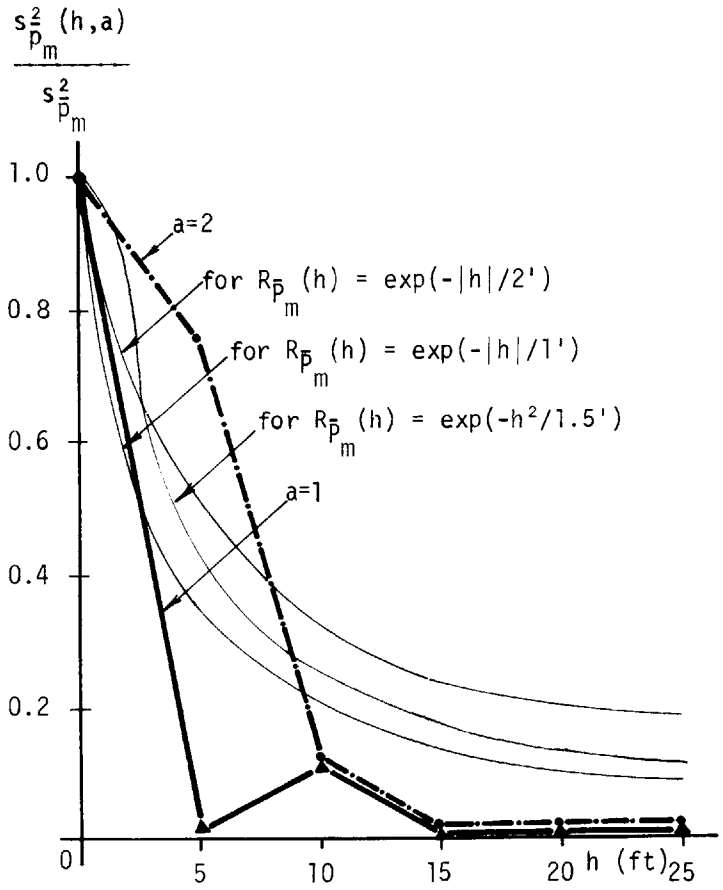


Figure 3.5.12 Normalized Variance Function for $\bar{P}_m$ Values

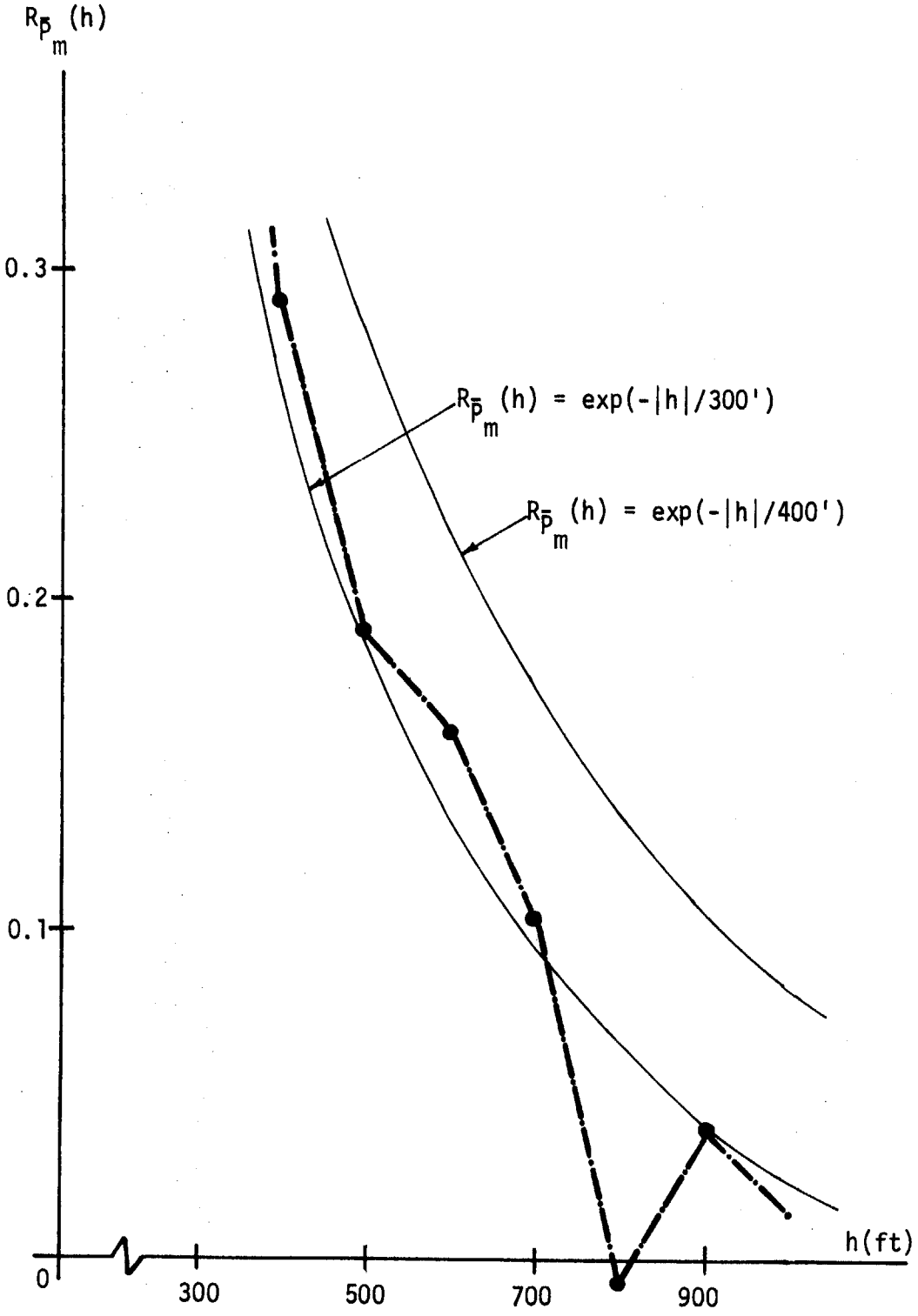


Figure 3.5.13 Horizontal Autocorrelation Function for $\bar{P}_m$ Values

CHAPTER 4

SPATIAL AVERAGES OF SOIL PROPERTIES

4.1 Introduction

The values of the soil properties (e.g., compressibilities) needed in the settlement analysis of structures can be usefully interpreted as spatial averages of point properties over finite volumes, layers or regions within the soil mass. To see this, consider that the load-induced vertical stresses are usually evaluated at the mid-depths of the layers, and that the corresponding layer (vertical) deformations are computed based on compressibility characteristics assigned to each layer midpoint.

For any soil volume, the spatial average $\langle U \rangle$ of a soil property is defined as follows:

$$\langle U \rangle = \frac{\iiint_{vol} U(x,y,z)\,dxdydz}{\text{volume}} \qquad (4.1.1)$$

in which U(x,y,z) represents the value of the property U at a point of coordinates (x,y,z) located within the volume. If U(x,y,z) is viewed as a function of z for given values of x and y (the coordinates of the point at which the settlement is evaluated), then the average of U over the layer thickness takes the form:

$$\langle U \rangle = \frac{\int_{z_1}^{z_2} U(z;x,y)dz}{(z_2 - z_1)} \qquad (4.1.2)$$

For example, $U(z;x,y)$ may represent the vertical compressibility at point (x,y,z), and $\langle U \rangle$ the average vertical compressibility of the layer whose thickness is $(z_2 - z_1)$.

In practice, the soil properties are measured through laboratory tests on specimens of finite size and do not really represent point values. Therefore, Eq. 4.1.2 may be rewritten as

$$\langle U \rangle = \frac{\frac{1}{n^*} \sum_{k=1}^{n^*} \int_{z^{(k)}}^{z^{(k)}+\Delta z} U dz}{\Delta z} = \frac{1}{n^*} \sum_{k=1}^{n^*} U_k \qquad (4.1.3)$$

where n^* is equal to the ratio of layer thickness $(z_2 - z_1)$ to specimen thickness Δz (i.e., the number of specimen-size "points" in the region), and U_k, the value of the soil property for the kth "point", is in itself the spatial average over the thickness of the kth specimen.

In the following sections, the probabilistic parameters of the spatial averages of soil properties are derived in the context of discretized models of the type implied by Eq. 4.1.3. These relationships will be used in the probabilistic settlement-prediction model developed in Chapter 6.

4.2 Means and Variances of Spatial Averages

In previous chapters, it was pointed out that in the analysis of the behavior of a soil mass, actual profiles are generally idealized as a number of layers. Assume that the means m_{U_k}, variances $\sigma^2_{U_k}$ and correlation coefficients ρ_{U_k,U_ℓ} are available for n* points within a region in one of these layers. Then, the mean and the variance of $\langle U \rangle$ can be evaluated as follows (see Appendix A):

$$m_{\langle U \rangle} = \frac{1}{n^*} \sum_{k=1}^{n^*} m_{U_k} \tag{4.2.1}$$

$$\sigma^2_{\langle U \rangle} = \frac{1}{(n^*)^2} \sum_{k=1}^{n^*} \sigma^2_{U_k} + \frac{2}{(n^*)^2} \sum_{k=1}^{n^*-1} \sum_{\ell=k+1}^{n^*} \rho_{U_k,U_\ell} \sigma_{U_k} \sigma_{U_\ell} \tag{4.2.2}$$

If it is assumed that the soil layer is "homogeneous", i.e., $m_{U_k} = m_U$, $\sigma_{U_k} = \sigma_U$, then the mean and the variance of $\langle U \rangle$ become:

$$m_{\langle U \rangle} = m_U \tag{4.2.3}$$

$$\sigma^2_{\langle U \rangle} = \sigma^2_U \left\{ \frac{1}{n^*} + \frac{2}{(n^*)^2} \sum_{k=1}^{n^*-1} \sum_{\ell=k+1}^{n^*} \rho_{U_k,U_\ell} \right\} = \sigma^2_U \Gamma^2_U \tag{4.2.4}$$

and

$$V_{\langle U \rangle} = V_U \Gamma_U \tag{4.2.5}$$

As discussed in Chapter 2, the correlation coefficient ρ_{U_k,U_ℓ} can frequently be described by an exponentially decaying function with a decay parameter d_U, the correlation distance. The factor Γ_U^2 will take values between 0 and 1. If the soil properties are uncorrelated, i.e., if $\rho_{U_k,U_\ell} = 0$ for $k \neq \ell$ (and $d_U = 0$ in Eqns. 2.4.4 and 2.4.5), then $\Gamma_U^2 = 1/n^*$ (†). On the other hand, when the soil properties are perfectly correlated, i.e., when $\rho_{U_k,U_\ell} = 1$ for all k,ℓ (and $d_U = \infty$ in Eqns. 2.4.4 and 2.4.5), then:

$$\Gamma_U^2 = \left\{ \frac{1}{n^*} + \frac{2}{(n^*)^2} \sum_{k=1}^{n^*-1} \sum_{\ell=k+1}^{n^*} 1 \right\} = \left\{ \frac{1}{n^*} + \frac{2}{(n^*)^2} \left[\frac{(n^*)^2-n^*}{2} \right] \right\} = 1 \tag{4.2.6}$$

In this case, the variance of the spatial average, $\sigma^2_{\langle U \rangle}$, is identical to the "point" variance σ_U^2. This result may justify the hypothesis of regarding specimen measurements as point values. As pointed out previously, soil properties obtained from specimens constitute spatial averages. Now, if the correlation distance is much larger than the dimensions of the specimen, then the values of soil properties at points within the specimen will be almost perfectly correlated, and therefore the mean and the variance of point and specimen properties will coincide. On a larger scale, the Γ_U values will depend on the relative values of the layer thickness and the correlation distance as illustrated in Figs. 4.2.1 and 4.2.2.

(†) If the soil properties are uncorrelated, then $\Gamma_U^2 = 0$ in the continuous case (i.e., the properties become an "ideal white noise").

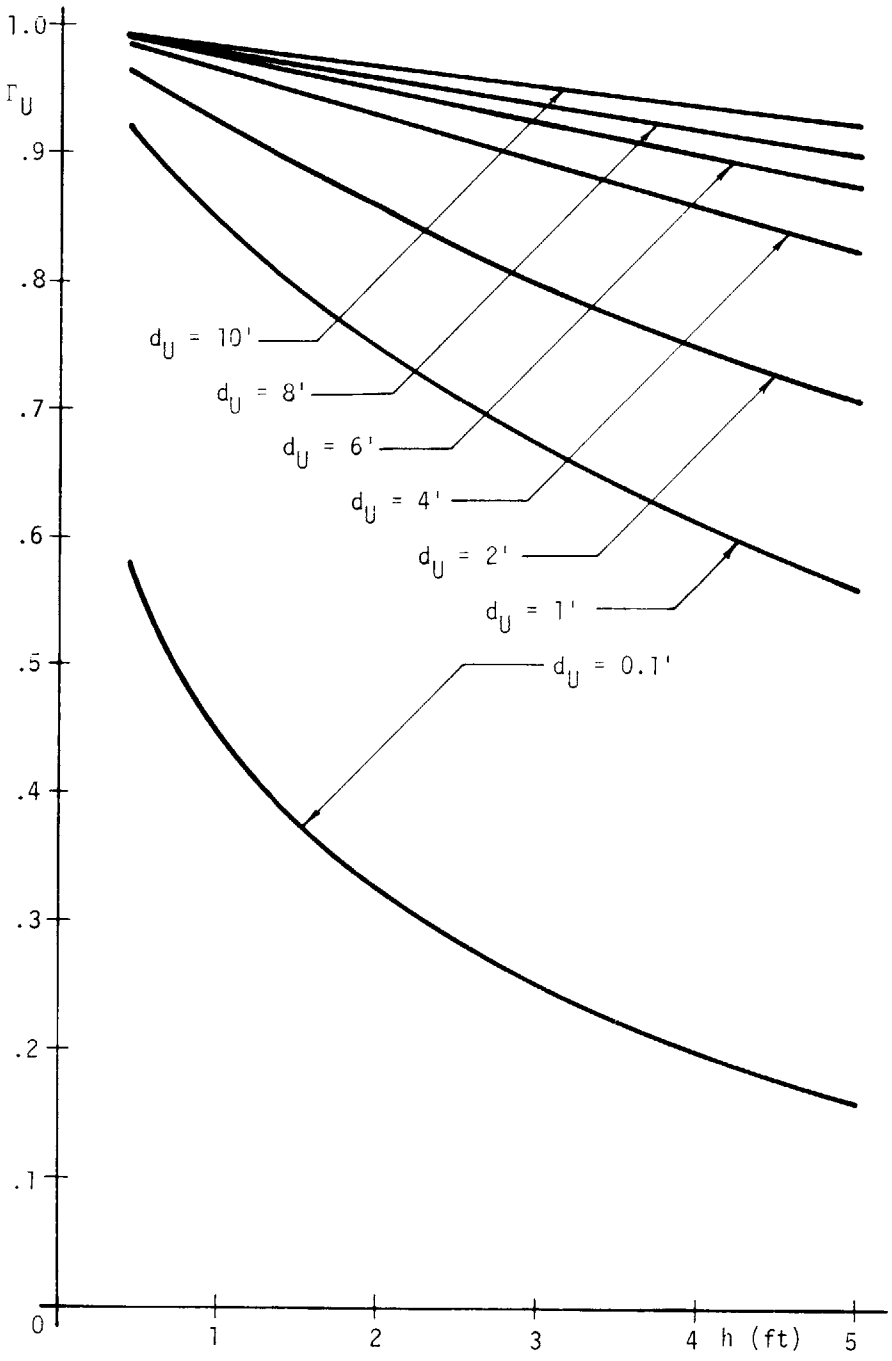


Figure 4.2.1 Γ_U Values for an Autocorrelation Function of the Form $R_U(h) = \exp(-|h|/d_U)$ and Specimens 1" Thick

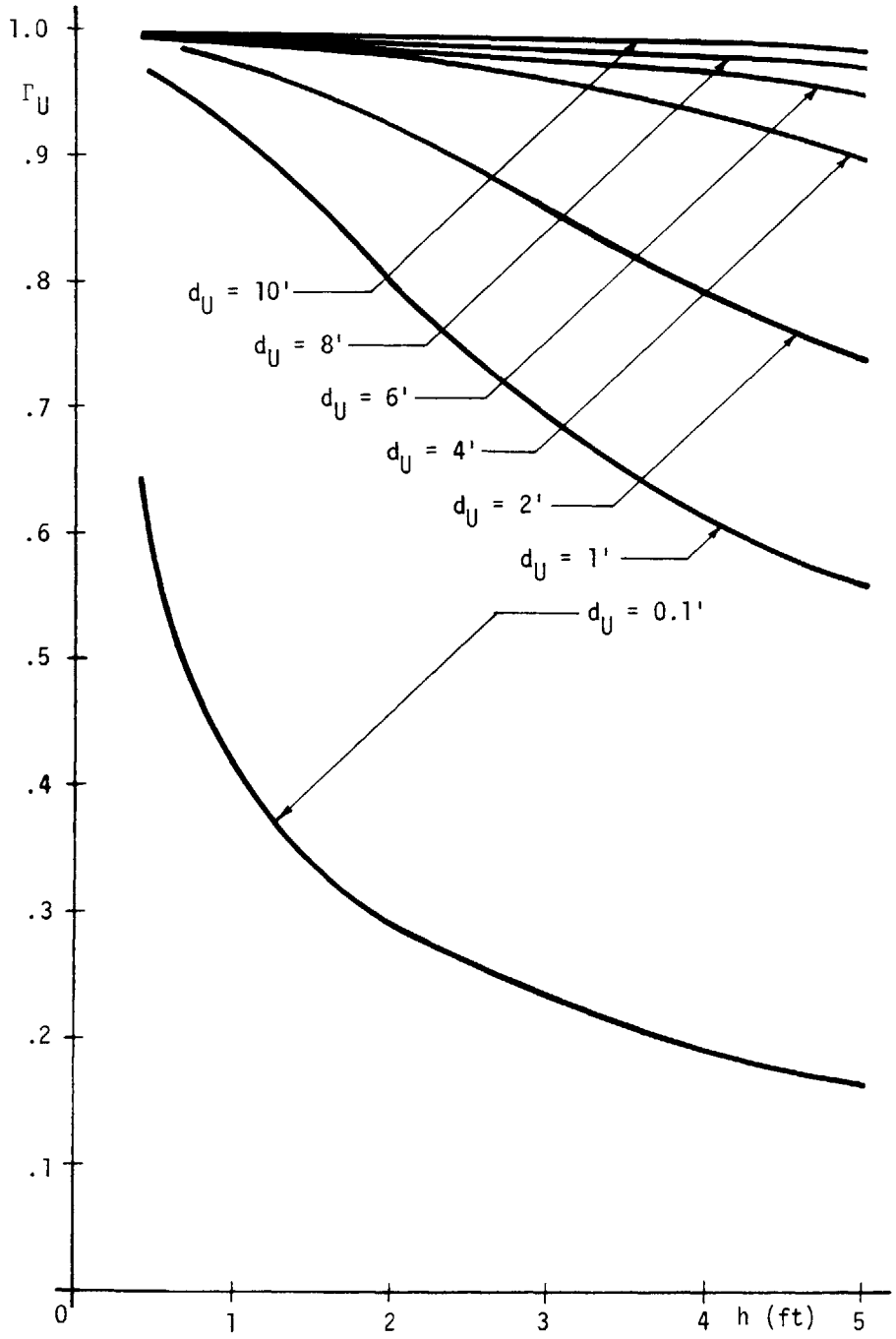


Figure 4.2.2 Γ_U Values for an Autocorrelation Function of the Form $R_U(h) = \exp(-h^2/d_U^2)$ and Specimens 1" Thick

Using the autocorrelation functions given in Eqns. 2.4.4 and 2.4.5, and assuming that the specimens are 1" thick (as those employed in oedometer tests), the values of Γ_U are evaluated in terms of the layer thickness, h, and the correlation distance, d_U. The factor Γ_U^2 may be interpreted as a correction factor which transforms the variance measured from specimens into the variance of the spatial average $\langle U \rangle$. As an example, in the case study of the previous chapter, the coefficient of variation for the recompression ratio of a homogeneous volume of clay is found to be $V_{RR} = 0.79$, based on measurements on 1" thick specimens. For a 3' thick layer of this material, and based on an autocorrelation function of the form $R_{RR}(h) = \exp(-|h|/1')$ (as shown in Fig. 3.5.11), the coefficient of variation of the spatial average (over the layer thickness) of the recompression ratio may be obtained from Fig. 4.2.1. The value is $V_{\langle RR \rangle} = 0.68\ V_{RR} = 0.68 \times 0.79 = 0.54$. Note that the assumption of perfect correlation would yield conservative estimates of the variability of spatial averages.

4.3 Covariances Between Spatial Averages

The covariance between the spatial averages $\langle U \rangle_i^{(a)}$ and $\langle U \rangle_j^{(b)}$ for the property U at two locations i and j within two soil layers a and b (see Fig. 4.3.1) may be computed as (see Eq. A.8 in Appendix A):

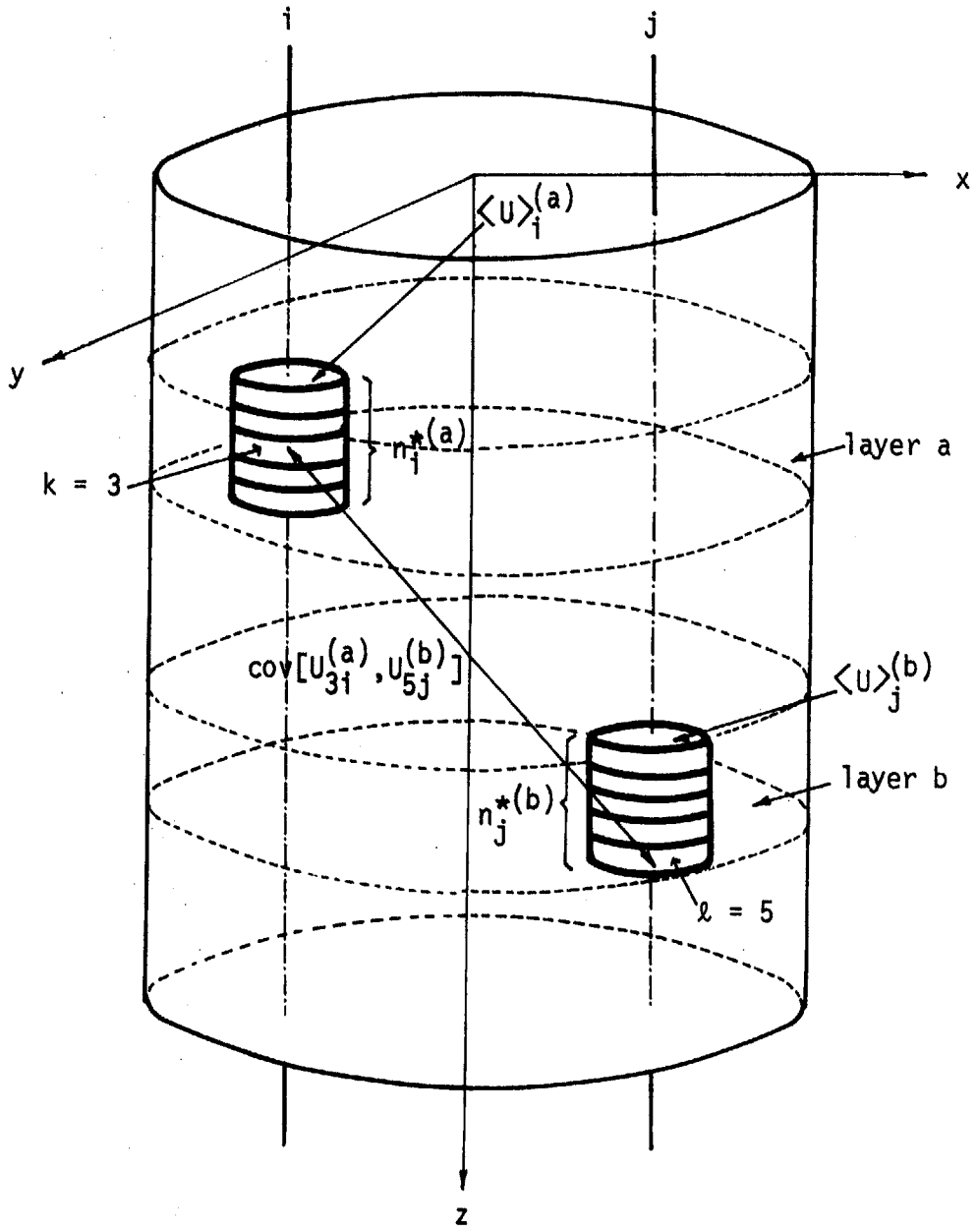


Figure 4.3.1 Schematic Representation of Two Spatial Averages $\langle U \rangle_i^{(a)}$ and $\langle U \rangle_j^{(b)}$

$$\mathrm{cov}[\langle U\rangle_i^{(a)},\langle U\rangle_j^{(b)}] = \frac{1}{n_i^{*(a)}}\,\frac{1}{n_j^{*(b)}}\sum_{k=1}^{n_i^{*(a)}}\sum_{\ell=1}^{n_j^{*(b)}} \rho_{U_{ki}^{(a)},U_{\ell j}^{(b)}}\,\sigma_{U_{ki}^{(a)}}\,\sigma_{U_{\ell j}^{(b)}} \tag{4.3.1}$$

where $n_i^{*(a)}$ and $n_j^{*(b)}$ represent the number of points in each region and $U_{ki}^{(a)}$ is the kth value of the property U in the region ai.

For "homogeneous" layers of constant thickness with different properties from layer to layer, Eq. 4.3.1 can be expressed as:

$$\mathrm{cov}[\langle U\rangle_i^{(a)},\langle U\rangle_j^{(b)}] = \sigma_{U(a)}\,\sigma_{U(b)}\left[\frac{1}{n^{*(a)}n^{*(b)}}\sum_{k=1}^{n^{*(a)}}\sum_{\ell=1}^{n^{*(b)}} \rho_{U_{ki}^{(a)},U_{\ell j}^{(b)}}\right]$$

$$= \sigma_{U(a)}\,\sigma_{U(b)}\,\nu_U \tag{4.3.2}$$

in which the correlation coefficients may, in principle, be computed with a three-dimensional autocorrelation function of the form given in Eqns. 2.4.8 or 2.4.9. The factor ν_U may be interpreted as a correlation coefficient which transforms the covariance between points to the covariance between spatial averages. If the two regions are in the same layer and are of the same size, then the factor ν_U can be expressed as the product $\Gamma_U^2\,\rho^*$ in which ρ^* is the correlation coefficient (as defined for point values) between the two regions and Γ_U is the factor discussed in Section 4.2. In other words, in this case the variances of the soil properties are first transformed from point to spatial averages through multiplication by Γ_U, and in

the remainder of the analysis the spatial average effects are neglected, i.e., one proceeds as if all the properties were perfectly correlated within each region.

If the soil volume considered is homogeneous throughout and if all the layers are of equal thickness:

$$\mathrm{cov}[\langle U\rangle_i^{(a)},\langle U\rangle_j^{(b)}] = \sigma_U^2 \left[\frac{1}{(n^*)^2}\sum_{k=1}^{n^*}\sum_{\ell=1}^{n^*}\rho_{U_{ki}^{(a)},U_{\ell j}^{(b)}}\right]$$

$$= \sigma_U^2\ \nu_U \qquad (4.3.3)$$

and the correlation coefficients now depend only on the differences of coordinates between the points in the two regions.

4.4 Experimental Variability and Testing Errors

In the context of the discussion of Section 3.4, when calculating the parameters of spatial averages, disturbance and testing variability should also be taken into account.

Let $\langle\hat{U}\rangle$ denote the spatial average of specimen-measured soil properties taking into account sampling and testing variability. Eqns. 3.4.2 to 3.4.4 can be generalized in the following way:

$$m_{\langle \hat{U} \rangle} = m_U + m_{E_d} \tag{4.4.1}$$

$$\sigma^2_{\langle \hat{U} \rangle} = \sigma^2_U \Gamma^2_U + \sigma^2_{E_d} + \frac{\sigma^2_{E_t}}{n^*} \tag{4.4.2}$$

$$\mathrm{cov}[\langle \hat{U} \rangle_i^{(a)}, \langle \hat{U} \rangle_j^{(b)}] = \sigma_{U(a)} \sigma_{U(b)} \nu_U + \sigma^2_{E_d} \quad , \; i \neq j \text{ or } a \neq b \tag{4.4.3}$$

CHAPTER 5

THE PREDICTION OF SETTLEMENTS OF STRUCTURES: A DETERMINISTIC PROCEDURE

5.1 Introduction

In this chapter, a settlement-prediction model is developed for structures supported on shallow foundations. The method accounts for the interaction between the structure and the soil through the redistribution of vertical loads due to uneven settlements of the foundation. Elastic structural behavior is implied throughout the analysis, however, in the case of stiffness degradation, the calculated differential settlements (based on the original structural stiffness) as well as the secondary stresses induced in the structural members will tend to constitute lower bounds to the true values. Conservative values can usually be obtained by neglecting the soil-structure interaction effects.

A one-dimensional approach is followed in which it is assumed that no lateral deformations of the soil are generated and that the vertical deformation of a compressible layer may be expressed as a summation of contributions due to a number of sublayers. However, the model does not depend on the particular stress-strain characteristics of each one of these sublayers and can accommodate any type of load-settlement relationships commonly employed in the modeling of actual soil behavior. A particular application of the method to cohesive soils is developed and illustrated at the end of the chapter.

5.2 The One-dimensional Settlement Model

Often in structures supported on shallow foundations, the loaded area is large compared to the thickness of the compressible strata. In such cases, the induced settlements are primarily due to one-dimensional strains resulting from volume changes. In this context, the vertical deformation, s, of a compressible stratum is given by:

$$s = \sum_{i=1}^{k} f^{(i)} \, \Delta\bar{p}^{(i)} \qquad (5.2.1)$$

where $f^{(i)}$ = soil flexibility of the ith sublayer, $\Delta\bar{p}^{(i)}$ = sum of vertical stresses induced by the applied loads in the ith sublayer, and k is the number of compressible sublayers in which the stratum has been discretized (so that along each sublayer thickness both $f^{(i)}$ and $\Delta\bar{p}^{(i)}$ may be assumed of constant value). The summation in Eq. 5.2.1 includes all the compressible layers below the point at which the settlement is to be evaluated, as shown in Fig. 5.2.1.

The soil flexibility f

If the stress-strain relationship of the soil is linear, then the flexibility parameter, f, will simply be equal to the thickness of the sublayer divided by the modulus of elasticity of the soil. In general, of course, the behavior will be non-linear and the value of f will become stress-dependent. In such a case, the parameter f may be referred to as the "pseudo-flexibility" and defined as the value of the slope of an imaginary straight line in the stress-settlement diagram,

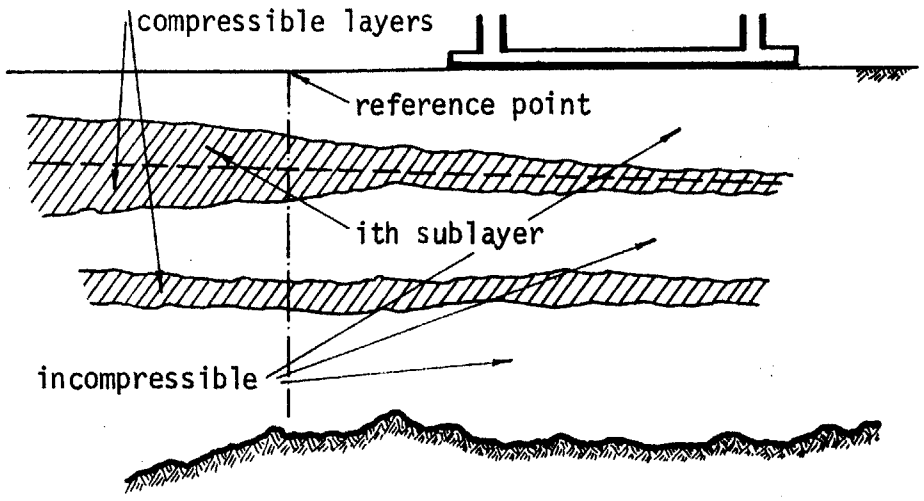


Figure 5.2.1 Soil Profile for Settlement Estimation

as illustrated by the broken line in Fig. 5.2.2. The product of the pseudo-flexibility f and the induced stress $\Delta\bar{p}$ must be equal to the settlement s* as if computed from the non-linear relation, or:

$$f = \frac{s^*}{\Delta\bar{p}} \qquad (5.2.2)$$

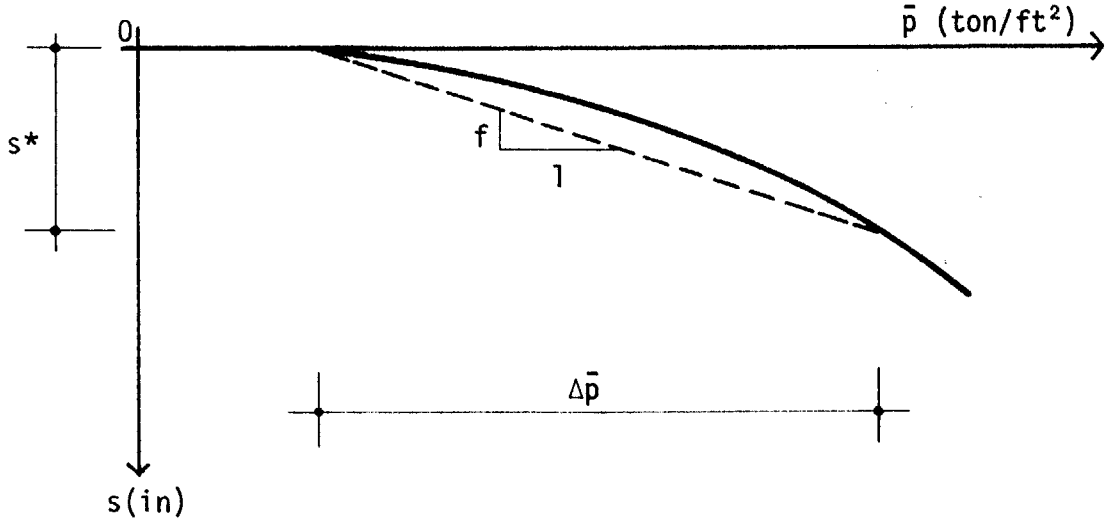


Figure 5.2.2 Definition of the Pseudo-flexibility Parameter f

The stress increments $\Delta\bar{p}$

For point loads and uniformly distributed loads, the induced vertical stress increments are calculated using the formulas derived from the theory of elasticity (29,43,46) shown in Fig. 5.2.3.

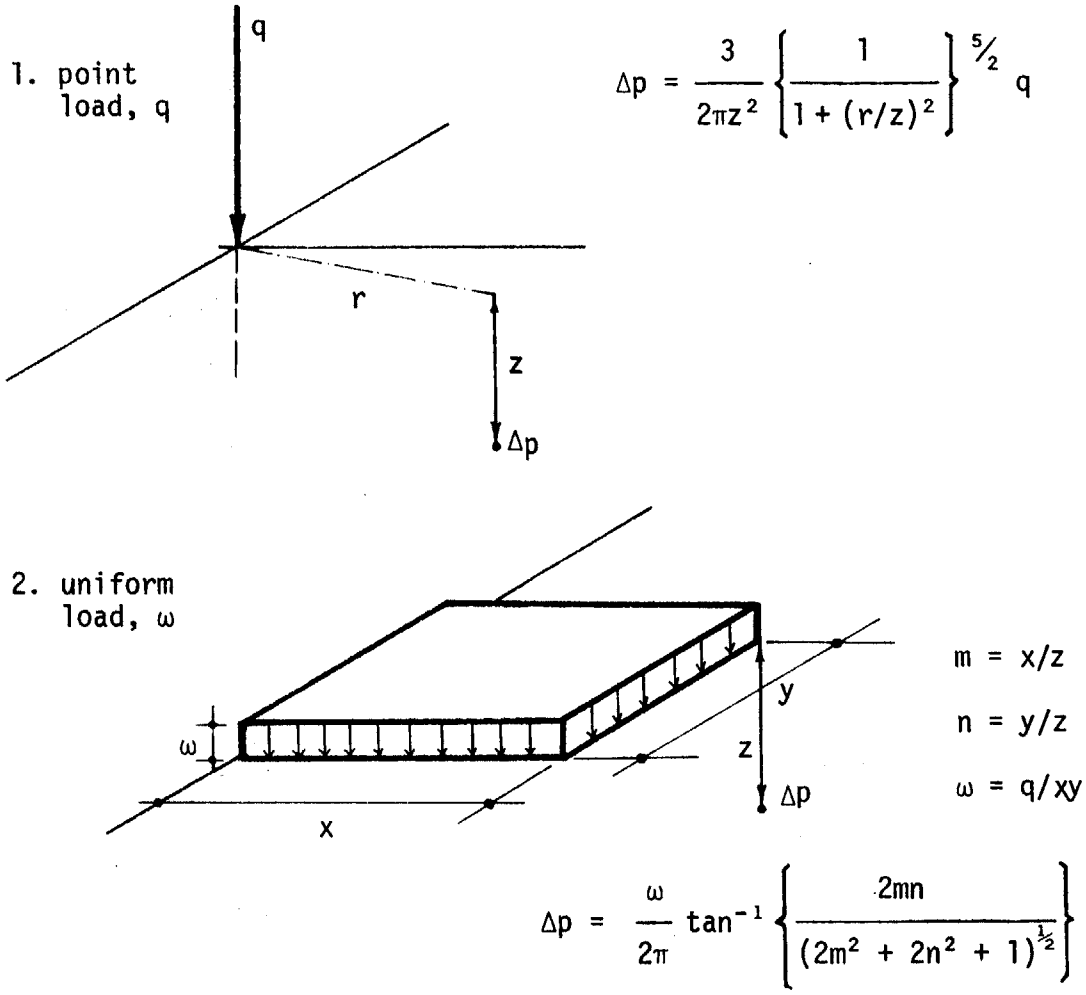


Figure 5.2.3 Stress Coefficients for Point Loads and Uniformly Distributed Loads

The expressions are based on the assumption that the soil is semi-infinite, homogeneous and isotropic, and that its stress-strain behavior follows the elastic theory. It is true that these assumptions are seldom satisfied when dealing with real soil problems, but in the case of vertical stresses, comparisons between measured and predicted vertical stresses (45) have shown a reasonable agreement.

In general, the effective stress increment $\Delta\bar{p}_{ij}$ (or the total stress increment since $\Delta\bar{p} = \bar{p}_{final} - \bar{p}_{initial} = \Delta p$) at a point i in the soil, induced by the load q_j acting at a point j on the soil surface, is given by:

$$\Delta\bar{p}_{ij} = \alpha_{ij}\, q_j \tag{5.2.3}$$

where α_{ij} = stress coefficient which can be obtained from Fig. 5.2.3 for point loads and uniform loads.

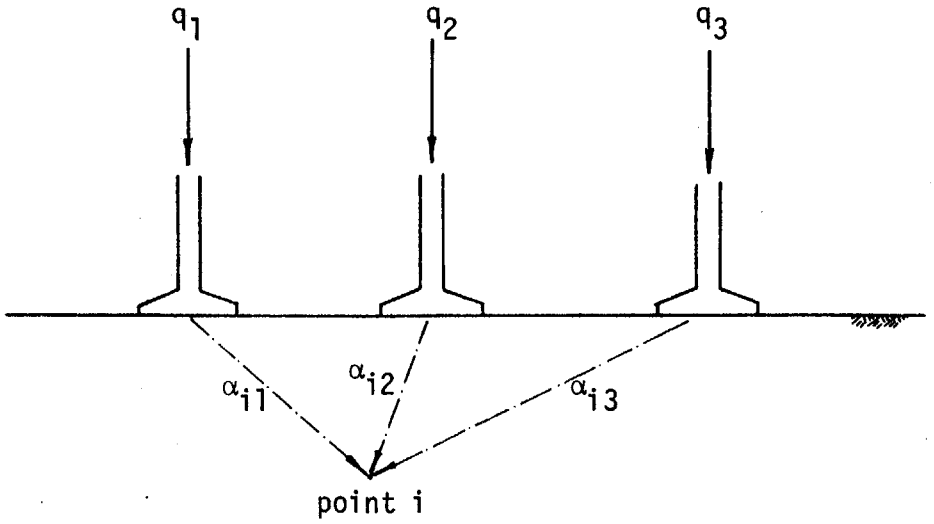


Figure 5.2.4 Vertical Stress at a Point Induced by a Number of External Loads

If n loads contributing to the stress increment at a particular point in the soil (see Fig. 5.2.4) are represented by a vector $\underset{\sim}{q}$, then a size m vector of induced stresses $\Delta\underset{\sim}{\bar{p}}$ may be evaluated using

$$\Delta\underset{\sim}{\bar{p}} = \alpha\, \underset{\sim}{q} \qquad (5.2.4)$$

where α is an $m \times n$ matrix of stress coefficients.

5.3 Soil-structure Interaction

In the above discussion on settlement estimation, no reference was made to the type of structural system under consideration. The only information needed about the superstructure is the values of the loads discharged to the foundation by the supporting walls or columns. The loading system has been idealized as a set of independent (point or line) loads applied at the ground level and structural continuity effects have been ignored (this would indeed be the case for a perfectly flexible structure which is referred to as "the flexible case" in what follows). However, it is evident that the loads cannot be uncoupled from the deformations they generate. If a particular column is very heavily loaded, the settlement underneath it is likely to be large. This will cause a redistribution of forces and part of the load will be transferred to less stressed support points, thus changing the settlement profile. By ignoring the soil-structure interaction, conservative upper bounds to the differential settlements are usually obtained. Thus, the interaction is frequently neglected. However, in choosing among various sub- and superstructure alternatives,

the stiffness effect will often constitute an important factor. It can significantly change the estimated movements and distortions of the structure, as well as the corresponding levels of superstructure and foundation distress and the associated costs of damage.

In soil-structure interaction models, the redistribution of vertical loads is often described in terms of so-called "load transfer coefficients" first proposed by Chamecki (4) and later used by Flores and Esteva (12) and Larnach (25). These are simply structure-dependent parameters and, for a structure supported on n points, define a square matrix T of order n. A typical element of this matrix, T_{ij}, represents the value of the vertical reaction generated at the ith support point when the jth settles a unit amount while the other supports are prevented from displacing vertically. This idea is clarified in Fig. 5.3.1a. which shows a two-bay one-story frame supported on spread footings. The T matrix for this frame is a 3×3 matrix whose elements are the nine reactions illustrated in Fig. 5.3.1b., c., and d. It is important to note that when a support moves, both tension and compression forces may be generated. Each row of the T matrix is equivalent to a vertical reaction influence line for settlements. Furthermore, the matrix is symmetric (since $T_{ij} = T_{ji}$ from Maxwell's Theorem) and, from vertical equilibrium, the elements of each column add up to zero.

The original column (or wall) reactions (obtained based on the assumption of unyielding supports)define the load vector $\underset{\sim}{q}$. If $\underset{\sim}{s}$ is a size n vector of calculated settlements, the product $T\underset{\sim}{s}$ will give

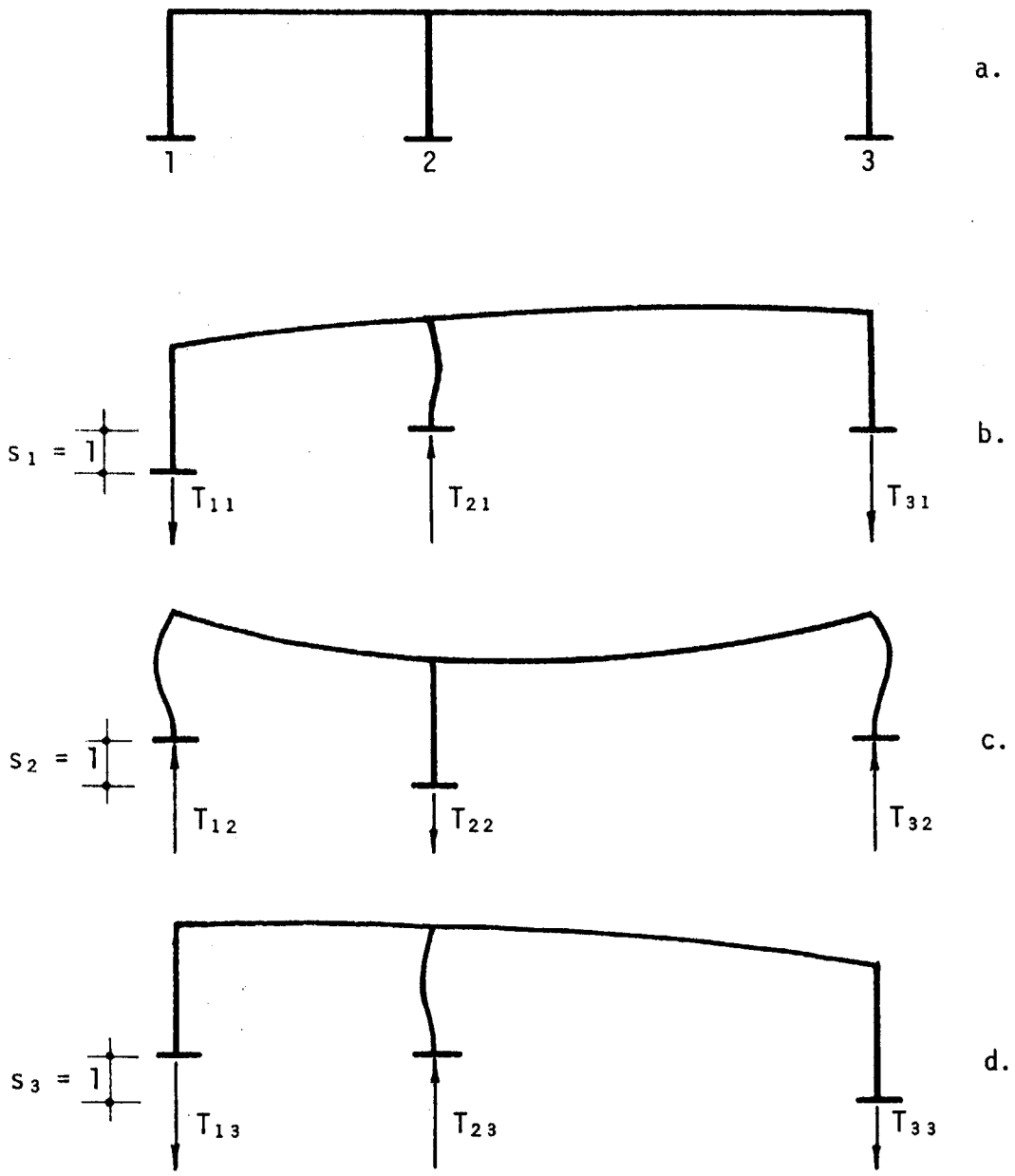


Figure 5.3.1 Load Transfer Coefficients for a Two-bay One-story Frame

the values of the redistributed loads. The elements of the vector $\underset{\sim}{q}$ must be corrected by these values to obtain the true loading condition . The stiffer the structure (and the larger the elements of the T matrix), the more the load corrections gain in importance. In the flexible case, the T matrix is equal to the null matrix and no corrections are necessary.

If a linear and constant load-settlement relationship is employed, it is possible to formulate the soil-structure interaction problem in closed form and to solve it in one step*. However, as soon as the parameters of the model become stress-dependent, their revision is necessary after the redistribution of stresses is known. If, in addition, a non-linear stress-strain relation is used, it is necessary to assume initially and then revise in an iterative way the final load-induced stress levels. In these instances, it becomes necessary to resort to an iterative procedure.

For the frame shown in Fig. 5.3.1a., assuming it is underlain by a single compressible sublayer (see also Fig. 5.3.2), the soil-structure interaction equations are:

$$f_{11}\{(q_1 + T_{11}s_1 + T_{12}s_2 + T_{13}s_3)\alpha_{11}$$

$$+ (q_2 + T_{21}s_1 + T_{22}s_2 + T_{23}s_3)\alpha_{12}$$

$$+ (q_3 + T_{31}s_1 + T_{32}s_2 + T_{33}s_3)\alpha_{13}\} = s_1$$

---

* In the case of very rigid structures or very compressible soils, an iteration procedure requiring small load corrections in each cycle should be used.

$$f_{22}\{(q_1 + T_{11}s_1 + T_{12}s_2 + T_{13}s_3)\alpha_{21}$$
$$+ (q_2 + T_{21}s_1 + T_{22}s_2 + T_{23}s_3)\alpha_{22}$$
$$+ (q_3 + T_{31}s_1 + T_{32}s_2 + T_{33}s_3)\alpha_{23}\} = s_2$$

$$f_{33}\{(q_1 + T_{11}s_1 + T_{12}s_2 + T_{13}s_3)\alpha_{31}$$
$$+ (q_2 + T_{21}s_1 + T_{22}s_2 + T_{23}s_3)\alpha_{32}$$
$$+ (q_3 + T_{31}s_1 + T_{32}s_2 + T_{33}s_3)\alpha_{33}\} = s_3$$

(5.3.1)

or, in matrix form:

$$\begin{bmatrix} f_{11} & 0 & 0 \\ 0 & f_{22} & 0 \\ 0 & 0 & f_{33} \end{bmatrix} \begin{bmatrix} \alpha_{11} & \alpha_{12} & \alpha_{13} \\ \alpha_{21} & \alpha_{22} & \alpha_{23} \\ \alpha_{31} & \alpha_{32} & \alpha_{33} \end{bmatrix} \left\{ \begin{bmatrix} q_1 \\ q_2 \\ q_3 \end{bmatrix} + \begin{bmatrix} T_{11} & T_{12} & T_{13} \\ T_{21} & T_{22} & T_{23} \\ T_{31} & T_{32} & T_{33} \end{bmatrix} \begin{bmatrix} s_1 \\ s_2 \\ s_3 \end{bmatrix} \right\} = \begin{bmatrix} s_1 \\ s_2 \\ s_3 \end{bmatrix}$$

(5.3.2)

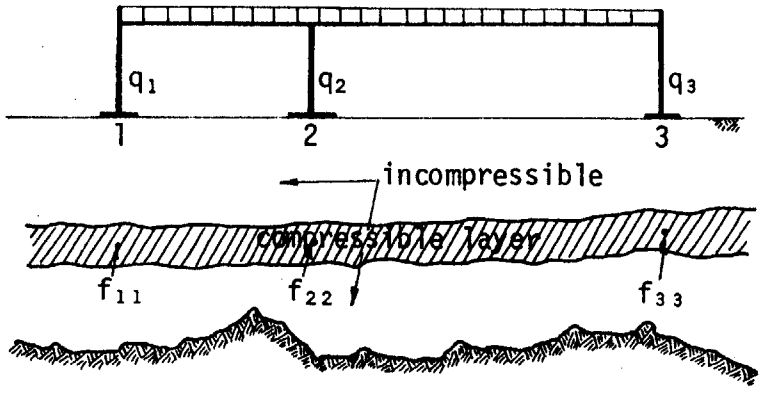


Figure 5.3.2 Soil-structure Interaction Problem: Three-supports Case

For the general case illustrated in Fig. 5.3.3, the problem may be formulated in matrix form as:

$$\{\sum_{i=1}^{k} f_d^{(i)}\alpha^{(i)}\}\{\underset{\sim}{q} + T\underset{\sim}{s}\} = \underset{\sim}{s} \qquad (5.3.3)$$

where k = the number of compressible layers or sublayers; $f_d^{(i)}$ = $n \times n$ diagonal matrix whose diagonal elements are the pseudo-flexibilities, $f_{jj}^{(i)}$, at mid-depth in sublayer i under support j; and $\alpha^{(i)}$ = $n \times n$ matrix of stress coefficients referred to layer i.

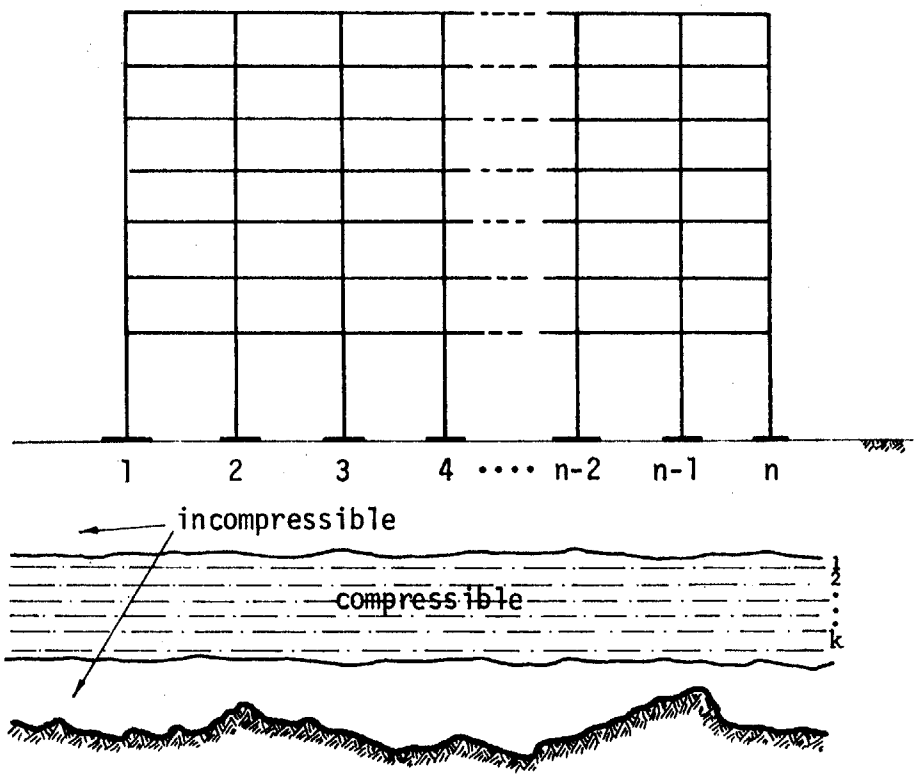


Figure 5.3.3 Soil-structure Interaction Problem: General Case

The above expression can be simplified by denoting the matrix $\sum_{i=1}^{k} f_d^{(i)}{}_{\alpha}{}^{(i)}$ by ω:

$$\omega\{\underset{\sim}{q} + T\underset{\sim}{s}\} = \underset{\sim}{s} \tag{5.3.4}$$

The solution of this system of linear equations is:

$$\underset{\sim}{s} = \{I - \omega T\}^{-1}\, \omega\, \underset{\sim}{q} \tag{5.3.5}$$

where I is an $n \times n$ identity matrix.

Using Eq. 5.3.5, the stresses in each sublayer can be evaluated and the pseudo-flexibilities may be revised. A few iterations will result in a rapid convergence to the correct solution* (Fig. 5.3.4).

The method is completely general: plane frames and tridimensional structures may be handled in the same way. A continuous foundation may be discretized into a set of virtual supports (41) and its rigidity-damped settlements may be computed by using Eq. 5.3.5. In this case, the T matrix will reflect not only the stiffness of the superstructure but that of the foundation as well.

If K, the stiffness matrix of the structure, is known, the load transfer coefficients may be easily obtained by appropriate matrix operations (see Appendix C for more details). However, if a computer is not used and approximate methods are necessary, careful attention must be paid to empirical procedures, e.g., the method of reducing a multi-story frame to a one-story frame with stiffness equal to the

---

* See footnote at the bottom of page 68.

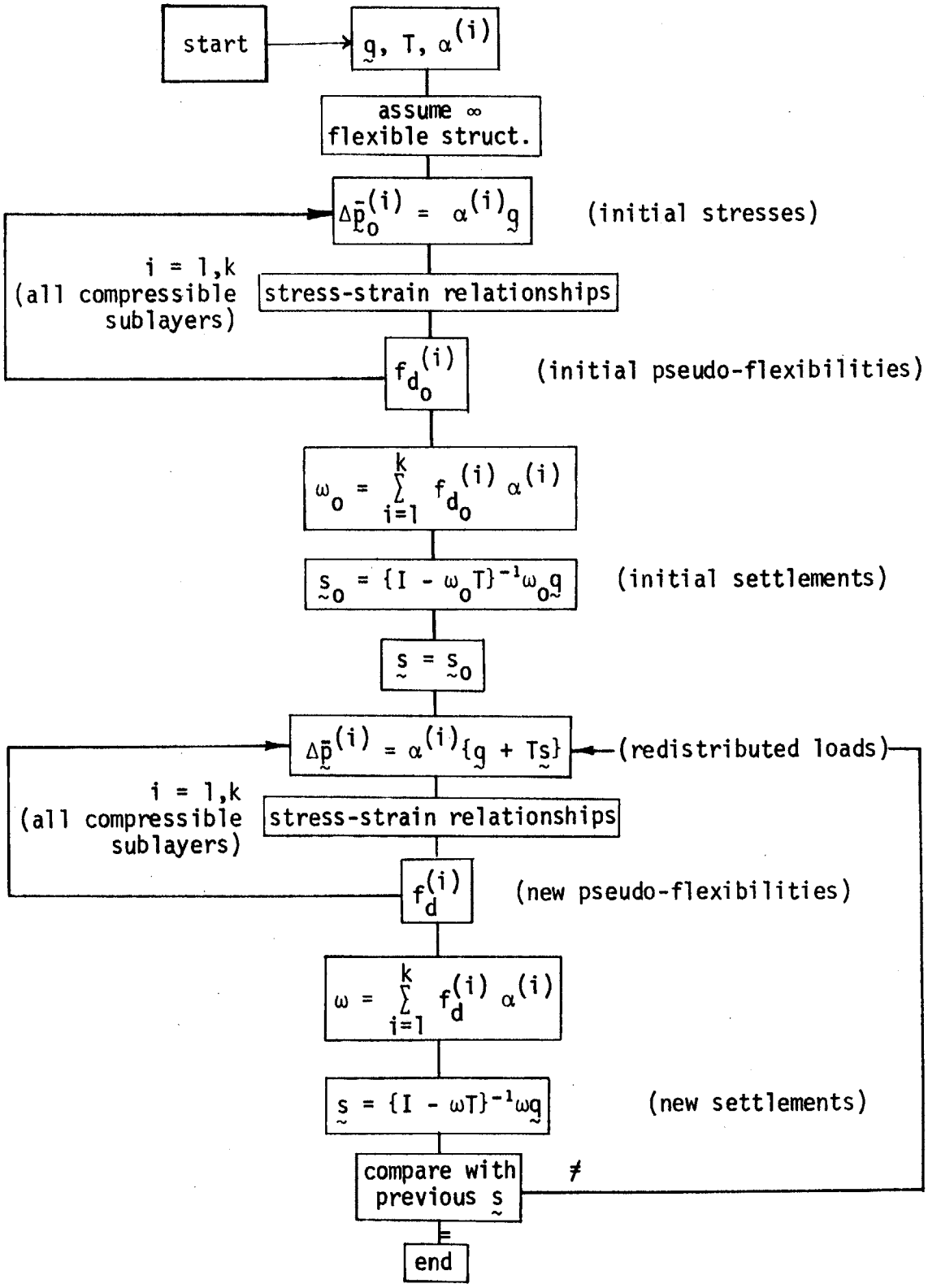


Figure 5.3.4 Algorithm for Solving the Deterministic Soil-structure Interaction Problem

summation of story stiffnesses along the total height of the building. Litton and Buston (26) have shown that in the case of tall, rigid steel frames, the lower half of the structure gives the predominant resistance to induced settlements. Thus, the above rule may prove unconservative. Measurements of movements in constructed buildings should be made and related to various rigidity parameters to establish good approximate rules regarding equivalent structural stiffness for settlement considerations (31).

As mentioned previously, if stiffness effects are neglected, upper bounds to the differential settlements and to the settlement-induced joint displacements and secondary stresses in the structure are usually obtained. On the other hand, recognition of the interaction between the structure and the soil will yield more accurate estimates of deformations and deformation-induced forces. However, it should be noted that the concept of load redistribution (on which the above interaction is based) presumes elastic structural behavior. In cases where the settlement-induced strains exceed the elastic limits of the materials, yielding and/or cracking of the structure will occur with accompanying stiffness degradation. In these instances, the calculated differential movements and forces will tend to constitute lower bounds to their true values. Furthermore, in concrete structures where the settlements may occur at a slower rate than the creep of concrete (e.g., in structures supported on soils of very low permeability) the elastic modulus of the material will tend to change with time in a relatively rapid way compared to the settlements. This

will tend to reduce soil-structure interaction effects (19,30).

5.4 Settlements of Structures on Cohesive Soils

The predominant deformation mechanism of a saturated stratum of ordinary clay when it is subjected to a rapid change in the exterior pressure is that of slow water drainage and transference of stress from the water particles to the soil skeleton, with accompanying volume changes (24,44). This process is known as consolidation and is the only type of settlement which is considered in the examples throughout this work.

To measure the vertical compressibility of the soil, confined compression (oedometer) tests (23,24,44) are performed in the laboratory. The stress-strain behavior of a soil sample is generally studied through e - log $\bar{p}$ curves, i.e., plots of void ratio versus the logarithm of the effective stress, as shown in Fig. 5.4.1. Since in an oedometer test a change in void ratio (Δe), a change in axial strain ($\Delta\varepsilon$), and the initial void ratio (e_o) are directly related (by $\Delta\varepsilon = -\Delta e/(1 + e_o)$), an e - log $\bar{p}$ plot completely defines a stress-strain characteristic. The point $\bar{p}_m$ in Fig. 5.4.1 corresponds to a value of the effective stress equal to the maximum which the sample has ever experienced during its lifetime. This soil parameter is known as the maximum past pressure, and generally differs from the existing overburden stress ($\bar{p}_o$) because of phenomena such as desiccation, fluctuations of the water table, etc. Table 5.4.1, which is taken from Ladd (22), lists the many mechanisms influencing the

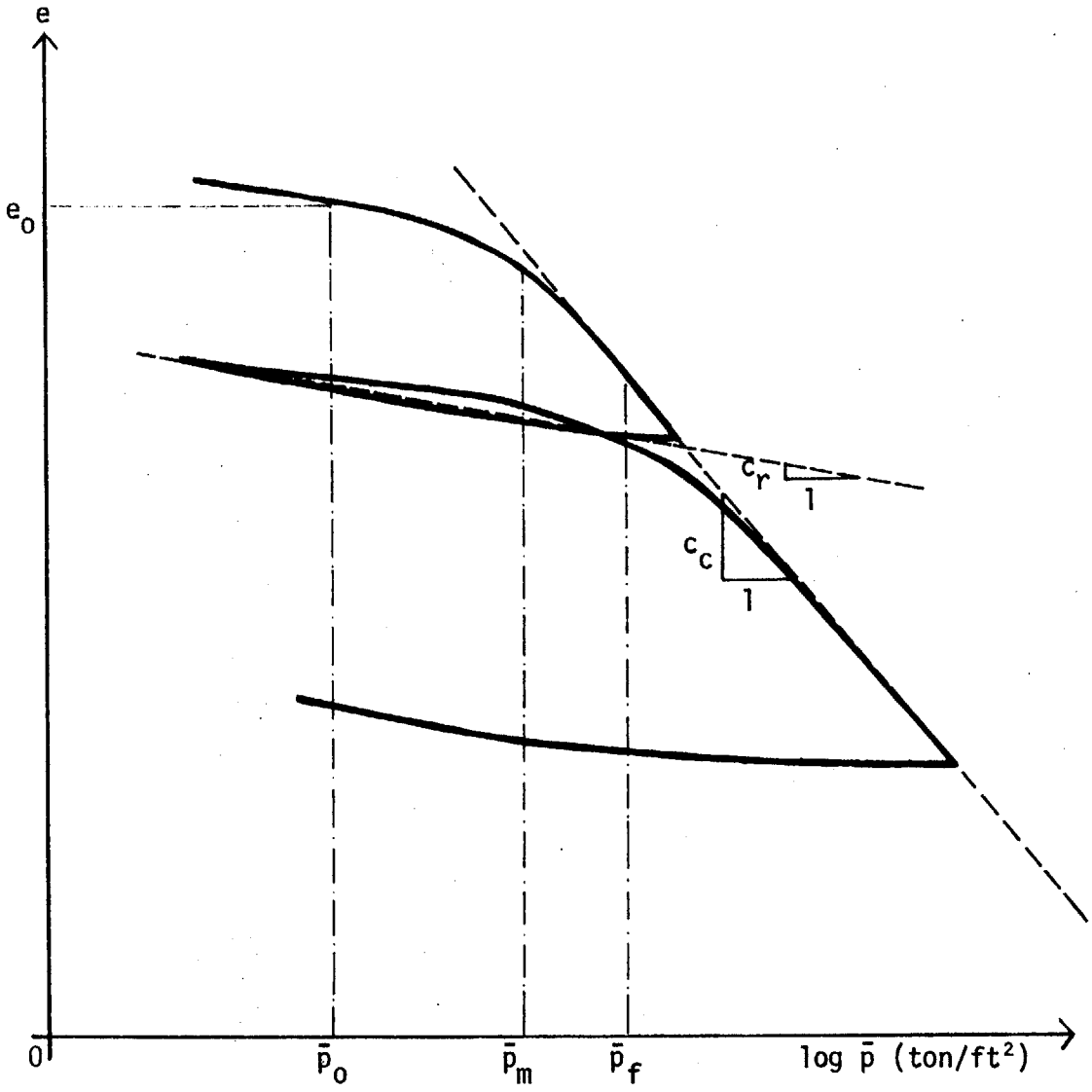


Figure 5.4.1 e - log $\bar{p}$ Plot for a Cohesive Material

A. Change in Total Stress Due to:
1. Removal of overburden
2. Past structures
3. Glaciation
B. Change in Pore Water Pressure Due to:
1. Change in water table elevation
2. Artesian pressure
3. Deep pumping
4. Desiccation due to drying
5. Desiccation due to plant life
C. Changes in Soil Structure Due to:
1. Secondary compression (aging)
2. Changes in environment, such as pH, temperature, salt concentration, etc.
3. Chemical alterations due to: "weathering", precipitation of cementing agents, ion exchange, etc.

Table 5.4.1 Mechanisms Causing a Maximum Past Pressure*

maximum past pressure. It is evident from the approximate bilinear nature of the e - log $\bar{p}$ curve that the stress history of the soil will play a definitive role in its stress-strain behavior. If the final load-induced effective stress, $\bar{p}_f$, is smaller than $\bar{p}_m$, the deformations will be small and the stresses are said to be acting in the "recompression zone". However, as soon as $\bar{p}_f$ becomes larger than $\bar{p}_m$, the induced settlements increase rapidly. In this case, part of the stress increment is acting in the "virgin compression zone" (see Fig. 5.4.2).

---

* From Ladd (22)

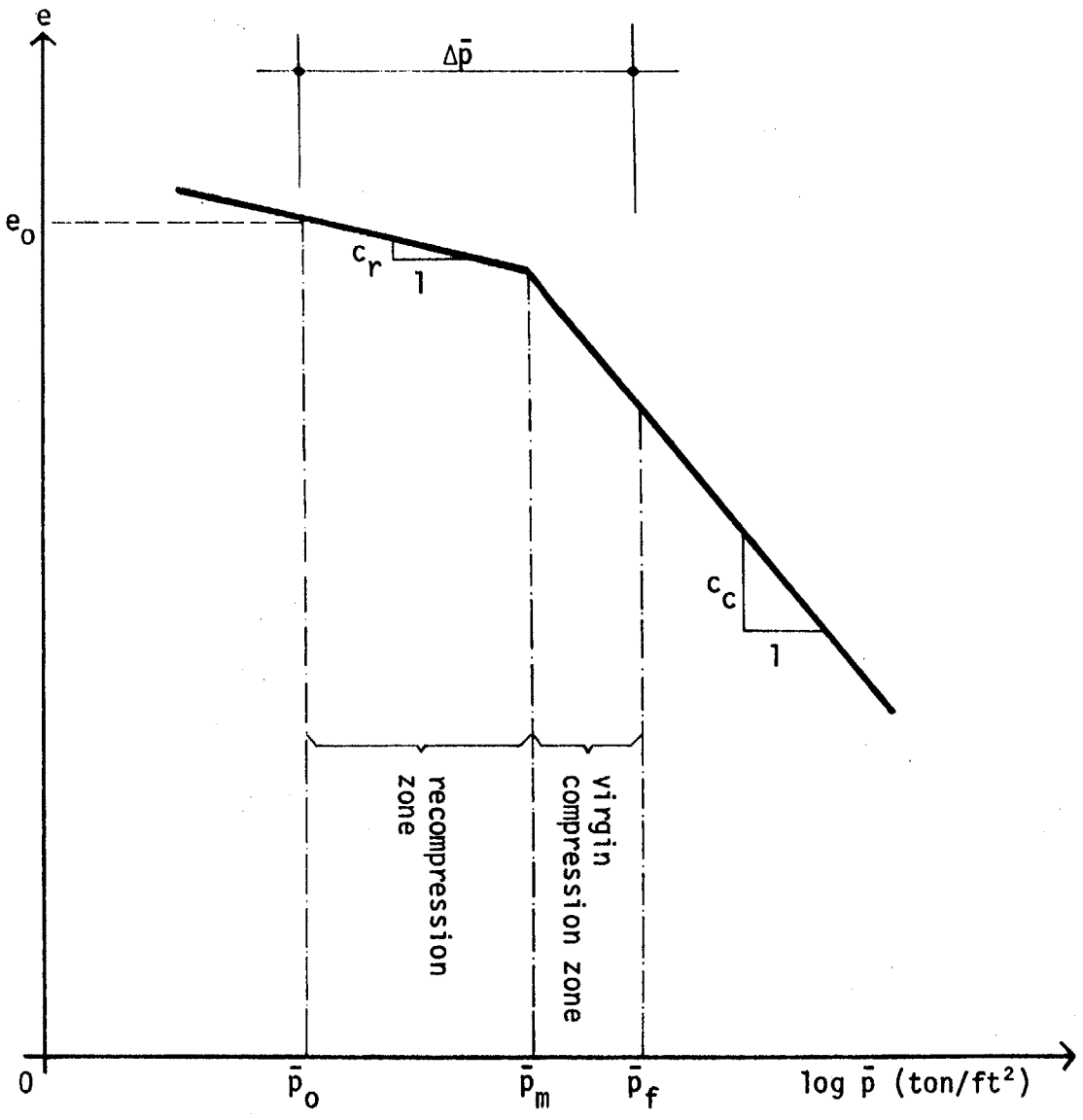


Figure 5.4.2 Idealized e - log $\bar{p}$ Plot for a Cohesive Material

An oversimplified explanation of this phenomenon is that a major part of the deformation of clays is due to the rearrangement of its particles, so that, when the soil is in a recompressed state, an irreversible deformation is already present and therefore stress increments which do not exceed $\bar{p}_m$ do not cause a great deal of additional settlement.

It should be mentioned that most clays are slightly recompressed and exhibit a stress-strain characteristic whose general features are similar to those discussed above. An approximately linear e - log $\bar{p}$ relationship can be used for normally consolidated soils. These exhibit only a virgin compression zone and are, of course, undesirable from the point of view of settlement-related performance.

Once the stress-strain relationship of a material is available, its modulus of volume change or volume compressibility, m_v, can be estimated quite easily. First consider the e - log $\bar{p}$ characteristic which is a straight line (as for a normally consolidated soil). The slope of the line, c, defines a constant relationship between Δe and $\Delta \log \bar{p}$, i.e.,

$$c = - \frac{\Delta e}{\Delta \log \bar{p}} \tag{5.4.1}$$

where

$$\Delta \log \bar{p} = \log \bar{p}_2 - \log \bar{p}_1 = \log \left(\frac{\bar{p}_2}{\bar{p}_1} \right) = 0.435 \ln \left(\frac{\bar{p}_2}{\bar{p}_1} \right)$$

$$\Delta \log \bar{p} \doteq 0.435 \times 2 \left[\frac{\bar{p}_2 - \bar{p}_1}{\bar{p}_2 + \bar{p}_1} + \ldots \right] \doteq \frac{0.87\, \Delta \bar{p}}{\bar{p}_1 + \bar{p}_2} \tag{5.4.2}$$

where $\bar{p}_1$ and $\bar{p}_2$ ($\bar{p}_1 < \bar{p}_2$) are the initial and the final effective stresses, respectively. The volume compressibility m_v represents the soil compressive strain per unit of original thickness due to a unit increase in the vertical pressure. It is measured by the ratio of the change in axial strain to the change in axial stress in a state of confined compression:

$$m_v = \frac{\Delta \varepsilon}{\Delta \bar{p}} = - \frac{1}{(1 + e_o)} \frac{\Delta e}{\Delta \bar{p}} \doteq \frac{0.87\, c}{(1 + e_o)(\bar{p}_1 + \bar{p}_2)} \tag{5.4.3}$$

For most clays, the e - log $\bar{p}$ relationship can be idealized as bilinear with the two straight lines intersecting at the value of $\bar{p}_m$, the maximum past pressure, as shown in Fig. 5.4.2. The recompression and the virgin compression indices c_r and c_c are defined by the slopes of the two lines. The corresponding compressibility parameters m_v' and m_v'' are:

$$\left.\begin{aligned} m_v' &\doteq \frac{0.87\, c_r}{(1 + e_o)(\bar{p}_o + \bar{p}_m)} = \frac{0.87\, rr}{\bar{p}_o + \bar{p}_m} \\ m_v'' &\doteq \frac{0.87\, c_c}{(1 + e_o)(\bar{p}_m + \bar{p}_f)} = \frac{0.87\, cr}{\bar{p}_m + \bar{p}_f} \end{aligned}\right\} \quad \bar{p}_f > \bar{p}_m \tag{5.4.4}$$

in which $rr = cr/(1 + e_o)$, the recompression ratio, and $cr = cc/(1 + e_o)$, the compression ratio.

Clearly, if the load-induced vertical stresses, the overburden stress and the maximum past pressure are assumed to be constant within a sublayer of a compressible stratum, then the compressibility moduli can also be dealt with as constants (see Fig. 5.4.3).

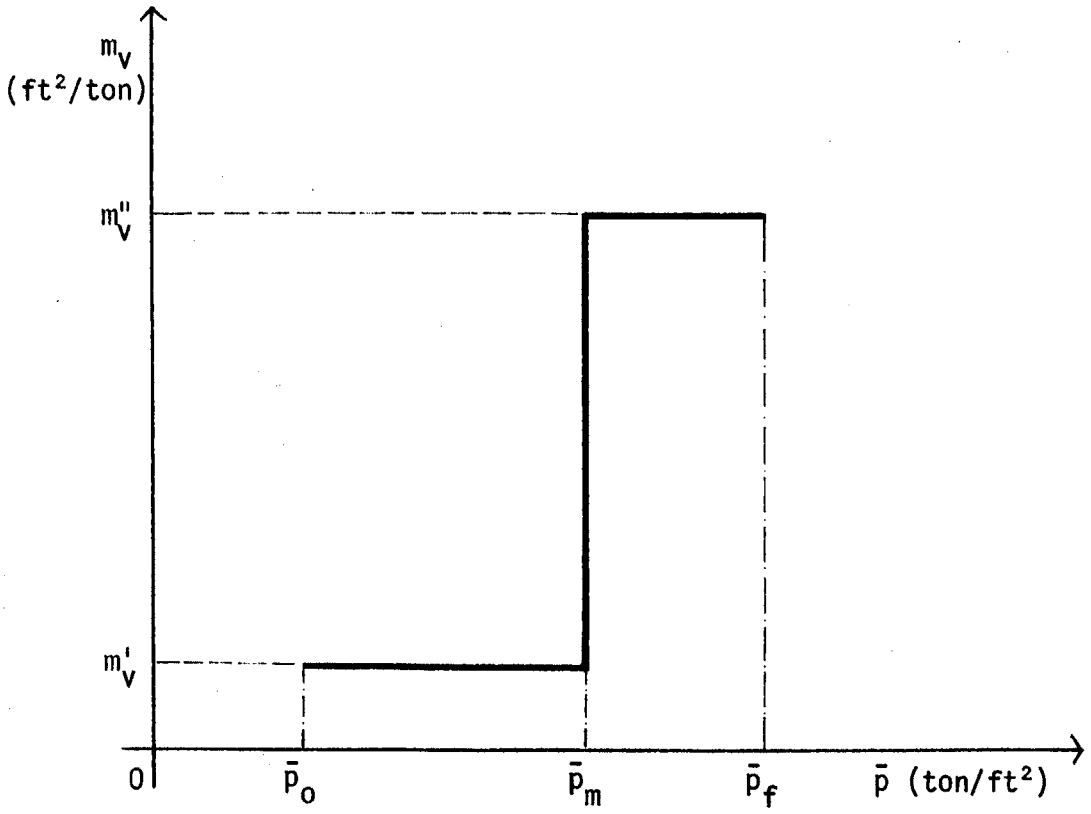


Figure 5.4.3 Compressibility Moduli as Functions of Stress

If the stress increment is not large enough for the final stress to exceed $\bar{p}_m$, only the recompression modulus needs to be defined. In this case,

$$m_v' \doteq \frac{0.87\ rr}{\bar{p}_o + \bar{p}_f} \qquad \bar{p}_f \leq \bar{p}_m \tag{5.4.5}$$

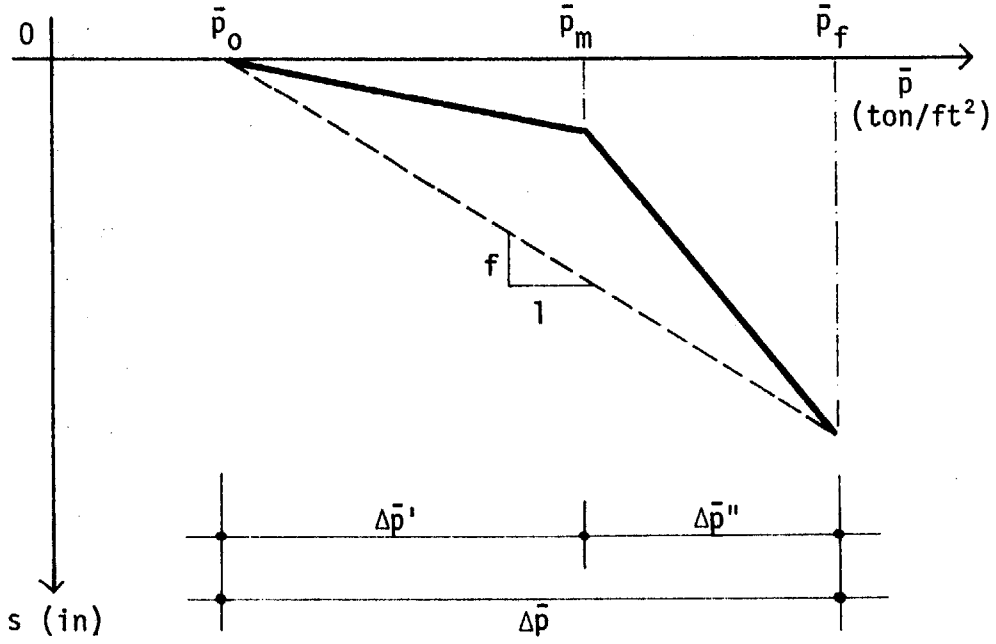


Figure 5.4.4 Idealized Stress-settlement Characteristic for a Cohesive Soil

The pseudo-flexibility, f, may now be defined in terms of the above parameters:

$$f = \frac{h(m_v' \Delta\bar{p}' + m_v'' \Delta\bar{p}'')}{\Delta\bar{p}} \quad , \text{ for } \bar{p}_f > \bar{p}_m \tag{5.4.6}$$

or, $f = h\, m'_v$, for $\bar{p}_f \leq \bar{p}_m$ (5.4.7)

in which h = thickness of the sublayer; the load-induced stresses $\Delta\bar{p}'$ and $\Delta\bar{p}''$ act in the recompression and in the virgin compression zones, respectively. This formulation is equivalent to defining a stress-settlement characteristic as that shown in Fig. 5.4.4.

5.5 Illustrations

In this section, the above-described methodology is applied to the two-bay three-story frame shown in Fig. 5.5.1. The structure under study is a symmetrically loaded and symmetrically supported frame. The foundation consists of a group of isolated footings which are designed for an allowable bearing pressure of 4 ton/ft^2. The corresponding footing dimensions are 10×6 ft^2 for the exterior columns and 10×14 ft^2 for the interior column.

For analysis purposes, the clay stratum is subdivided into 2 ft thick sublayers. The overburden pressure and the maximum past pressure are assumed to vary with depth as shown in Fig. 5.5.2. All the sublayers are assumed to be homogeneous, having equal values of the recompression and the compression ratios (as referred to their mid-depths), rr = 0.02; cr = 0.20.

Settlement preformance may be estimated through the values of an induced maximum differential settlement, δ_{max}, measured from the deformed shape of the foundation after the uniform settlement and the tilt have been removed (16,40). Fig. 5.5.3 illustrates this definition for a continuous foundation and for a three-footing structure

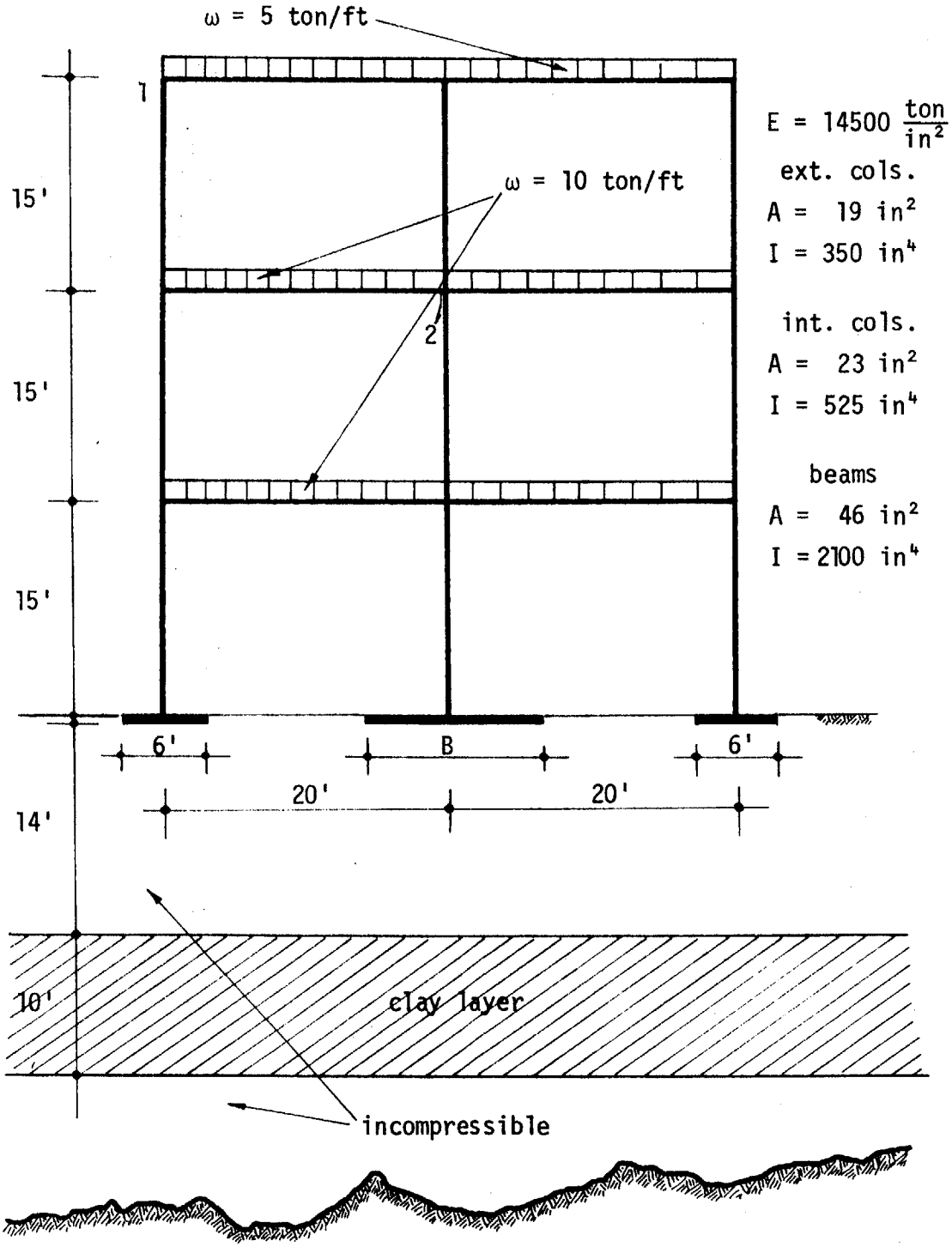


Figure 5.5.1 Example Frame: Spread Footings Foundation

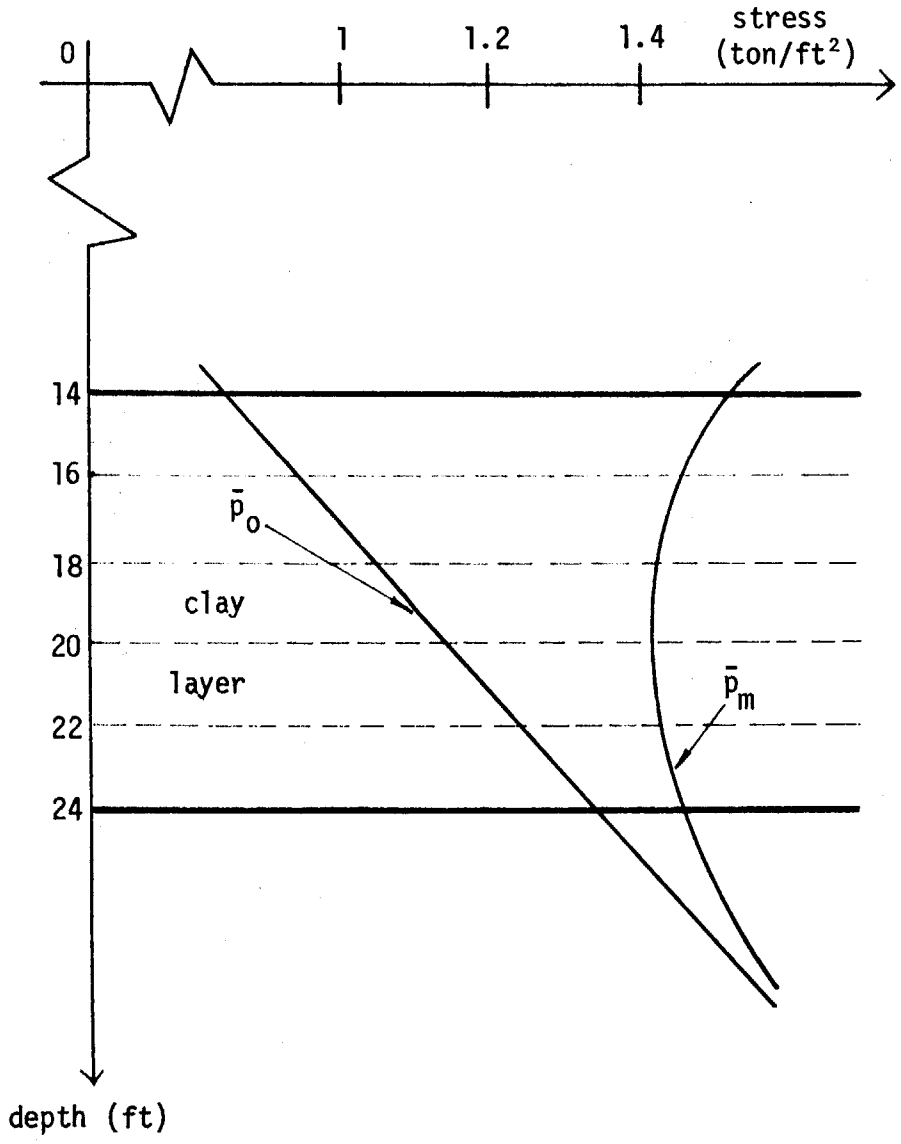


Figure 5.5.2 Variation with Depth of $\bar{p}_o$ and $\bar{p}_m$ for Example Problem

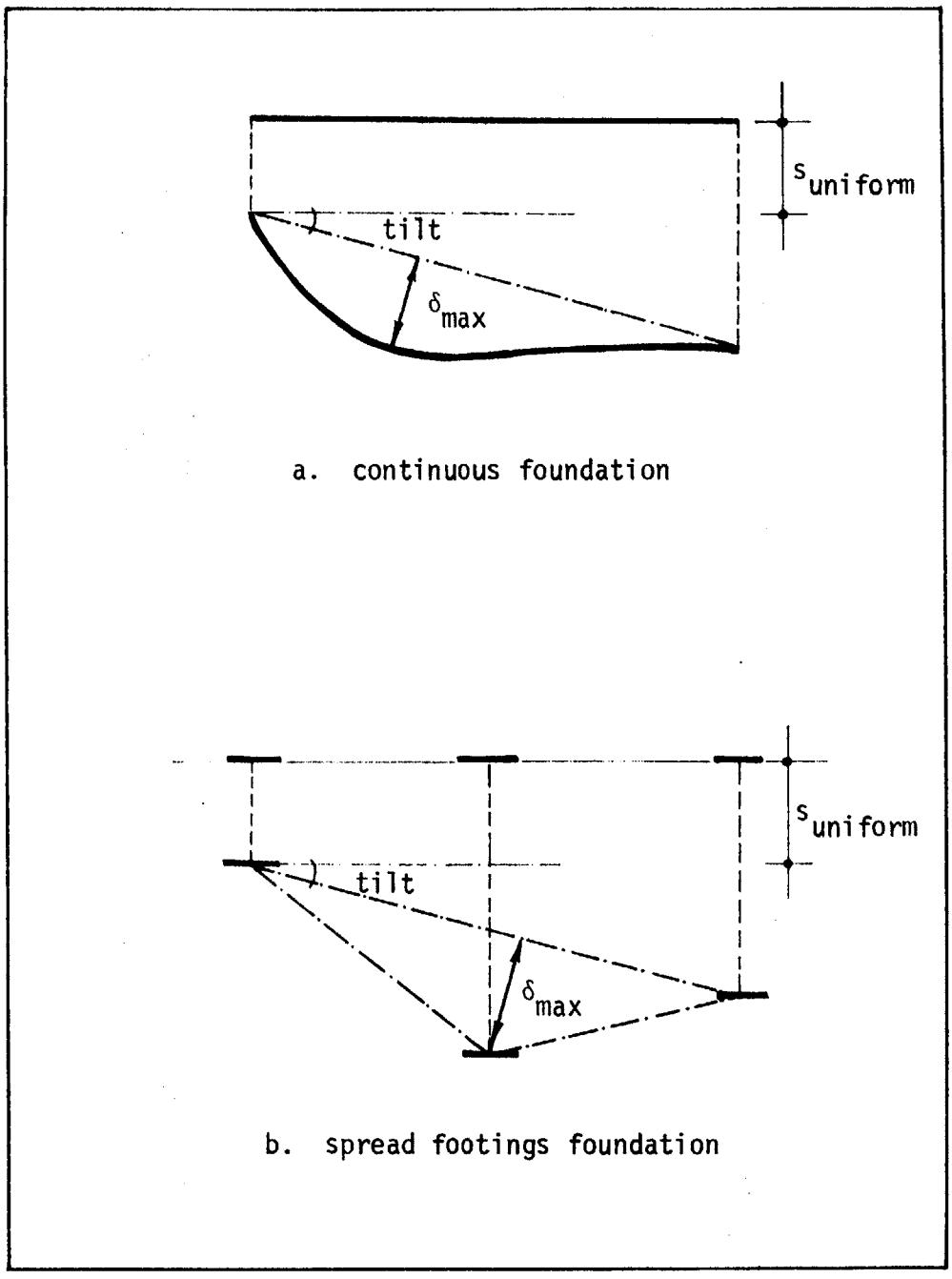


Figure 5.5.3 Definition of the Maximum Differential Settlement δ_{max}

where the middle support settles more than the exterior ones. In a symmetric case, the value of the tilt is zero and therefore, δ_{max} is simply computed as the difference between the total settlements for the central and the exterior support points.

To compare various foundation design alternatives, different analyses were made while varying the interior footing width B. The results are shown in Fig. 5.5.4 which presents the settlements as functions of the dimension B and in Table 5.5.1 where the effect of stiffness is shown.

A common serviceability constraint requires that the maximum net slope $(\delta/\ell)_{max}$ be limited to a value less than or equal to 1/300 (16, 40). For a span length ℓ = 20 ft, this limitation is equivalent to specifying an allowable differential settlement δ_{all} of 0.8". When soil-structure interaction is accounted for, all the alternatives

B (ft)	δ_{max}(in) when neglecting stiffness effect	δ_{max}(in) when including stiffness effect
14	0.96	0.72
16	0.86	0.64
18	0.75	0.58
20	0.65	0.52

Table 5.5.1 δ_{max} Values for Example Frame

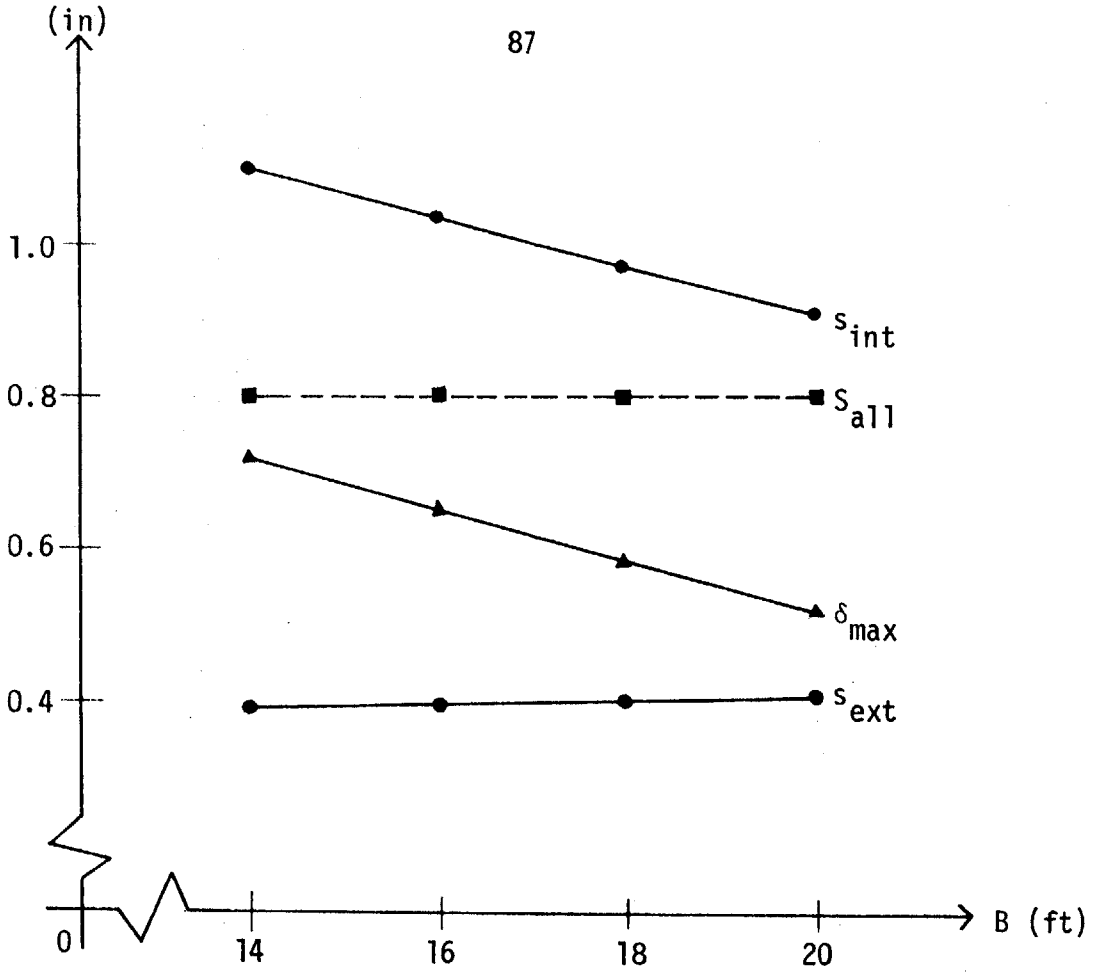


Figure 5.5.4 Settlements as Functions of the Footing Width B Including Stiffness Effect

considered above satisfy this requirement. In this case, the value B = 14 ft appears preferable to other values, because it gives the minimum foundation cost while satisfying the serviceability limitation. If the interaction is neglected, B has to be increased to 18 ft in order to fulfill this constraint.

As an additional example, the foundation for the above structure was changed to a raft 3 ft thick and 10 ft wide (the same width as for the footings in the previous case). The foundation is modeled

by 11 discrete elements as illustrated in Fig. 5.5.5. The values of the settlements under each element are given in Table 5.5.2. Note that in this case, the maximum differential settlement δ_{max} is 0.14".

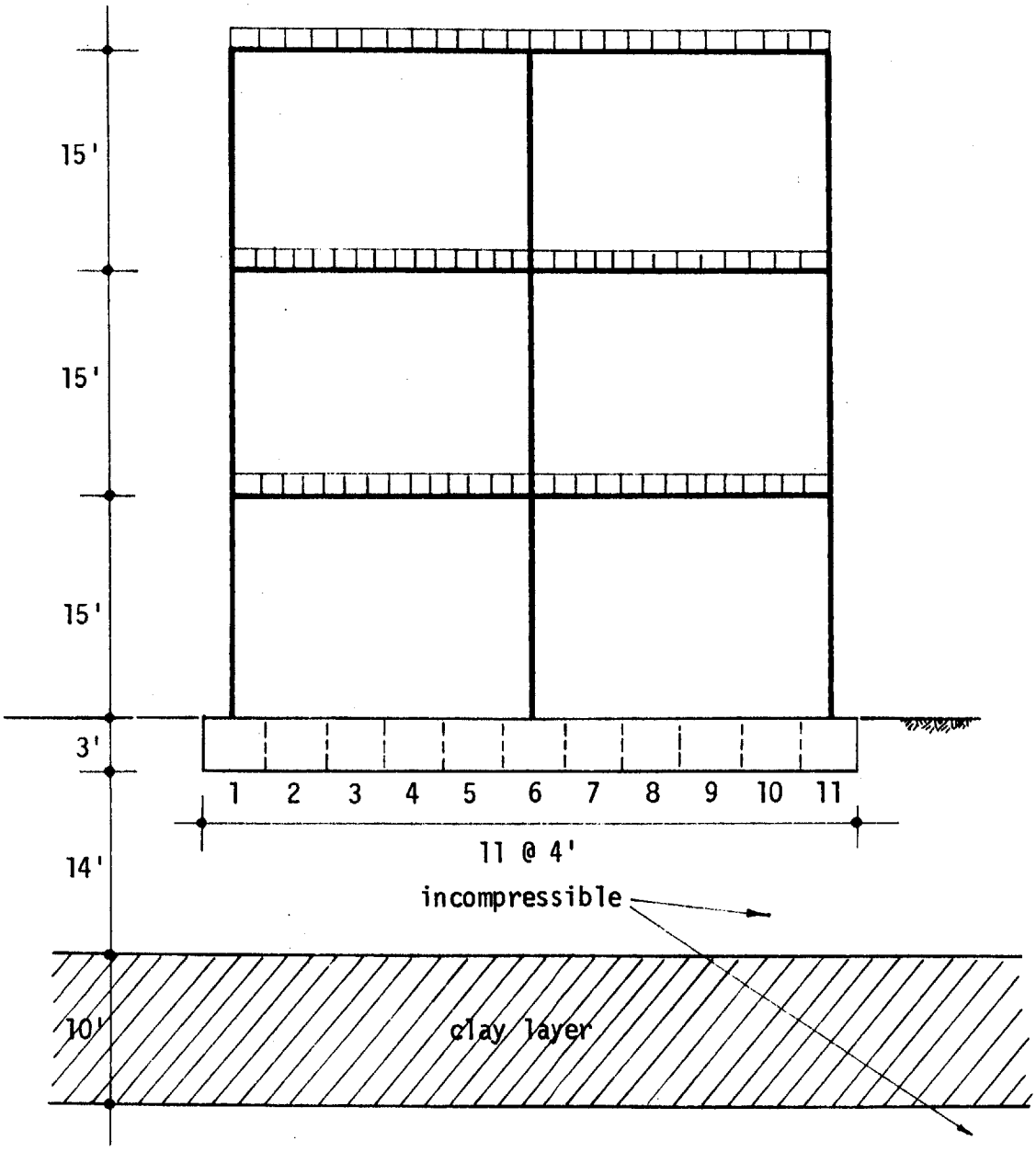


Figure 5.5.5 Example Frame: Raft Foundation

element	1 or 11	2 or 10	3 or 9	4 or 8	5 or 7	6
s_i (in)	0.47	0.52	0.55	0.58	0.61	0.61

Table 5.5.2 Total Settlements for Raft Foundation

CHAPTER 6

THE PREDICTION OF SETTLEMENTS OF STRUCTURES: A PROBABILISTIC MODEL

6.1 Introduction

Thus far, a methodology has been developed for predicting foundation settlements in which the different input and output quantities are deterministic, mostly best estimates or average values. This presents a serious limitation in problems where interest focuses on differential settlements, particularly in problems involving foundations designed to eliminate differences between the estimated settlements. It is not possible, in these cases, to evaluate fully and quantitatively the merits of different foundation design alternatives. Furthermore, engineers have always been aware that the variables involved are not deterministic but random*. As discussed previously, soil properties exhibit a high degree of variability due to various phenomena. Loads are also random and vary not only as functions of space but of time as well. An important consequence of all this is that different foundation systems may have the same average settlement behavior while exhibiting, at the same

---

* Getzler (15), for example, incorporated uncertainty measures in his settlement-prediction method to account for "deviations due to the inhomogeneity of the soil, to unexpected moisture fluctuations, unexpected load distribution or concentration, and other factors not yielding themselves to analytical treatment" by representing the soil properties by the ratios of maximum to minimum values.

time, quite different degrees of scatter about these average values. However, very few attempts have been made to account explicitly or systematically for the uncertainties involved.

There appears to be a need for a settlement-prediction model which permits not only the computation of best estimates of foundation movements but of the uncertainties of these estimates as well. Probability theory is an invaluable tool in extending the deterministic settlement-prediction model presented in the previous chapter into a probabilistic one. However, it is quite impractical to attempt a full probabilistic model at this time. For this to be possible, it would be necessary to know or assume the joint probability distribution of the many random variables entering into the analysis. The approach followed here is a first-order probabilistic analysis in which only the means and the covariance structure of the settlements and the differential settlements are evaluated. In what follows, the probabilistic model is developed and illustrated by a particular application to structures supported on cohesive soils.

6.2 The One-dimensional Settlement Model

In Section 5.2, a one-dimensional model for estimating settlements of structures supported on shallow foundations was given as:

$$s = \sum_{i=1}^{k} f^{(i)} \, \Delta\bar{p}^{(i)} \qquad (6.2.1)$$

In the framework of a probabilistic analysis, all the variables in Eq. 6.2.1 will now be treated as random variables, and are denoted by capital letters:

$$S = \sum_{i=1}^{k} F^{(i)} \, \Delta\bar{P}^{(i)} \tag{6.2.2}$$

in which, S = (random) settlement; $F^{(i)}$ = (random) soil flexibility of the ith compressible sublayer; and $\Delta\bar{P}^{(i)}$ = (random) load-induced vertical stress in the ith sublayer.

Uncertainty in the soil parameters

In the settlement-prediction model formulated in Chapter 5, a measure of the soil compressibility at a certain point within the soil was referred to as the pseudo-flexibility f and defined in terms of the soil properties and the level of stress at the point in question. In a probabilistic model, it becomes important to regard each soil property value used in the analysis as a kind of spatial average rather than a point value (see Chapter 4). In this context, a soil layer is assumed to be made up of a number of sublayers within each of which the soil properties (whose spatial averages are needed in the settlement analysis) vary from point to point in a random but stationary manner. The sublayers will often be the same as those used in solving the deterministic problem but further subdividing may sometimes prove necessary. The spatial averages will be computed for regions within the sublayers and along a number of vertical

lines through the points at which the settlements are to be evaluated (see Fig. 6.2.1).

In the framework of a first-order probabilistic analysis, the soil parameters used in estimating the settlements of a structure supported on n points and founded on top of k compressible sublayers (see Fig. 5.3.3), will be characterized by k diagonal ($n \times n$) matrices of mean values $m^{(a)}_{\langle F \rangle_d}$ (one matrix for each sublayer) and by a $kn \times kn$ covariance matrix $C_{\langle F \rangle}$. Typical elements of these matrices are $E[\langle F \rangle_i^{(a)}]$ and $cov[\langle F \rangle_i^{(a)}, \langle F \rangle_j^{(b)}]$ which represent, respectively, the expected value and the covariance of the spatial averages of the pseudo-flexibilities $\langle F \rangle_i^{(a)}$ and $\langle F \rangle_j^{(b)}$. The elements along the main diagonal of the matrix $C_{\langle F \rangle}$ are the variances $Var[\langle F \rangle_i^{(a)}]$.

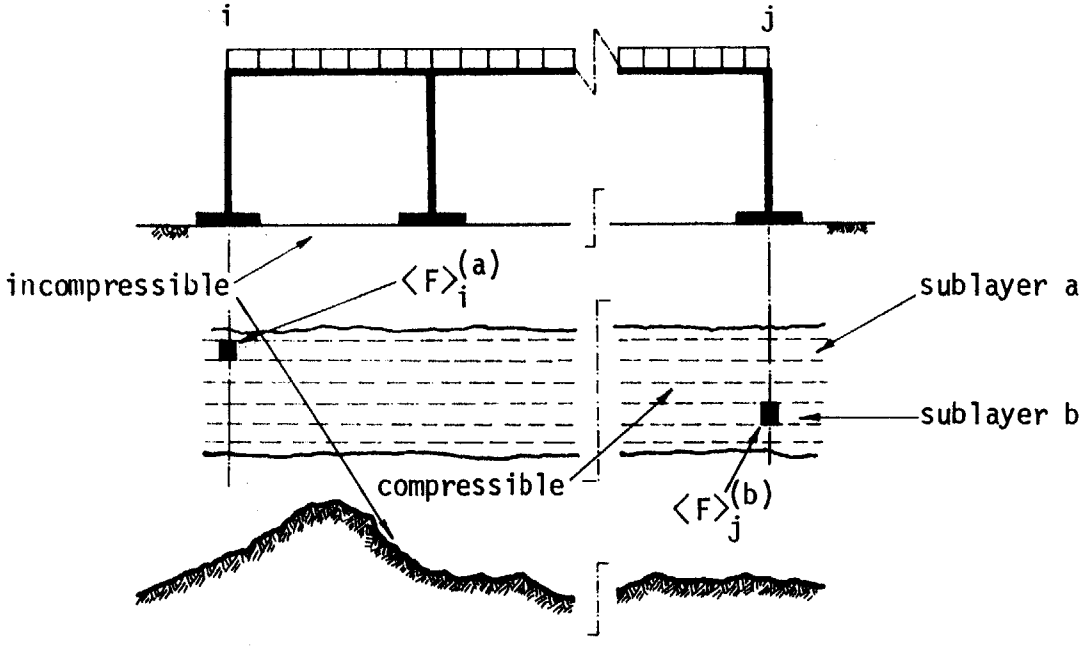


Figure 6.2.1 Spatial Averages of Soil Properties for Settlement Prediction

When using a non-linear stress-settlement characteristic, the parameter F becomes itself a non-linear function of soil and stress variables. Its expected value and its covariances may only be estimated in an approximate way by linearizing the function with a Taylor-series expansion about the mean values of the different variables involved (see Appendix D).

Uncertainty in the loads

It is evident that the loads acting upon a structure are random quantities. Permanent loads exhibit variability due to discrepancies between specified and real member dimensions and due to fluctuations of volumetric weights, but mainly, uncertainty in dead loads is related to the weight of non-structural elements whose final location, composition and weight is unknown in the design stage. Furthermore, live loads vary not only spatially but also temporally. The effects of furniture, personnel, changes of tenants and emergency loadings are obviously impossible to predict with certainty. For all these reasons, probabilistic load models have been proposed (33) and in the last few years the concepts of load variability have been finding their way into structural engineering problems through building codes and safety investigations.

Live loads exhibit more variability than permanent loads. However, when studying the long-time performance of a structure, only a fraction of the live loads (about 1/3) is included in the analysis. Hence, if dead and live loads are assumed to be stochas-

tically independent, the resulting variability of their sum will be of the same order of magnitude as that attributed to the dead loads (with a coefficient of variation of the order of 10%).

In the context of a first-order probabilistic model, the applied loads will be characterized by a size r vector of mean values $\underset{\sim}{m}_L$ and a $r \times r$ covariance matrix C_L. The element (i,j) of the matrix C_L is defined as $cov[L_i,L_j] = \rho_{L_i,L_j} \sigma_{L_i} \sigma_{L_j}$, where ρ_{L_i,L_j} represents the coefficient of correlation* between the ith and the jth loads on the structure, and $\sigma_{L_i} \sigma_{L_j}$ is the product of their standard deviations. For the ith load, the standard deviation σ_{L_i} may be computed as the product of the expected value m_{L_i} and the coefficient of variation V_{L_i}, or simply as the square root of the ith element in the principal diagonal of the matrix C_L.

In terms of the above <u>applied</u> load characteristics, the probabilistic properties of the vertical reactions at the foundation level may be obtained:

$$\underset{\sim}{m}_Q = A \, \underset{\sim}{m}_L \tag{6.2.3}$$

$$C_Q = A \, C_L \, A^T \tag{6.2.4}$$

where, for a structure supported on n points, $\underset{\sim}{m}_Q$ and C_Q represent, respectively, a size n vector of expected values and an $n \times n$ matrix

---

* Autocorrelation functions similar to those proposed in Chapter 3 for soil properties have been used to describe load correlation effects in terms of a "load correlation distance", d_L (18,33).

of covariances for the vertical reactions at the level of the foundation (obtained based on the assumption of rigid supports). The matrix A is a transformation matrix of size $n \times r$ derived in Appendix C . It should be noted that even if the applied loads were assumed as independent random variables, the induced reactions would be correlated by the effect of the A matrix.

6.3 Methodology

The solution to the deterministic soil-structure interaction problem has been obtained in the preceding chapter (Eq. 5.3.5):

$$\underset{\sim}{s} = \{I - \omega T\}^{-1} \omega \underset{\sim}{q} \tag{6.3.1}$$

where,

$$\omega = \sum_{i=1}^{k} f_d^{(i)} \alpha^{(i)} \tag{6.3.2}$$

In a first-order probabilistic approach, the means, variances and correlations of the settlements are obtained by taking a multi-dimensional Taylor-series expansion (Appendix D) of Eq. 6.3.1 about the expected values of all the random variables involved. The results are in the form of a size n vector of mean settlements, $\underset{\sim}{m}_S$, and an $n \times n$ matrix of covariances between settlements, C_S:

$$\underset{\sim}{m}_S \doteq \{I - \Omega T\}^{-1} \Omega \underset{\sim}{m}_Q \tag{6.3.3}$$

$$C_S \doteq \Lambda C_{\langle F \rangle} \Lambda^T + \Theta C_Q \Theta^T \tag{6.3.4}$$

where,

$$\Omega = \sum_{i=1}^{k} m_{\langle F \rangle_d}^{(i)} \alpha^{(i)} \tag{6.3.5}$$

$$\Theta = \{I - \Omega T\}^{-1} \Omega \tag{6.3.6}$$

and Λ is an $n \times kn$ matrix whose elements are the partial derivatives of the settlements with respect to the spatial averages of the pseudo-flexibilities evaluated at the mean values of the random variables. That is,

$$\Lambda_{ij}^{(a)} = \left. \frac{\partial S_i}{\partial \langle F \rangle_j^{(a)}} \right|_{m_{\langle F \rangle_d} \, \underset{\sim}{m}_Q} \tag{6.3.7}$$

In the derivation of Eq. 6.3.4 it is assumed that the loads and the soil parameters are stochastically independent*.

Each <u>column</u> of the matrix Λ may be calculated with the following relationship (35):

$$\underset{\sim}{\Lambda}_i^{(a)} = \left[-\{I - \Omega T\}^{-1} \frac{\partial}{\partial \langle F \rangle_j^{(a)}} [I - \Omega T] \Big|_{m_{\langle F \rangle_d}} \{I - \Omega T\}^{-1} \right] \Omega \, \underset{\sim}{m}_Q + \\ + \{I - \Omega T\}^{-1} \frac{\partial}{\partial \langle F \rangle_j^{(a)}} [\Omega \underset{\sim}{Q}] \Big|_{m_{\langle F \rangle_d} \, \underset{\sim}{m}_Q} \tag{6.3.8}$$

---

* Actually, a cyclic procedure was tested wherein, starting from the flexible case and updating the information after the matrix C_S was known, the covariance matrix of load-induced stresses was calculated and the correlation effects between the loads and the pseudo-flexibilities were included in the analyses. However, these effects proved to be of negligible importance.

in which,

$$\left.\frac{\partial}{\partial \langle F\rangle_j^{(a)}}\,[I - \Omega T]\right|_{m_{\langle F\rangle_d}} \cdot$$

$$= \begin{bmatrix} 0 & \cdots & 0 \\ \vdots & & \vdots \\ -\sum_{\ell=1}^{n} \alpha_{j\ell}^{(a)}\, T_{\ell 1} & -\sum_{\ell=1}^{n} \alpha_{j\ell}^{(a)}\, T_{\ell 2} \cdots -\sum_{\ell=1}^{n} \alpha_{j\ell}^{(a)}\, T_{\ell n} \\ \vdots & & \vdots \\ 0 & \cdots & 0 \end{bmatrix} \qquad (6.3.9)$$

and,

$$\left.\frac{\partial}{\partial \langle F\rangle_j^{(a)}}\,[\Omega \underset{\sim}{Q}]\right|_{m_{\langle F\rangle_d}\, \underset{\sim}{m}_Q} = \begin{bmatrix} 0 \\ \vdots \\ \sum_{\ell=1}^{n} \alpha_{j\ell}^{(a)}\, m_{Q\ell} \\ 0 \\ \vdots \\ 0 \end{bmatrix} \qquad (6.3.10)$$

Note that the solution to a probabilistic settlement-prediction model where the applied loads are treated as deterministic is given by the same equations. It suffices to substitute $\underset{\sim}{Q}$ by $\underset{\sim}{m}_Q$ and to drop the second term in Eq. 6.3.4.

6.4 Model Uncertainty

Geotechnical engineers recognize that the mathematical models employed in representing actual soil behavior will not be exact. For example, in the settlement-prediction model presented above, the load-induced stresses are calculated based on the assumption that the soil is an elastic, homogeneous and isotropic half-space. Also, lateral deformations of the soil are neglected by assuming a one-dimensional strain field. For these and other reasons, a certain variability in the output is expected even for situations with identical and perfectly-known input variables.

This additional source of uncertainty, model uncertainty, may be accounted for, in a crude way, through a multiplicative non-dimensional random term, Φ, in the following manner (5):

$$\underset{\sim}{S} = \Phi\{I - \Omega T\}^{-1} \Omega \underset{\sim}{Q} \qquad (6.4.1)$$

in which Φ represents the ratio of observed to model-predicted output. If the model is "unbiased", then the mean of Φ will be 1, and Eq. 6.3.3 will correctly predict the expected values of the settlements.

Model uncertainty is measured through the variance σ_Φ^2 which

can, in principle, be obtained through direct comparisons between computed and actual settlement data (9), perhaps supplemented by subjective estimation. The covariance matrix C_S now has a third term which reflects the added uncertainty:

$$C_S \doteq \Lambda\, C_{\langle F \rangle}\, \Lambda^T + \Theta\, C_Q\, \Theta^T + \sigma_\Phi^2\, \underset{\sim}{m}_S\, \underset{\sim}{m}_S^T \qquad (6.4.2)$$

6.5 Settlements of Structures on Cohesive Soils

For structures supported on cohesive soils, a pseudo-flexibility parameter was defined in Section 5.4 as a function of the moduli m_v' and m_v''. However, the soil parameters used in the definitions of these moduli (Eq. 5.4.4) show a high degree of variability and can be usefully treated as random variables. Their properties were analyzed in Chapter 3.

Uncertainty in the soil parameters

In Chapter 5, a bilinear stress-settlement characteristic was employed to define the pseudo-flexibility parameter. However, when estimating the variability of F, the bilinear formulation poses a problem because for stresses acting only in the recompression zone, the pseudo-flexibilities have constant values independent of $\bar{P}_m$ and M_v'' (see Eq. 5.4.7). However, since both the maximum past pressure and the load-induced stress increments are actually random variables, a mean value of the final stress acting only in the recompression zone does not rule out the possibility that the true final stress

acts in the virgin compression zone. For this reason, while estimating the covariances of the pseudo-flexibilities, smooth curves are employed to define the stress-settlement relationships. The curve shown in Fig. 6.5.1 approximates the bilinear model and provides a smooth transition from one straight line to the other in the neighborhood of the maximum past pressure. The non-linear relationship used is of the form:

$$s = h\{m''_v\,\Delta\bar{p} + (m'_v - m''_v)(\bar{p}_m - \bar{p}_o)(1 - \exp(-\Delta\bar{p}/(\bar{p}_m - \bar{p}_o)))\} \tag{6.5.1}$$

so that the pseudo-flexibility is given by

$$f = h\{m''_v + \frac{(m'_v - m''_v)(\bar{p}_m - \bar{p}_o)(1 - \exp(-\Delta\bar{p}/(\bar{p}_m - \bar{p}_o)))}{\Delta\bar{p}}\} \tag{6.5.2}$$

when $\Delta\bar{p} \to 0$, Eq. 6.5.2 takes the form:

$$f \to h\{m''_v + \frac{(m'_v - m''_v)(\bar{p}_m - \bar{p}_o)\Delta\bar{p}}{(\bar{p}_m - \bar{p}_o)\Delta\bar{p}}\} = h\,m'_v \tag{6.5.3}$$

and when $\Delta\bar{p} \to \infty$, it becomes:

$$f \to h\,\{\frac{m'_v(\bar{p}_m - \bar{p}_o) + m''_v(\bar{p}_o + \Delta\bar{p} - \bar{p}_m)}{\Delta\bar{p}}\}$$

$$= h\,\{\frac{m'_v\,\Delta\bar{p}' + m''_v\,\Delta\bar{p}''}{\Delta\bar{p}}\} \tag{6.5.4}$$

These are the exact limiting values for the bilinear model.

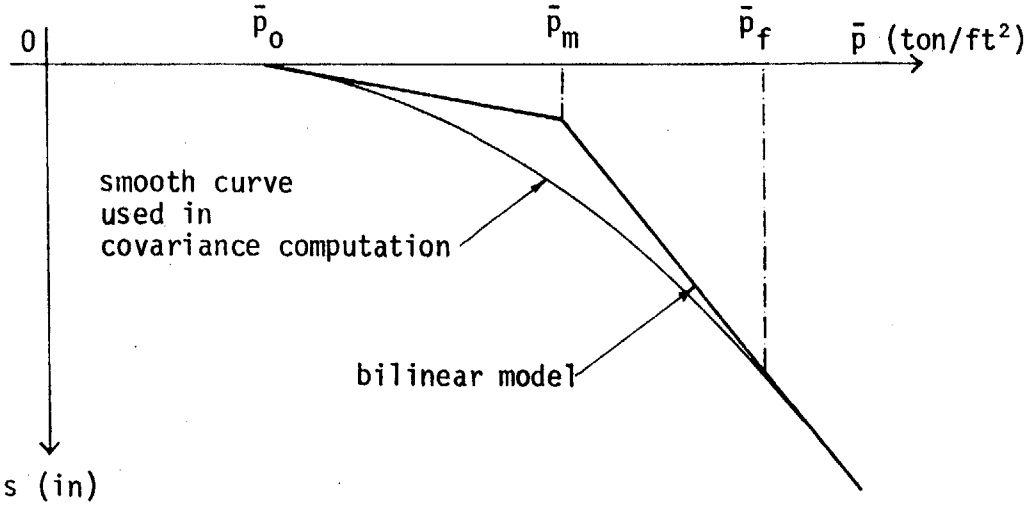


Figure 6.5.1 Stress-settlement Characteristic Employed in Estimating the Matrix $C_{\langle F \rangle}$ for a Cohesive Soil

In this case, the mean value, $E[\langle F \rangle_i^{(a)}]$, of the pseudo-flexibility $\langle F \rangle_i^{(a)}$ of layer a below surface point i, may be approximated by using the relationships derived from the bilinear model with each variable substituted by its expected value:

$$E[\langle F \rangle_i^{(a)}] = E[H_i^{(a)}] \left\{ \frac{E[\langle M_v' \rangle_i^{(a)}]E[\langle \Delta \bar{P}' \rangle_i^{(a)}] + E[\langle M_v'' \rangle_i^{(a)}]E[\langle \Delta \bar{P}'' \rangle_i^{(a)}]}{E[\Delta \bar{P}_i^{(a)}]} \right\}$$

$$, \text{ for } E[\bar{P}_{f_i}^{(a)}] > E[\langle \bar{P}_m \rangle_i^{(a)}] \qquad (6.5.5)$$

$$E[\langle F\rangle_i^{(a)}] = E[H_i^{(a)}]E[\langle M'_v\rangle_i^{(a)}] \quad , \text{ for } E[\bar{P}_{f_i}^{(a)}] \leq E[\langle \bar{P}_m\rangle_i^{(a)}] \tag{6.5.6}$$

The first-order approximation for the covariance, $\text{cov}[\langle F\rangle_i^{(a)}, \langle F\rangle_j^{(b)}]$, takes the following form:

$$\begin{aligned}\text{cov}[\langle F\rangle_i^{(a)}, \langle F\rangle_j^{(b)}] \doteq \\ \doteq A_i^{(a)}A_j^{(b)}\text{cov}[H_i^{(a)},H_j^{(b)}] + B_i^{(a)}B_j^{(b)}\text{cov}[\langle M'_v\rangle_i^{(a)},\langle M'_v\rangle_j^{(b)}] + \\ + C_i^{(a)}C_j^{(b)}\text{cov}[\langle M''_v\rangle_i^{(a)},\langle M''_v\rangle_j^{(b)}] + D_i^{(a)}D_j^{(b)}\text{cov}[\langle \bar{P}_m\rangle_i^{(a)},\langle \bar{P}_m\rangle_j^{(b)}] + \\ + C_i^{(a)}D_j^{(b)}\text{cov}[\langle M''_v\rangle_i^{(a)},\langle \bar{P}_m\rangle_j^{(b)}] + D_i^{(a)}C_j^{(b)}\text{cov}[\langle \bar{P}_m\rangle_i^{(a)},\langle M''_v\rangle_j^{(b)}]\end{aligned} \tag{6.5.7}$$

Exact expressions for the constants $A_i^{(a)}$, $B_i^{(a)}$, etc., and for the covariance and the expected value factors are given in Appendix E.

In deriving Eq. 6.5.7, only the soil parameters RR, CR, $\bar{P}_m$ and H were treated as random variables and they were assumed to be mutually independent. The importance of possible correlation effects between RR and CR was in fact tested by hypothesizing various functional relationships between them of the form*:

---

* Ladd (22) suggests a value of γ between 0.1 and 0.2. The parameters α and β were assumed to vary between 0.3 and 1.0 and between 0.2 and 1.0, respectively (8,46).

$$\left.\begin{aligned} RR &= \gamma CR \\ CR &= \alpha(E_o - \beta)/(1 + E_o) \end{aligned}\right\} \qquad (6.5.8)$$

However, a sensitivity analysis indicated that the effects are negligible and that, for all practical purposes, RR and CR may be treated as independent variables. The variability of the applied stresses also proved to be of only secondary importance in the pseudo-flexibility computations. These were therefore also neglected in the derivation of Eq. 6.5.7.

Sensitivity analysis of the probabilistic model

The number of variables involved in the above probabilistic model is quite large. To understand the relative importance of the various components of uncertainty, a parametric study was performed. The coefficient of variation, $V_.$, and the horizontal correlation distance, $d_{h_.}$, of each random variable were allowed to vary in relation to the reference values given in Table 6.5.1. The structure employed in the analyses is the two-bay, one-story frame illustrated in Fig. 6.5.2. It is assumed that there is only a single cohesive stratum with perfectly correlated soil properties in the vertical direction. It is possible, however, to test the sensitivity of the results to changes in the vertical correlation structure of a particular soil property by replacing its coefficient of variation $V_.$ by the product $V_.\Gamma_.$ in which the parameter $\Gamma_.$ depends on the vertical correlation distance of the soil property being studied.

variable	E[•]	$V_{\cdot}$	$d_{h_{\cdot}}$ * (ft)
$\bar{P}_o$ (ton/ft^2)	0.3	-	-
RR	0.02	0.50	10.0
CR	0.20	0.15	10.0
$\bar{P}_m$ (ton/ft^2)	0.5	0.20	300.0
H (ft)	4.0	0.15	50.0
L_1 & L_2 (ton)	30.0	0.10	10.0
Φ	1	0	-
E_d	0	0	∞
E_t	0	0	0

Table 6.5.1 Values of the Parameters for the Basic Case

* $R(x) = \exp(-x/d_{h_{\cdot}})$

The results are displayed in Figs. 6.5.3 and 6.5.4 for the coefficients of variation and in Fig. 6.5.5 for the horizontal correlation distances. The plots show the coefficient of variation of the maximum differential settlement $V_{\Delta_{max}}$ (see Eq. 6.6.1 and Fig. 6.6.1), as a function of the stiffness of the beams K_1. The value $K_1 = 0$ corresponds to the case of a "perfectly flexible" structure (i.e., soil-structure interaction is not taken into account), and the value $K_1 = 1$ identifies the case shown in Fig. 6.5.2 where

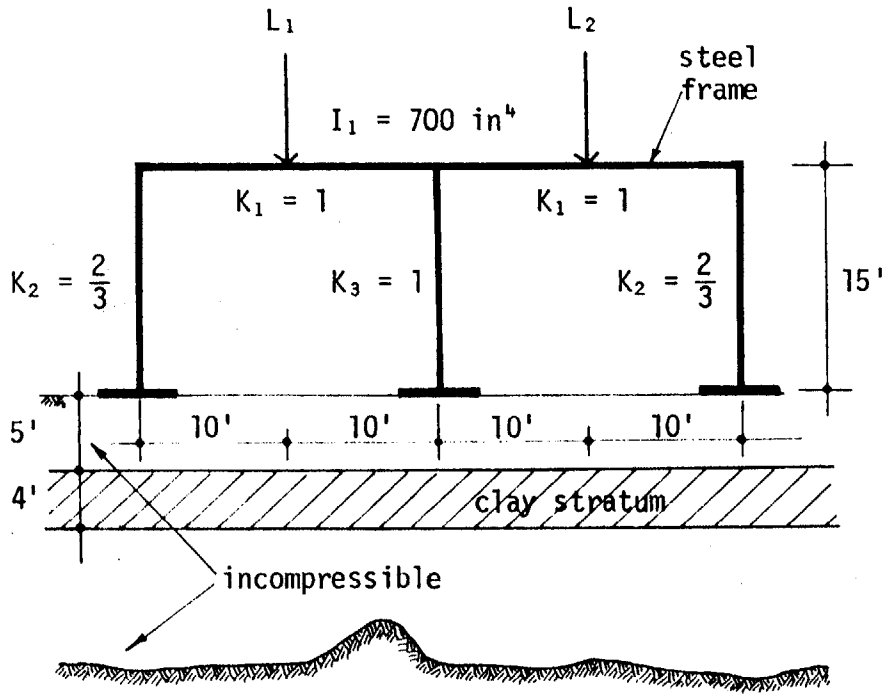


Figure 6.5.2 Two-bay, One-story Frame Employed in the Sensitivity Analysis

the stiffness of the beams is that necessary just to meet strength requirements. The other points, for which $K_1 > 1$, are obtained by increasing the stiffness of the beams while keeping the column stiffnesses constant. If the effect of the superstructure is taken into account, the values of $V_{\Delta_{max}}$ are likely to be much smaller than those obtained for the $K_1 = 0$ case. This means that even though the mean value of Δ_{max} decreases with increasing stiffness of the frame, its standard deviation decreases even more rapidly.

The results show that for soil properties strongly correlated in the vertical direction, the settlement variability is most sensitive

to the uncertainty in the maximum past pressure. The compression ratio and the stratum thickness are of somewhat lesser importance. Recall that in the case study of Chapter 3, it was found that $\bar{P}_m$ has a weak vertical correlation compared to that of CR. If this is the case, the value of the parameter $\Gamma_{\bar{P}_m}$ will not be close to 1. For example, $\Gamma_{\bar{P}_m} = 0.75$ is obtained from Fig. 4.2.1 for h = 4' and $dv_{\bar{P}_m} = 2'$. Therefore, a plot for $V_{\bar{P}_m} = 0.4$ and $dv_{\bar{P}_m} = 2'$ appears just like that corresponding to $V_{\bar{P}_m} = 0.4 \times 0.75 = 0.3$ and $dv_{\bar{P}_m} = \infty$ (see the broken line in Figs. 6.5.3 and 6.5.4). It follows that, accounting for vertical correlation effects, all three variables $\bar{P}_m$, CR, and H may be about equal in importance as regards the sensitivity of $V_{\Delta_{max}}$.

The results appear to be relatively insensitive to the uncertainty in the recompression ratio, RR. Treating this soil property as deterministic will, in general, not result in any appreciable loss of accuracy in the results (in particular if $d_{V_{RR}}$ is small as in the case study of Chapter 3). Finally, the effects due to the variability in the loads also seem to be small. In many cases, this effect will not be of importance when compared to the effects due to the uncertainty in the soil behavior.

When quantifying the effects of varying the horizontal correlation distances, once again the results seem to be most sensitive to the influence of the maximum past pressure $\bar{P}_m$, but the horizontal correlation structure of H may have an important influence as well. Note that these results are independent of the degree of vertical

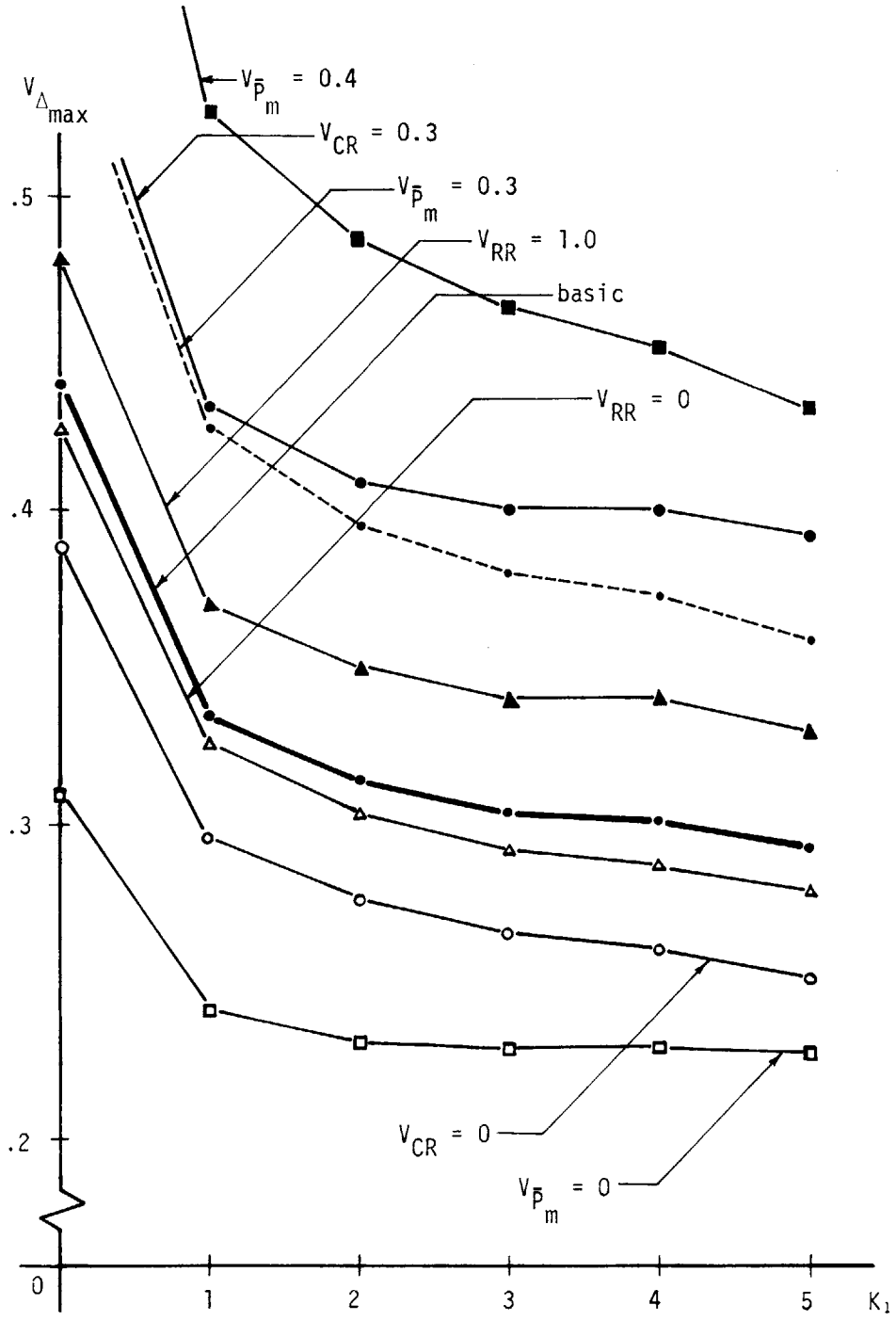


Figure 6.5.3 Coefficients of Variation: RR, CR and $\bar{P}_m$

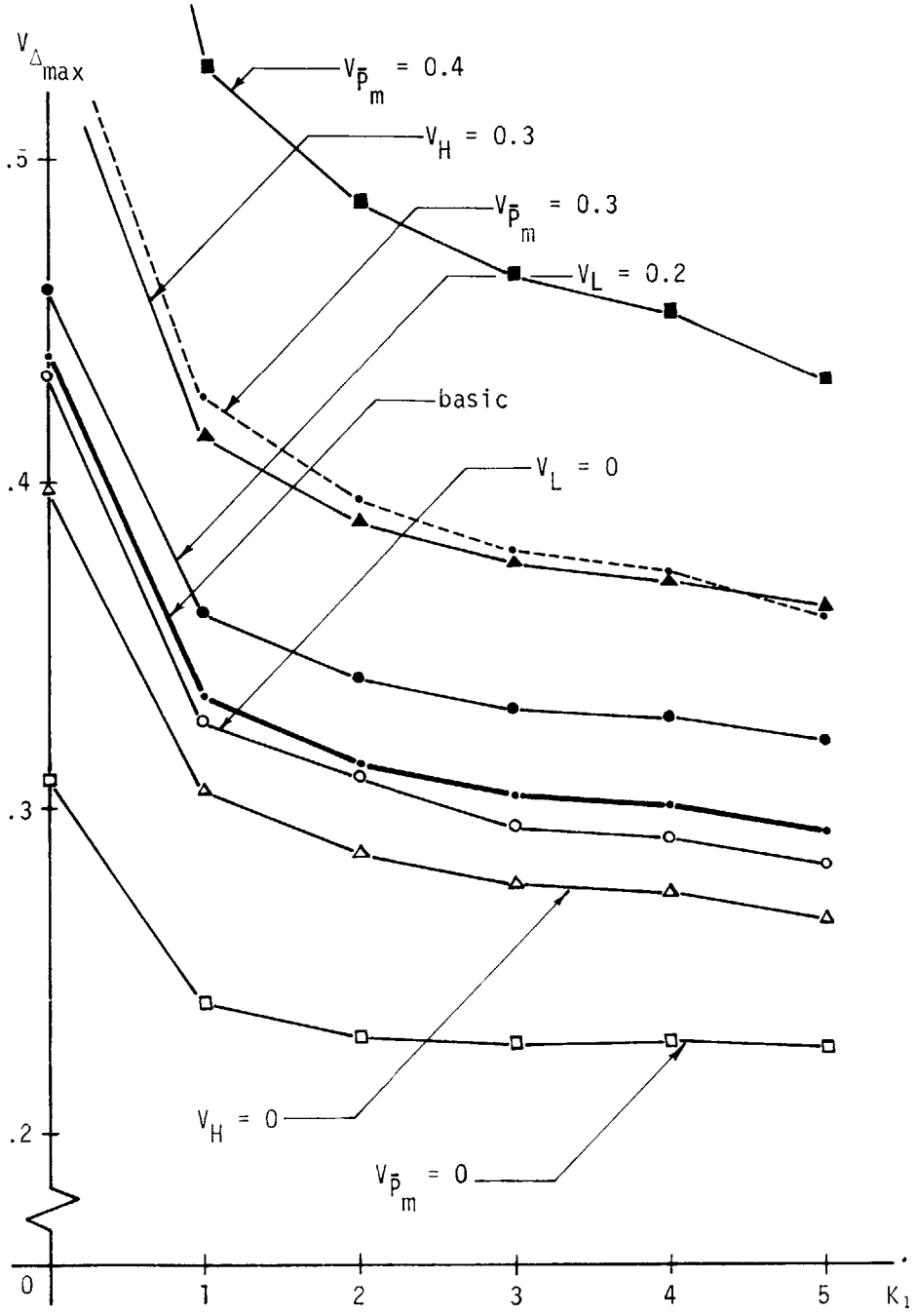


Figure 6.5.4 Coefficients of Variation: $\bar{P}_m$, H and L

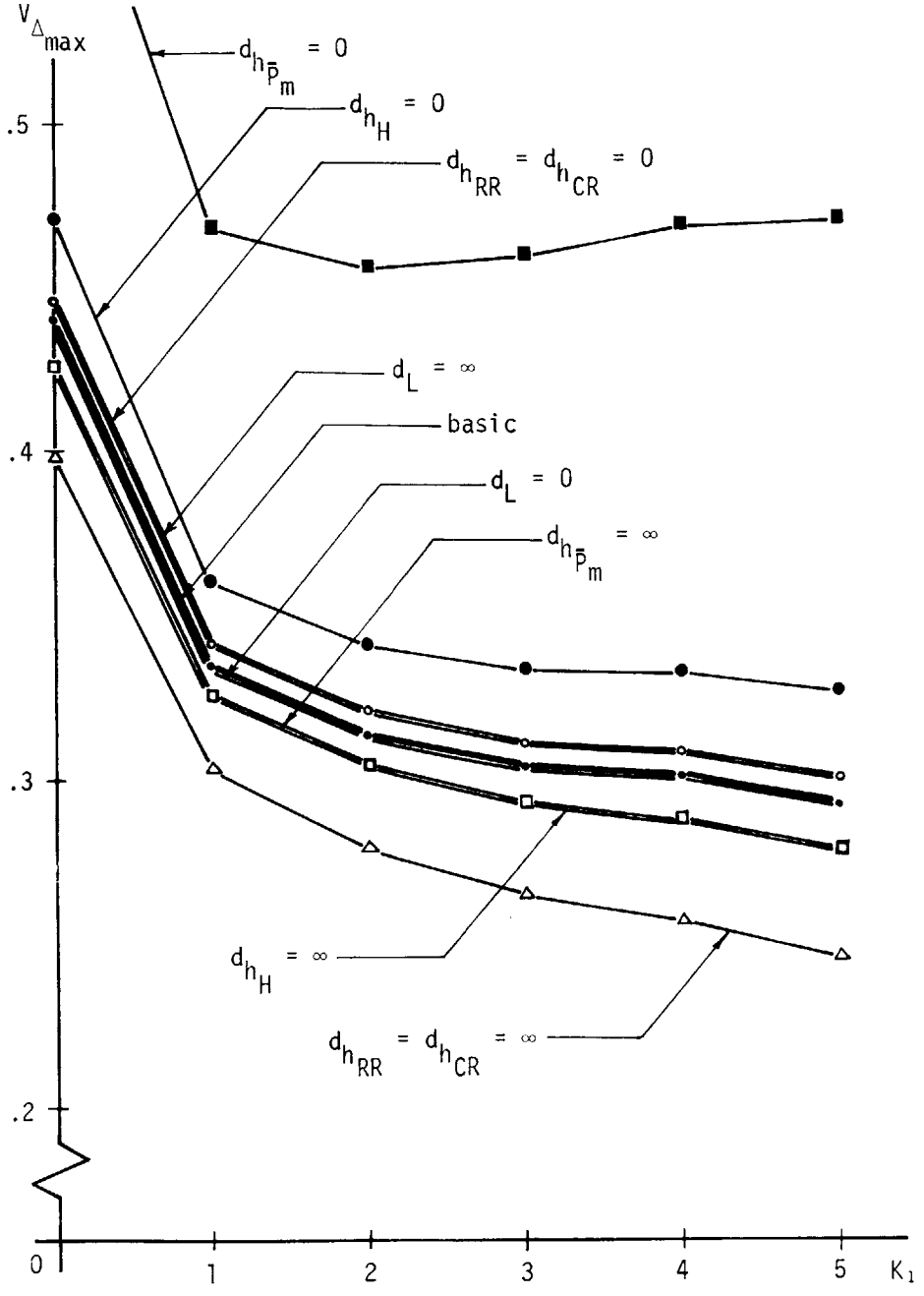


Figure 6.5.5 Horizontal Correlation Distances

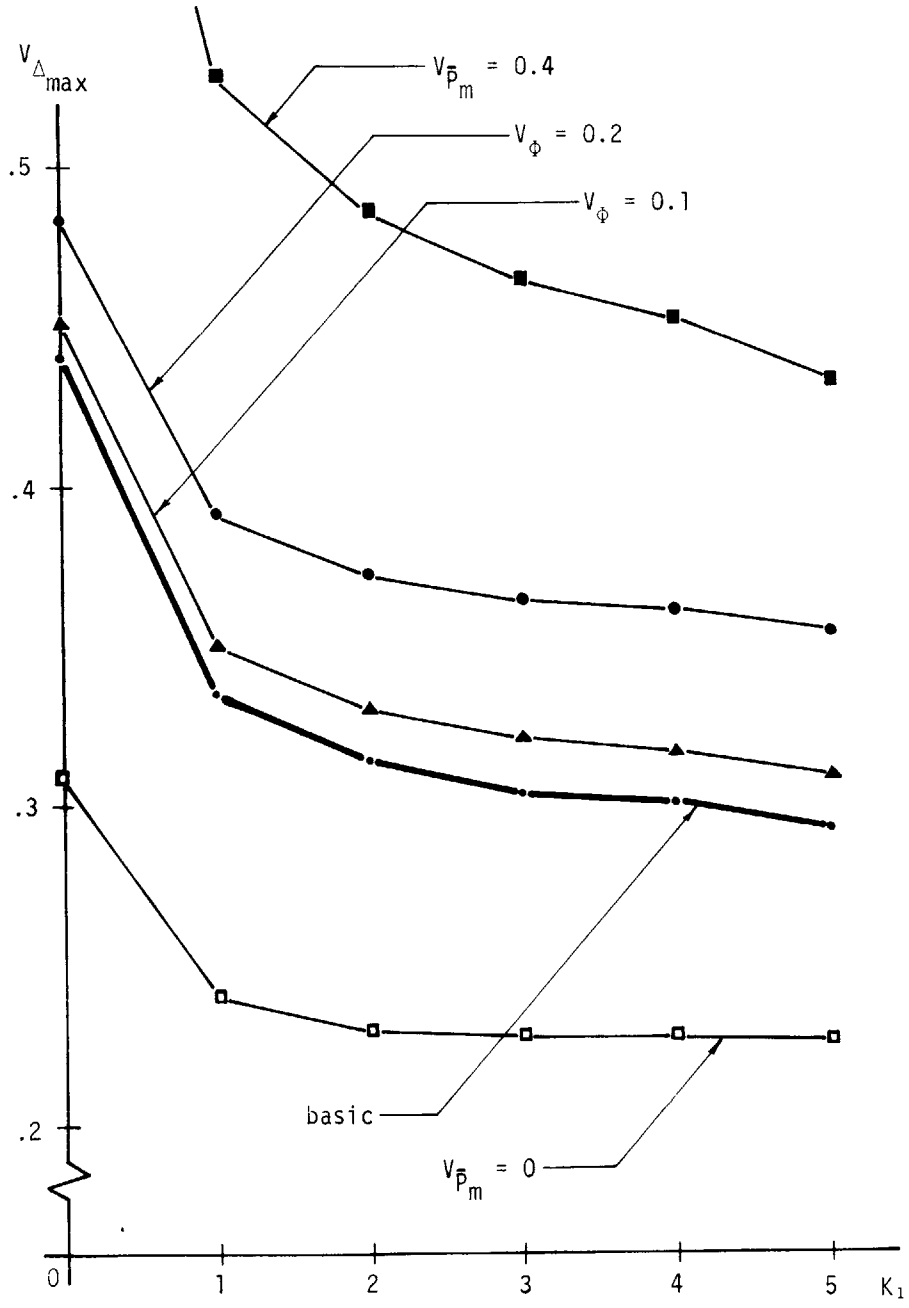


Figure 6.5.6 Model Uncertainty

correlation.

Fig. 6.5.6 shows the sensitivity of the results with respect to the uncertainty in the model. The plots indicate that a coefficient of variation V_Φ as high as 20% still has a small effect on the results compared to the effect of the soil variability. A value of V_Φ of 10% or less may be neglected in the analysis.

6.6 Illustrations

The frame shown in Fig. 5.5.1 for which deterministic analyses were discussed in Chapter 5, is now studied in a probabilistic framework. The recompression and the virgin compression ratios as well as the maximum past pressure are the only variables treated as random. Sampling and testing variabilities, and model uncertainty are not accounted for. Moreover, it is assumed that the soil properties in the compressible sublayers employed in the deterministic problem satisfy the proper stationarity conditions. Their characteristics are shown in Table 6.6.1 and, excepting the mean value of $\bar{P}_m$ (which varies with depth), they are assumed to be equal for all sublayers. The values of the other parameters are the same as those used in the examples in Section 5.5.

In a deterministic context, the serviceability performance of various designs was evaluated by comparing the maximum induced differential settlement, δ_{max}, with a specified allowable value, δ_{all}. Within a probabilistic framework, this maximum differential settlement becomes a random variable denoted by Δ_{max}. With a first-order

random variable	E[·]	$V_{\cdot}$	$d_{h_{\cdot}}^{*}$ (ft)	$d_{v_{\cdot}}^{*}$ (ft)
RR	0.02	0.50	10.0	1.0
CR	0.20	0.15	10.0	10.0
$\bar{P}_m$	†	0.20	300.0	1.0

Table 6.6.1 Values of the Random Soil Parameters for Example Problem

probabilistic model, it is possible to estimate not only the expected value of Δ_{max}, but its variability as well.

Due to the random nature of the problem, even for a symmetrically loaded and symmetrically supported structure, the load-induced tilt may not be zero. In this case, Δ_{max} may be approximately defined for a three-footing structure as illustrated in Fig. 6.6.1:

$$\Delta_{max} = S_2 - \frac{1}{2}(S_1 + S_3) \qquad (6.6.1)$$

where S_2, S_1 and S_3 are the total load-induced random settlements of the interior and the exterior supports, respectively. In most cases, the tilt will be small and thus the error involved in measuring Δ_{max}

---

† See Fig. 5.5.2

* $R_{\cdot}(x,z) = \exp\{-(x/d_{h_{\cdot}} + z/d_{v_{\cdot}})\}$

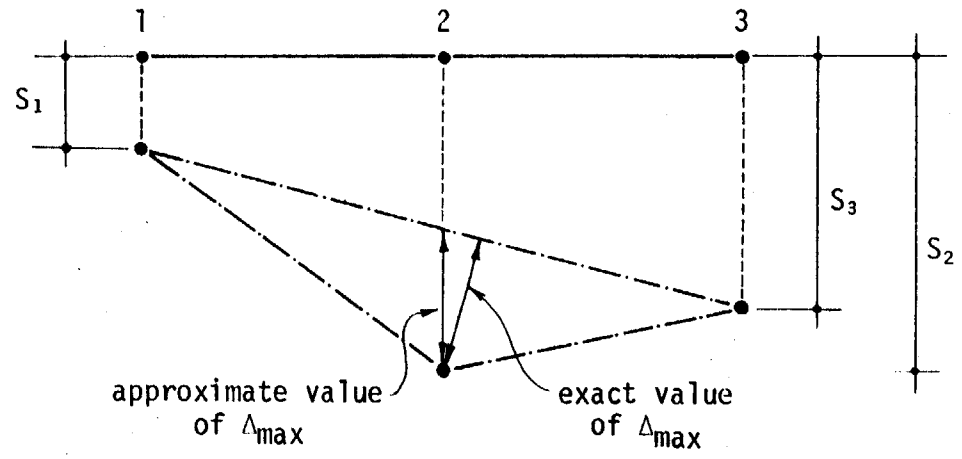


Figure 6.6.1 Definition of Δ_{max}

along a vertical line and not along a perpendicular to the line joining the exterior supports will also be small.

For a continuous foundation it becomes difficult to define exactly the location of the maximum differential settlement (see Fig. 5.5.3a.). However, considering that for a stiff continuous foundation the settlements at various points throughout its length will be strongly correlated, an approximate value of Δ_{max} for the symmetric examples discussed in here may be estimated with the same Eq. 6.6.1.

The mean and the variance of Δ_{max} are obtained in terms of the means, variances and correlation coefficients of the total settlements:

$$E[\Delta_{max}] = E[S_2] - \frac{1}{2}\{E[S_1] + E[S_3]\} \qquad (6.6.2)$$

$$\begin{aligned} Var[\Delta_{max}] = Var[S_2] + \frac{1}{4}\{Var[S_1] + Var[S_3]\} - \\ - \{cov[S_2,S_1] + cov[S_2,S_3]\} + \\ + \frac{1}{2} cov[S_1,S_3] \end{aligned} \qquad (6.6.3)$$

Spread footings foundation

Incorporating stiffness effects, Fig. 5.5.4 shows the average Δ_{max} as a function of the central footing width B. The same type of relationship is now illustrated in Fig. 6.6.2 for the standard deviation of Δ_{max}.

The probabilistic information obtained here will allow comparison of different foundation design alternatives in a more rational way. It permits one to determine approximately the probability of exceedance which corresponds to a given allowable value for the load-induced differential settlement. If Δ_{max} is assumed to be a normally distributed random variable, its mean and standard deviation will completely define its probability distribution. Hence, the probability that Δ_{max} will exceed a certain value δ_{all} is simple to compute. For example, Table 6.6.2 shows the probability that Δ_{max} exceeds 0.8" for different footing sizes. This is the allowable value used in the illustrations in Chapter 5.

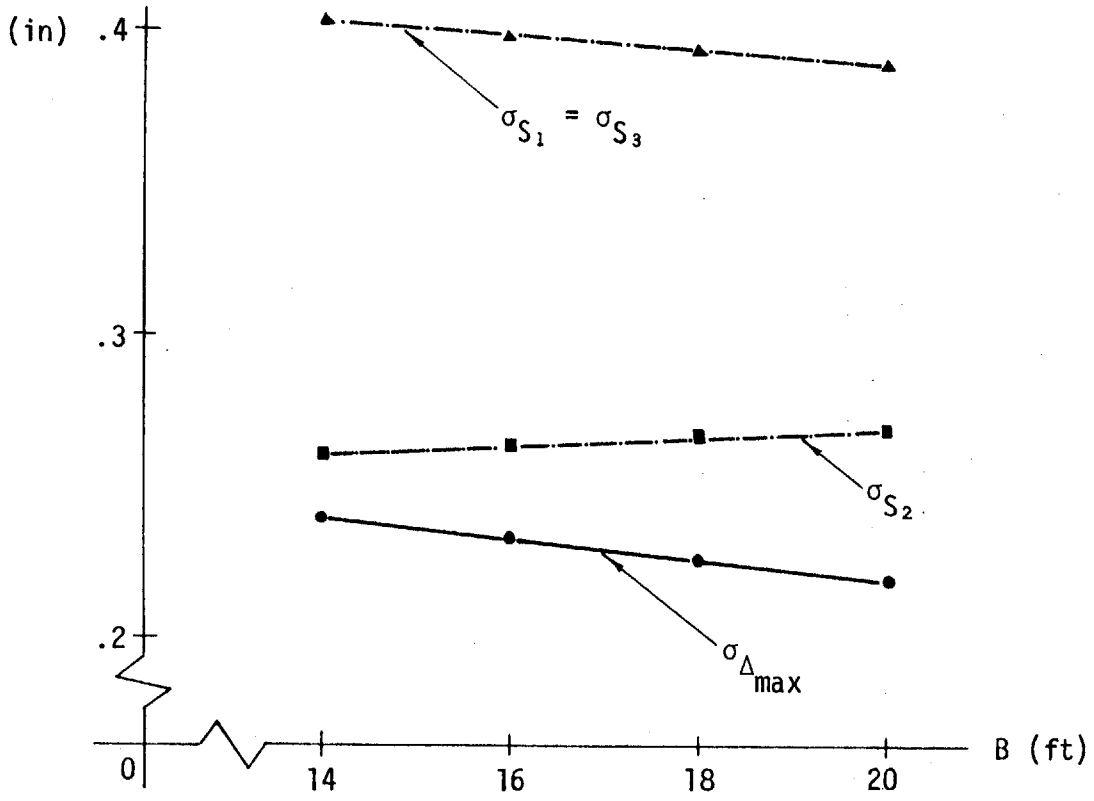


Figure 6.6.2 Standard Deviations of Settlements as Functions of the Footing Width B, Including Stiffness Effect

In Table 6.6.2, as B increases, $m_{\Delta_{max}}$, $\sigma_{\Delta_{max}}$ and $P[\Delta_{max} \geq 0.8"]$ decrease. If soil-structure interaction is neglected in the analysis, both the mean of the differential settlement and its standard deviation constitute upper bounds to their respective true values. Therefore, the value of the probability of exceedance of δ_{all} obtained in this manner is conservative. If the structure remains elastic after the settlements have occurred, the soil-structure interaction methodology described herein may indeed provide accurate values for $m_{\Delta_{max}}$

B (ft)	$E[\Delta_{max}]$ (in)	$\sigma_{\Delta_{max}}$ (in)	$V_{\Delta_{max}}$	$P[\Delta_{max} \geq 0.8"]$
14	0.96*	0.30	0.32	0.70
	0.72	0.24	0.33	0.37
16	0.86*	0.29	0.34	0.58
	0.64	0.23	0.36	0.24
18	0.75*	0.28	0.37	0.43
	0.58	0.23	0.39	0.17
20	0.65*	0.26	0.40	0.28
	0.52	0.22	0.42	0.10

Table 6.6.2 First-order Probabilistic Parameters of Δ_{max}: Spread Footings Foundations

and $\sigma_{\Delta_{max}}$. On the other hand, if stiffness degradation accompanies the deformation of the frame or if creep effects become important, then the computed results will tend to constitute lower bounds. Actual values may be expected to lie between the two limits.

Raft Foundation

Tables 6.6.3 and 6.6.4 show, respectively, the standard deviations and the coefficients of correlation for the total settlements

---

* No interaction effects.

of the (assumed) discrete supports in the raft foundation illustrated in Fig. 5.5.5. Note that the values of the standard deviations are essentially the same for all the support points and that the values of the correlation coefficients are large. In this case, the value of $\sigma_{\Delta_{max}}$ computed from Eq. 6.6.3 is equal to 0.05". This value is much smaller than the ones given in Table 6.6.2 for a number of spread footings foundations.

element	$E[S_.]$ (in)	$\sigma_{S_.}$ (in)	$V_{S_.}$
1 or 11	0.47	0.32	0.68
2 or 10	0.52	0.30	0.58
3 or 9	0.55	0.29	0.52
4 or 8	0.58	0.28	0.47
5 or 7	0.61	0.27	0.45
6	0.61	0.27	0.44

Table 6.6.3 Standard Deviations of Settlements: Raft Foundation

1	2	3	4	5	6	7	8	9	10	11	element
1.00	1.00	0.98	0.96	0.93	0.88	0.83	0.80	0.72	0.66	0.60	1
	1.00	1.00	0.98	0.96	0.92	0.88	0.83	0.78	0.72	0.66	2
		1.00	0.99	0.98	0.95	0.92	0.88	0.83	0.78	0.72	3
			1.00	1.00	0.98	0.96	0.92	0.88	0.83	0.78	4
				1.00	1.00	0.98	0.96	0.92	0.88	0.83	5
					1.00	1.00	0.98	0.95	0.92	0.88	6
						1.00	1.00	0.98	0.96	0.93	7
							1.00	0.99	0.98	0.96	8
								1.00	1.00	0.98	9
									1.00	1.00	10
										1.00	11

Table 6.6.4 Settlement Correlation Matrix:
Raft Foundation

CHAPTER 7

SOME DECISION PROBLEMS IN SETTLEMENT-CONTROLLED DESIGN

7.1 Introduction

The methodology developed in the preceding chapter allows the estimation of first-order probabilistic information about the settlements of a structure. With it, it becomes possible to make rational comparisons among a number of alternate designs in order to select "the best" one. One way of doing the optimization is to calculate the total expected costs (TEC) for various foundation alternatives and to select the alternative which yields the minimum value. The cost components include the initial cost of the foundation, C_o, the cost of obtaining new or additional information about the soil properties, C_i, and the future "cost of damage" (the cost of damage, C_d, times the probability of damage, p_d).

In a simple approach to the problem, the probability p_d may be defined as the probability that the maximum differential settlement, Δ_{max}, exceeds a prescribed allowable value δ_{all}. This parameter may arise from a code-like serviceability constraint which limits, for example, the maximum net slope $(\Delta/\ell)_{max}$. The cost C_d may reflect some simple utility function as discussed by Rosenblueth (37) and Folayan et al. (13).

On a more sophisticated level, if probabilistic information about structural member deformations and about related damage and costs are

available, then the expected cost of damage may be calculated by weighting various levels of settlement-induced costs by their probabilities of occurrence.

Another problem which is dealt with in this chapter is that of updating information and of improving reliability estimates through additional sampling of soil properties.

7.2 Cost Minimization Problem

Fig. 7.2.1 illustrates how the foundation design problem may be cast in a cost minimization format. The example used here is the same as that presented in Section 6.6 with p_d defined as the probability that Δ_{max} exceeds 0.8" (see Table 6.6.2). As the footing width B increases, the expected cost of damage decreases. At the same time, the initial cost of the foundation increases. For a fixed amount of sampling, the "optimum" solution may be obtained by minimizing the expression:

$$\min(TEC) = C_o + p_d C_d \qquad (7.2.1)$$

As an example, assume that $C_o = [20 + 2.5(B - 14)^2]\beta$ and $C_d = 200\beta$, where β is some constant. The solution is obtained graphically in Fig. 7.2.1. Only footing widths between 14 ft and 20 ft have been considered. The optimum footing size is approximately B = 15 ft if soil-structure interaction is included, and B = 17 ft if it is not (i.e., in the flexible case).

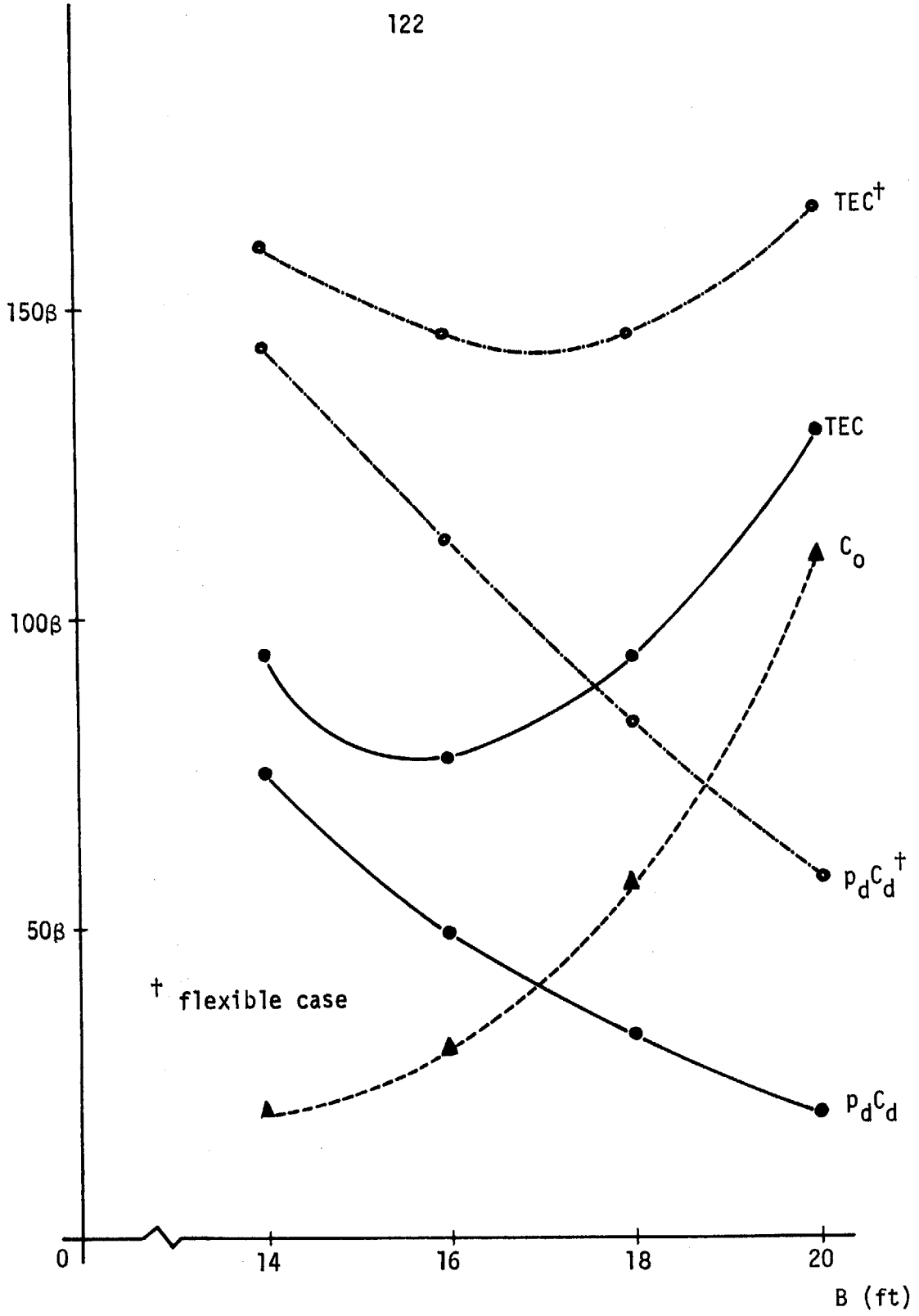


Figure 7.2.1 Footing Optimization Problem: Fixed Amount of Sampling

7.3 The Uncertainty of Settlement-induced Displacements and Forces

Given that first-order probabilistic information about the settlements of a structure is available, it is possible to calculate means, variances and correlations of settlement-induced displacements and forces.

Referring to Eq. C.1 in Appendix C, the expected (free) joint displacements induced by the vertical movements of the supports may be computed as follows:

$$\underset{\sim}{m}_{D_1} = -K_{11}^{-1} B^* \underset{\sim}{m}_S \tag{7.3.1}$$

where $\underset{\sim}{m}_{D_1}$ = size r vector of mean (free) joint displacements; K_{11}^{-1} = $r \times r$ inverse matrix of the partition K_{11} of the stiffness matrix of the structure; B^* = $r \times n$ transformation matrix; and $\underset{\sim}{m}_S$ = size n vector of mean settlements. The columns of the matrix B^* are equal to the columns of the partition K_{12} which correspond to the degrees of freedom of the vertical support displacements.

The relationship between all the mean joint displacements and the expected settlements is:

$$\underset{\sim}{m}_D = B \underset{\sim}{m}_S \tag{7.3.2}$$

where $\underset{\sim}{m}_D$ = size j vector of mean displacements. The matrix B is given by,

$$\underset{(j \times n)}{B} = \begin{bmatrix} -K_{11}^{-1} B^* \\ \hline J \end{bmatrix} \tag{7.3.3}$$

If the prescribed support displacements are ranked last among the elements of the vector $\underset{\sim}{d}_2$ (see Appendix C), then the upper part of the matrix J becomes a null matrix of size $\frac{2}{3}(j - r)$ and the lower part is a size $\frac{1}{3}(j - r)$ identity matrix.

Once the matrix B is known, the $j \times j$ displacement covariance matrix C_D may be obtained as a function of the $n \times n$ settlement covariance matrix C_S:

$$C_D = B\ C_S\ B^T \tag{7.3.4}$$

To obtain probabilistic information about the forces in the members, vectors of expected displacements $\underset{\sim}{m}_D^*$ and covariance matrices of displacements C_D^* (in general of size 6 and 6×6, respectively) may be assembled for each member from the vector $\underset{\sim}{m}_D$ and the matrix C_D. If k^* defines a 6×6 member stiffness matrix, the vector of mean member forces, $\underset{\sim}{m}_F^*$, and the covariance matrix of member forces, C_F^*, will be given by:

$$\underset{\sim}{m}_F^* = k^*\ \underset{\sim}{m}_D^* \tag{7.3.5}$$

$$C_F^* = k^*\ C_D^*\ k^{*T} \tag{7.3.6}$$

As an illustration, the above described methodology was applied to the frame shown in Fig. 5.5.1 and discussed in Section 6.6. Different analyses were done for different widths of the interior footing. Some typical results are shown in Tables 7.3.1 and 7.3.2 for the rotation Θ of an exterior joint of the frame (joint 1 in

Fig. 5.5.1) and the bending moment M in one of the beams (section 2 in Fig. 5.5.1), respectively.

The effects of increasing the central footing width, B, are evident. As B increases, the expected values of the joint displacements and forces as well as their standard deviations decrease. It should be noted that the coefficients of variation are large and of the same order as those of the corresponding maximum differential settlements (see Table 6.6.2).

B (ft)	$E[\Theta]$ $\times 10^{-2}$	σ_Θ $\times 10^{-2}$	V_Θ
14	0.405*	0.133	0.329
	0.301	0.108	0.358
16	0.362*	0.128	0.353
	0.271	0.105	0.389
18	0.317*	0.122	0.385
	0.242	0.103	0.423
20	0.272*	0.116	0.428
	0.218	0.099	0.456

Table 7.3.1 Coefficients of Variation for the Rotation of a Joint

* No interaction effects.

B (ft)	E[M] (ton in)	σ_M (ton in)	V_M
14	1939.7*	614.6	0.317
	1442.1	481.8	0.334
16	1734.1*	586.3	0.338
	1299.4	469.1	0.361
18	1520.9*	557.0	0.366
	1160.6	454.6	0.392
20	1303.6*	527.5	0.405
	1045.8	437.3	0.418

Table 7.3.2 Coefficients of Variation for the Bending Moment in a Beam

7.4 Updating Information about Soil Properties Through Further Exploration

In probabilistic subsurface modeling, actual profiles are idealized as a number of (statistically) homogeneous volumes, and the theory of stochastic processes is used to represent the soil properties. In each homogeneous soil volume (or layer, in this case)

* No interaction effects

a "global" mean, m_U, a "global" variance, σ_U^2, and an autocorrelation function are estimated for each soil property U from available geological and local boring data. For all points where no sample has been taken, it is assumed that the "local" and the global estimates of the parameters will coincide. However, these estimates will be equal only if the values of U are independent from point to point in the layer. In the context of spatial averages, the relationships derived in Chapter 4 are valid only if the independence condition really holds and if the sampling is done outside the region over which the average is taken, or if the sampled points are sufficiently far away from the region (such that the correlation effects become negligible).

In general, after a soil volume is sampled, the local estimates of the parameters at non-sampled points will be influenced by the results of the sampling. The degree of influence will depend on the degree of correlation between the soil properties. As mentioned above, if there is no correlation, the effect will be nill. On the other extreme, if the soil properties are perfectly correlated and no sampling or testing errors are present, just one sample will be sufficient to describe the layer completely. The local estimates of the parameters may therefore be interpreted as conditional on the observations.

In the case of a linear* prediction model and a single error-

---

* A model of the form: $U_\ell = \alpha + \beta_k \, u_k$

free measurement u_k, the conditional mean and variance of the soil properties at a point ℓ, $m_{U_\ell|u_k}$ and $\sigma^2_{U_\ell|u_k}$, will be given by (34):

$$m_{U_\ell|u_k} = m_U + \rho_{U_k,U_\ell} (u_k - m_U) \tag{7.4.1}$$

$$\sigma^2_{U_\ell|u_k} = (1 - \rho^2_{U_k,U_\ell}) \sigma^2_U \tag{7.4.2}$$

in which ρ_{U_k,U_ℓ} is the correlation coefficient (prior to the sampling) of the property U between the points k and ℓ.

For the general case, if there are n_t points (or rather, elementary volumes) in the region and n_s of these are sampled, the new mean value vector, $\underset{\sim}{m}_{U|u}$, and the new covariance matrix, $C_{U|u}$, for the n_t points <u>after</u> the sampling (the posterior local parameters of the soil properties) may be calculated as follows (6 ,34):

$$\underset{\sim}{m}_{U|u} = \underset{\sim}{m}_U + C_U \, \xi^T \, (C^*_u + C_\varepsilon)^{-1} (\underset{\sim}{u} - \xi \underset{\sim}{m}_U) \tag{7.4.3}$$

$$C_{U|u} = C_U - C_U \, \xi^T \, (C^*_u + C_\varepsilon)^{-1} \, \xi \, C_U \tag{7.4.4}$$

where C_U and C^*_u are prior covariance matrices of the property U for n_t and n_s points, respectively, and the matrix C_ε is the covariance matrix due to the error terms. In the context of the discussion presented in Section 3.4:

$$C_{\underset{(n_s \times n_s)}{\varepsilon}} = \begin{bmatrix} \sigma^2_{E_d} + \sigma^2_{E_t} & \sigma^2_{E_d} & \cdots & \sigma^2_{E_d} \\ \sigma^2_{E_d} & \ddots & & \vdots \\ \vdots & & \ddots & \sigma^2_{E_d} \\ \sigma^2_{E_d} & \cdots & \sigma^2_{E_d} & \sigma^2_{E_d} + \sigma^2_{E_t} \end{bmatrix} \qquad (7.4.5)$$

The vector $\underset{\sim}{u}$ represents the n_s values corrected for bias (if any). If the n_t points are labeled in such a way that the n_s sampled points rank last, then ξ will be a rather simple $n_s \times n_t$ matrix:

$$\xi = [N \,\vdots\, I] \qquad (7.4.6)$$

in which N is a $(n_t - n_s) \times n_s$ null matrix and I is an $n_s \times n_s$ identity matrix.

It is interesting to recognize that if disturbance and testing errors are not taken into account, then:

$$C_U \, \xi^T \, C^{*-1}_u = \begin{bmatrix} A \\ \hline I \end{bmatrix} \qquad (7.4.7)$$

where I is an identity matrix and A is a matrix of "kriging" coefficients (1,10).

In the framework of spatial averages, the new, conditional parameters (which may vary from point to point in the region over

which the spatial average is taken) will substitute the corresponding global estimates. Following the above discussion, if n' of the n_s observations are made inside a region which contains a total of n* points, the spatial average of the property U may be written as:

$$U = \frac{1}{n^*}\left\{\sum_{k=1}^{n^*-n'} U_k + \sum_{\ell=1}^{n'} u_\ell\right\} \tag{7.4.8}$$

in which U_k is the unknown value of the property U at point k in the soil and u_ℓ is the measurement of the soil property at point ℓ.

The mean and the variance of the spatial average $\langle U \rangle$ may be obtained using the expressions given in Appendix A:

$$E[\langle U \rangle] = \frac{1}{n^*}\left[\sum_{k=1}^{n^*-n'} m_{U_k|u} + \sum_{\ell=1}^{n'} u_\ell\right] \tag{7.4.9}$$

$$\mathrm{Var}[\langle U \rangle] = \frac{1}{(n^*)^2}\left\{\sum_{k=1}^{n^*-n'} \mathrm{Var}[U_k|u] + n'(\sigma^2_{E_d} + \sigma^2_{E_t})\right\} + \frac{2}{(n^*)^2}\left\{\sum_{k=1}^{n^*-n'-1}\ \sum_{\ell=k+1}^{n^*-n'} \mathrm{cov}[U_k, U_\ell|u] + \left[\frac{(n')^2-n'}{2}\right]\sigma^2_{E_d}\right\} \tag{7.4.10}$$

where the conditional parameters are obtained from Eqs. 7.4.3 and 7.4.4.

As an illustration, the same problem studied in Sections 7.2 and 7.3 (which will be referred to as Case I) is re-analyzed after a boring is taken close to the central column and each sublayer is sampled at its mid-depth (Case II), as shown in Fig. 7.4.1.

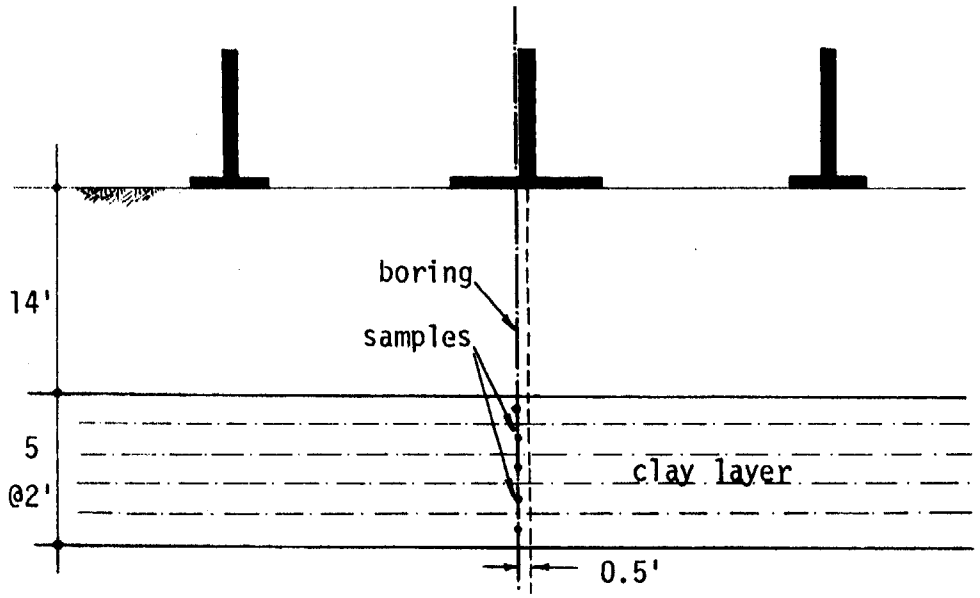


Figure 7.4.1 Location of Samples for Case II Example

Assuming that the prior and the posterior mean values of all the properties are the same and that $\sigma_{E_d} = \sigma_{E_t} = 0$, the effects of the new boring are shown in Table 7.4.1 for Δ_{max} and in Tables 7.4.2 and 7.4.3 for Θ and M. Note that in all cases, the uncertainty, measured by the standard deviation or the coefficient of variation, is greatly reduced.

For a $(\Delta/\ell)_{max}$ constraint, the total expected cost minimization problem is illustrated in Fig. 7.4.2. The curves for the Case II do not reflect the cost of sampling. This is a constant amount, C_i, which will only move the curves uniformly upward. Note that if $C_i < 15\beta$ then the Case II solutions yield smaller TEC values than those for the Case I.

B (ft)	$E[\Delta_{max}]$ (in)	Case I			Case II		
		$\sigma_{\Delta_{max}}$ (in)	$V_{\Delta_{max}}$	$\overset{\dagger}{P}[\Delta_{max} \geq 0.8"]$	$\sigma_{\Delta_{max}}$ (in)	$V_{\Delta_{max}}$	$\overset{\dagger}{P}[\Delta_{max} \geq 0.8"]$
14	0.96*	0.30	0.32	0.70	0.15	0.16	0.86
	0.72	0.24	0.33	0.37	0.13	0.18	0.27
16	0.86*	0.29	0.34	0.58	0.15	0.17	0.66
	0.64	0.23	0.36	0.24	0.13	0.19	0.11
18	0.75*	0.28	0.37	0.43	0.14	0.19	0.36
	0.58	0.23	0.39	0.17	0.12	0.21	0.03
20	0.65*	0.26	0.40	0.28	0.14	0.22	0.14
	0.52	0.22	0.42	0.10	0.12	0.23	0.01

Table 7.4.1 Comparison Between Case I and Case II Results for Δ_{max}

* No interaction effects.

† Assuming a normal distribution.

B (ft)	E[Θ] × 10^{-2}	Case I		Case II	
		σ_Θ × 10^{-2}	V_Θ	σ_Θ × 10^{-2}	V_Θ
14	0.405*	0.133	0.329	0.075	0.184
	0.301	0.108	0.358	0.066	0.220
16	0.362*	0.128	0.353	0.073	0.202
	0.271	0.105	0.389	0.066	0.243
18	0.317*	0.122	0.385	0.072	0.226
	0.242	0.103	0.423	0.065	0.270
20	0.272*	0.116	0.428	0.070	0.259
	0.218	0.099	0.456	0.065	0.297

Table 7.4.2 Case I and Case II Results for the Rotation of a Joint

---

* No interaction effects

B (ft)	E[M] (ton in)	Case I		Case II	
		σ_M (ton in)	V_M	σ_M (ton in)	V_M
14	1939.7*	614.6	0.317	310.6	0.160
	1442.1	481.8	0.334	256.1	0.178
16	1734.1*	586.3	0.338	300.8	0.173
	1299.4	469.1	0.361	252.6	0.194
18	1520.9*	557.0	0.366	291.0	0.191
	1160.6	454.6	0.392	248.8	0.214
20	1303.6*	527.5	0.405	281.5	0.216
	1045.8	437.3	0.418	244.1	0.233

Table 7.4.3 Case I and Case II Results for the Bending Moment in a Beam

---

* No interaction effects

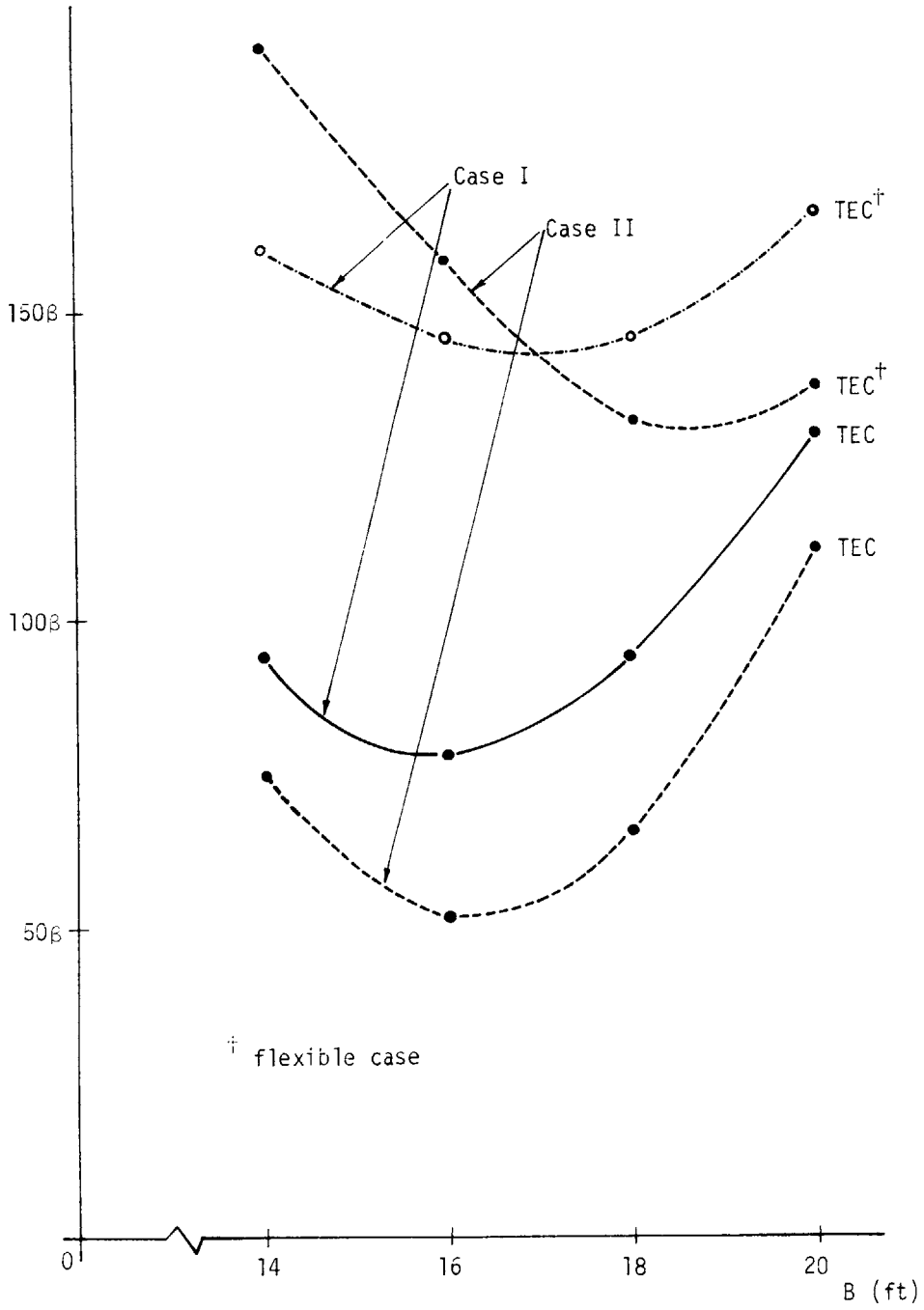


Figure 7.4.2 Footing Optimization Problem: Case I and Case II

CHAPTER 8

COMMENTS AND CONCLUSIONS

1. A probabilistic settlement-prediction model is developed in this work. The model yields first-order probabilistic information* about the settlements and the differential settlements of a structure in terms of a first-order probabilistic description of loads and soil properties.

2. The model accounts for "soil-structure interaction", i.e., the effect of redistribution of foundation loads due to uneven settlements of the supports, through a matrix of "load-transfer coefficients" which represents super- and/or sub-structure stiffness.

3. Only structures supported on shallow foundations are considered. However, no other restrictions are placed upon the configuration of the structure.

4. A one-dimensional settlement model is employed in which lateral deformations of the soil are neglected and the settlements are regarded as a summation of sublayer contributions. The stress-strain relationship of each sublayer characterizes the soil behavior. Most common relationships used to represent different soil types can be accommodated. The examples developed herein

---

* This means averages, variances and correlation coefficients.

make use of a non-linear stress-strain curve typical for cohesive materials.

5. The method assumes that the structure remains elastic after the settlements have occurred. In the cases where this assumption is not satisfied, the means and the variances of the differential settlements predicted by the proposed model will generally constitute lower bounds to the true values. Upper bounds are obtained when soil-structure interaction is neglected.

6. A sensitivity analysis of the model shows that, for structures on clay, the variance of the maximum past pressure gives the most important contribution to the variances of the settlements in an individual layer. On the other hand, the variability in the recompression ratio and in the applied loads tends to be small, and may be negligible in many cases.

7. The same analysis shows that the horizontal spatial correlation of the maximum past pressure has also an important effect on the settlement variability.

8. If the maximum past pressure is much less strongly correlated vertically than the compression ratio, then both properties may be about equal in importance as regards their effect on the variances of the settlements.

9. Higher horizontal correlation among soil properties results in smaller settlement variability. On the other hand, higher vertical correlation increases the variances of the settlements.

10. The test data on San Francisco "bay mud" samples analyzed in the case study shows maximum past pressures to have a small vertical and a high horizontal correlation. The compression ratio has a much higher vertical correlation than the recompression ratio or the maximum past pressure.

11. The inputs to the probabilistic settlement model are not the parameters of point soil properties but rather the parameters of spatial averages of soil properties. In general, the variability of these spatial averages will be smaller than that measured in laboratory or field tests.

12. With little additional computational effort, the settlement-prediction model can be used to yield first-order probabilistic information about displacements and secondary stresses in the structural members.

13. The results of further exploration and testing of soil samples may be combined with the prior information about the soil properties to obtain updated estimates of the input parameters to the model.

14. Employing the methodology developed in this work, future research in the area of settlement-controlled design will aim at establishing rational serviceability specifications related to the settlement behavior of buildings. Various methods can be used, which may differ in their level of sophistication and in the probable lead time to implementation in standard foundation projects. In a simple approach to the problem, current recommendations should be re-interpreted by taking into account the uncertainties involved. In this context, allowable levels may be defined in terms of the probability of their exceedance. In a more advanced formulation, the specifications may be stated not in terms of relative movements of the foundation but in terms of damage levels in the structural members and ultimately of human tolerance to damage. This criterion allows considerable freedom to the designer because the foundation-superstructure system may be conceived as a set of interacting subsystems among which trade-offs can be made. Eventually, it may become possible to compare all feasible design alternatives and to choose the best among them, and ultimately, an optimum solution may be obtained. In this context, it becomes necessary to estimate not only the uncertainty of load-induced settlements but also of settlement-induced deformations and related damage levels in the superstructure, and finally to update these settlement and damage estimates in the light of new information about the soil properties.

REFERENCES

1. Agterberg, F. P., "Autocorrelation Functions in Geology," Proc. of a Colloquium on Geostatistics, edited by D. F. Merriam, University of Kansas, 1970.

2. Benjamin, J. R., and C. A. Cornell, Probability, Statistics, and Decision for Civil Engineers, McGraw-Hill Book Co., New York, 1970.

3. Casagrande, A., "Role of the Calculated Risk in Earthwork and Foundation Engineering," Proc. ASCE, J. Soil Mech. and Found. Div., July, 1965.

4. Chamecki, S., "Structural Rigidity in Calculating Settlements," Proc. ASCE, J. Soil Mech. and Found. Div., January, 1956.

5. Cornell, C. A., "First-order Uncertainty Analysis of Soils Deformation and Stability," Proc. of Conf. on Applications of Statistics and Probability to Soil and Structural Engineering, University of Hong Kong, 1971.

6. Cornell, C. A., "Notes on First-order Uncertainty Analyses," unpublished paper, Department of Civil Engineering, MIT, January, 1971.

7. Cox, D. R., and H. D. Miller, The Theory of Stochastic Processes, John Wiley and Sons Inc., New York, 1965.

8. Cozzolino, E. V. M., "Statistical Forecasting of Compression Index," Proc. 5th Intl. Conf. Soil Mech. and Found. Eng., Paris, 1961.

9. D'Appolonia, D. J., E. E. D'Appolonia, and R. F. Brissette, "Settlement of Spread Footings on Sand," Proc. ASCE, J. Soil Mech. and Found. Div., May, 1968.

10. Davis, J. C., Statistics and Data Analysis in Geology, John Wiley and Sons Inc., New York, 1973.

11. de Mello, V. F. B., "Foundations of Buildings in Clay," State-of-the-art Report, Proc. 7th Intl. Conf. Soil Mech. and Found. Eng., Mexico, D.F., 1969.

12. Flores, A., y L. Esteva, "Análisis y Diseño de Cimentaciones sobre Terreno Compresible," Informe No. 258, Instituto de Ingeniería, UNAM, México, D.F., Febrero, 1970.

13. Folayan, J., K. H. Höeg, and J. R. Benjamin, "Decision Theory Applied to Settlement Predictions," Proc. ASCE, J. Soil Mech. and Found. Div., July, 1970.

14. Fredlund, D. G., and A. E. Dahlman, "Statistical Geotechnical Properties of Glacial Lake Edmonton Sediments," Proc. of Conf. on Applications of Statistics and Probability to Soil and Structural Engineering, University of Hong Kong, 1971.

15. Getzler, Z., "The Virtual Differential Settlement Method," J. Bos. Soc. of Civil Eng., April, 1966.

16. Grant, R., J. T. Christian, and E. H. Vanmarcke, "Tolerance of Buildings to Differential Settlements," Research Report R72-79, Department of Civil Engineering, MIT, December, 1972.

17. Hammitt, G. M., "Statistical Analysis of Data from a Comparative Laboratory Test Program Sponsored by ACIL," U.S. Army Engineers Waterways Experimental Station, Corps of Engineers, Misc. Paper No. 4-785, 1966.

18. Hauser, R., "Load Correlation Models in Structural Reliability," M.S. Thesis, Department of Civil Engineering, MIT, February, 1971.

19. Heil, H., "Studies on the Structural Rigidity of Reinforced Concrete Building Frames on Clay," Proc. 7th Intl. Conf. Soil Mech. and Found. Eng., Mexico, D.F., 1969.

20. Hilldale, C., "A Probabilistic Approach to Estimating Differential Settlement of Footings on Sand," M.S. Thesis, Department of Civil Engineering, MIT, June, 1971.

21. Krumbein, W. C., and F. A. Graybill, an introduction to Statistical Models in Geology, McGraw-Hill Book Co., New York, 1965.

22. Ladd, C. C., "Settlement Analyses for Cohesive Soils," Research Report R71-2, Department of Civil Engineering, MIT, August, 1971.

23. Lambe, T. W., Soil Testing for Engineers, John Wiley and Sons Inc., New York, 1951.

24. Lambe, T. W., and R. V. Whitman, Soil Mechanics, John Wiley and Sons Inc., New York, 1969.

25. Larnach, W. J., "Computation of Settlements in Building Frames," Civil Eng. and Public Works Review, September, 1970.

26. Litton, E., and J. M. Buston, "The Effect of Differential Settlement on a Large, Rigid, Steel-Framed Multi-Storey Building," The Struct. Eng., November, 1968.

27. Lumb, P.,"The Variability of Natural Soils," Canadian Geotechnical Journal, Vol. 3, No. 2, 1966.

28. Lumb, P., "Precision and Accuracy of Soil Tests," Proc. of Conf. on Applications of Statistics and Probability to Soil and Structural Engineering, University of Hong Kong, 1971.

29. Lysmer, J., and J. M. Duncan, "Stresses and Deflections in Foundations and Pavements," Department of Civil Engineering, University of California, Berkeley, 1969.

30. Meyerhof, G. G., "The Settlement Analysis of Building Frames," The Struct. Eng., September, 1947.

31. Ohsaki, Y., "Settlement and Crack Observation of Structures," Soil and Foundation, Vol. I, April, 1960.

32. Parzen, E., Stochastic Processes, Holden-Day Inc., San Francisco, 1962.

33. Peir, J. C., and C. A. Cornell, "Spatial and Temporal Variability of Live Loads," Proc. ASCE, J. Struct. Div., May, 1973.

34. Rao, C. R., Linear Statistical Inference and its Applications, John Wiley and Sons Inc., New York , 1965.

35. Reinschmidt, K. F., C. A. Cornell, and J. F. Brotchie, "Iterative Design and Structural Optimization," Proc. ASCE, J. Struct. Div., December, 1966.

36. Reséndiz, D., and I. Herrera, "A Probabilistic Formulation of Settlement-controlled Design," Proc. 7th Intl. Conf. Soil Mech. and Found. Eng., Mexico, D.F., 1969.

37. Rosenblueth, E., Discussion Session 2, Proc. 7th Intl. Conf. Soil Mech. and Found. Eng., Mexico, D.F., 1969.

38. Schultze, E., "Frequency Distributions and Correlations of Soil Properties," Proc. of Conf. on Applications of Statistics and Probability to Soil and Structural Engineering, University of Hong Kong, 1971.

39. Singh, A., and K. L. Lee, "Variability in Soil Parameters," Proc. Eighth Annual Conf. on Geological and Soil Eng., Idaho, 1970.

40. Skempton, A. W., and D. H. MacDonald, "The Allowable Settlements of Buildings," Proc. Inst. of Civil Eng., Vol. 5, Part III, December, 1956.

41. Sommer, H., "A Method for the Calculation of Settlements, Contact Pressures and Bending Moments in a Foundation Including the Influence of the Flexural Rigidity of the Superstructure," Proc. 6th Intl. Conf. Soil Mech. and Found. Eng., Montreal, 1965.

42. Terzaghi, K., "Sampling, Testing and Averaging," Proc. Purdue Conf. on Soil Mechanics and its Applications, Purdue University, Lafayette, Indiana, 1940.

43. Terzaghi, K., Theoretical Soil Mechanics, John Wiley and Sons Inc., New York, 1943.

44. Terzaghi, K., and R. B. Peck, Soil Mechanics in Engineering Practice, 2nd Edition, John Wiley and Sons Inc., New York, 1967.

45. Turnbull, W. J., A. A. Maxwell, and R. G. Ahlvin, "Stresses and Deflections on Homogeneous Soil Masses," Proc. 5th Intl. Conf. Soil Mech. and Found. Eng., Paris, 1961.

46. U.S. Navy, Design Manual - Soil Mechanics, Foundations and Earth Structures, NAVDOCKS DM-7, 1971.

47. Vanmarcke, E. H., "Memorandum on Variance Functions," unpublished paper, Department of Civil Engineering, MIT, December, 1970.

48. Yucemen, M. S., W. H. Tang, and A. H-S Ang, "A Probabilistic Study of Safety and Design of Earth Slopes," Civil Eng. Studies, Struct. Research Series No. 402, University of Illinois, Urbana, Illinois, July, 1973.

BIOGRAPHY

The author was born in México, D.F., on September 14, 1946. He entered the Universidad Nacional Autónoma de México in 1963 and received the degrees of Ingeniero Civil and of Maestro en Ingeniería in 1968 and in 1970, respectively.

From 1967 to 1970 the author worked at the Instituto de Ingeniería in the same university, first as a research assistant and then as a research associate in the Structures Division. At MIT, he has been a research and a teaching assistant since the fall of 1970 up to the present date.

APPENDIX A: Some Properties of the Expected Value Operator

If X_i, $i = 1....n$, are a group of random variables and c_i, $i = 1....n$, are constants, then the following relations will hold:

$$E[c_i] = c_i \tag{A.1}$$

$$E[c_i X_i] = c_i\, E[X_i] \tag{A.2}$$

$$E[\sum_{i=1}^{n} c_i X_i] = \sum_{i=1}^{n} c_i\, E[X_i] \tag{A.3}$$

$$Var[c_i] = 0 \tag{A.4}$$

$$Var[c_i X_i] = c_i^2\, Var[X_i] \tag{A.5}$$

$$Var[X_i] = E[X_i^2] - E^2[X_i] \tag{A.6}$$

$$Var[\sum_{i=1}^{n} c_i X_i] = \sum_{i=1}^{n} c_i^2\, Var[X_i] + 2 \sum_{i=1}^{n-1} \sum_{j=i+1}^{n} c_i c_j\, cov[X_i, X_j] \tag{A.7}$$

$$cov[\sum_{i=1}^{m} c_i X_i, \sum_{j=m+1}^{n} c_j X_j] = \sum_{i=1}^{m} \sum_{j=m+1}^{n} c_i c_j\, cov[X_i, X_j] \tag{A.8}$$

$$E[c_i c_j X_i X_j] = c_i c_j \; E[X_i] \; E[X_j] + c_i c_j \; \mathrm{cov}[X_i, X_j] \tag{A.9}$$

if the variables X_i and X_j are stochastically independent, then

$$\mathrm{cov}[X_i, X_j] = 0 \tag{A.10}$$

APPENDIX B: Additional Details About the Evaluation of Variance Functions

Starting at a certain layer a, Eq. 3.3.5 in Chapter 3 may be used to estimate the h-step variance function from boring data. If the soil volume under consideration is "homogeneous" throughout, then the variance function will depend only on the value of h. In this case, Eq. 3.3.5 is reduced to:

$$\frac{s_u^2(h)}{s_u^2} = \frac{1}{m(\ell-h+1)} \sum_{v=1}^{\ell-h+1} \sum_{j=1}^{m} \{ \sum_{i=v}^{h+v-1} u_j^{*(i)} \}^2 \qquad (B.1)$$

in which m is the number of borings, ℓ is the number of layers and

$$u_j^{*(i)} = \frac{u_j^{(i)} - \bar{u}}{s_u} \qquad (B.2)$$

where $u_j^{(i)}$ is the value of the property in the jth boring at the ith layer, $\bar{u}$ is the mean value of the soil property and s_u is the point standard deviation.

It should be noted that when either Eqns. 3.3.5 or B.1 are being used, it is assumed that measurements of the soil property under consideration are available for all the layers and at each one of the borings. In practice, this is seldom the case and the above formulas should be used with care. Observations which do not contribute to the variance function should not be considered when estimating

the layer variance or the total variance. For example, consider the situation illustrated in Fig. 3.2.1 which shows a three-boring, two-layer case in which no samples are taken from boring #3 at layer a. In this case, from Eq. 3.3.5:

$$\frac{s_u^2(2,a)}{s_u^2} = \frac{1}{2}\{(u_1^*(a) + u_1^*(b))^2 + (u_2^*(a) + u_2^*(b))^2\} \qquad (B.3)$$

and the normalizing layer standard deviations are,

$$s_u^{(a)} = \frac{1}{2}\{(u_1^{(a)})^2 + (u_2^{(a)})^2\} - (\bar{u}^{(a)})^2 \qquad (B.4)$$

$$s_u^{(b)} = \frac{1}{2}\{(u_1^{(b)})^2 + (u_2^{(b)})^2\} - (\bar{u}^{(b)})^2 \qquad (B.5)$$

APPENDIX C: The Load Transfer Coefficients and the A Matrix

Using the displacement method of structural analysis, the relationship between the joint displacements and forces may be written as:

$$\left[\begin{array}{c|c} K_{11} & K_{12} \\ \hline K_{21} & K_{22} \end{array}\right] \left[\begin{array}{c} \underset{\sim}{d}_1 \\ \hline \underset{\sim}{d}_2 \end{array}\right] = \left[\begin{array}{c} \underset{\sim}{f}_1 \\ \hline \underset{\sim}{f}_2 \end{array}\right] \qquad (C.1)$$

or

$$K\underset{\sim}{d} = \underset{\sim}{f} \qquad (C.2)$$

where K is the stiffness matrix of the structure (of size $j \times j$ for j degrees of freedom), $\underset{\sim}{d}$ and $\underset{\sim}{f}$ are vectors of joint displacements and forces, and the partitions of the matrix and the vectors correspond to r free and j-r prescribed degrees of freedom.

While calculating the T matrix, no loads act upon the structure and the vector $\underset{\sim}{f}_1$ is a null vector. However, one element of the vector $\underset{\sim}{d}_2$ is a prescribed unit vertical displacement for one of the supports (say the ith support) and hence the corresponding column of the matrix K_{12} (the ith column $k_{i2}^{(i)}$) must be transferred to the

load vector. The free displacements may now be computed as $\underset{\sim}{d}_1 = -K_{11}^{-1}\, k_{12}^{(i)}$ and the vector $\underset{\sim}{f}_2$ will follow directly. The load transfer coefficients are elements of the vector $\underset{\sim}{f}_2$ corresponding to the vertical reactions at the supports.

The A matrix employed in Eqns. 6.2.3 and 6.2.4 defines a relationship between the loads and the vertical reactions at the supports, or between elements of the vectors $\underset{\sim}{f}_1$ and $\underset{\sim}{f}_2$. When the loads are applied on the structure, the vector $\underset{\sim}{d}_2$ is a null vector. Hence, the free displacements may be calculated as $\underset{\sim}{d}_1 = K_{11}^{-1}\, \underset{\sim}{f}_1$ and the support reactions will be given by $\underset{\sim}{f}_2 = K_{21}\, K_{11}^{-1}\, \underset{\sim}{f}_1$. The force vector $\underset{\sim}{f}$ is referred to the joints of the structure. Thus, the vector $\underset{\sim}{f}_1$ is a function of the applied loads on the members, or $\underset{\sim}{f}_1 = G\underset{\sim}{\ell}$ where $\underset{\sim}{\ell}$ is a vector of applied <u>member</u> loads and the matrix G relates member to joint forces. If K* is a submatrix of the partition K_{21} which is referred only to vertical degrees of freedom for the supports, the matrix A will be computed as

$$A = K^*\, K_{11}^{-1}\, G \qquad (C.3)$$

APPENDIX D: A Multivariate Approximation for the Mean Value and the Covariance of Random Variables*

If Y_1 and Y_2 are a pair of variables which depend on the random variables $X_1, X_2, \ldots, X_n$, i.e.,

$$\left.\begin{aligned} Y_1 &= \phi_1(X_1, X_2, \ldots, X_n) \\ Y_2 &= \phi_2(X_1, X_2, \ldots, X_n) \end{aligned}\right\} \qquad (D.1)$$

then the means of Y_1 and Y_2 depend on the means of the independent variables, m_{X_i}, in the following approximate way:

$$m_{Y_j} \doteq \phi_j(m_{X_1}, m_{X_2}, \ldots, m_{X_n}) \; ; \; j = 1,2 \qquad (D.2)$$

The first-order approximation to the covariance of Y_1 and Y_2 is given by:

$$\mathrm{cov}[Y_1, Y_2] \doteq \sum_{i=1}^{n} \sum_{j=1}^{n} \left.\frac{\partial \phi_1}{\partial X_i}\right|_m \left.\frac{\partial \phi_2}{\partial X_j}\right|_m \mathrm{cov}[X_i, X_j] \qquad (D.3)$$

in which $\left.\partial\phi_1/\partial X_i\right|_m$ is the partial derivative of the function ϕ_1,

---

* From Benjamin and Cornell (2)

with respect to the variable X_i, evaluated at the mean values m_{X_1}, m_{X_2}, etc.

If the random variables $X_1, X_2, \ldots, X_n$ are assumed to be stochastically independent, then the variances of Y_1 and Y_2 can be written in terms of the variances of $X_1, X_2, \ldots, X_n$:

$$\mathrm{Var}[Y_j] \doteq \sum_{i=1}^{n} \left(\frac{\partial \phi_j}{\partial X_i} \bigg|_m \right)^2 \mathrm{Var}[X_i] \quad ; j = 1,2 \qquad (D.4)$$

The above expression indicates that each random variable X_i contributes to the uncertainty of the dependent variable Y_j by an amount equal to the product of its own variance and a sensitivity factor. When this product is small compared to other contributions, then the uncertainty of the random variable X_i may be neglected.

APPENDIX E: Probabilistic Parameters of the Spatial Averages of Pseudo-flexibilities for a Cohesive Soil

Using a pseudo-flexibility parameter as defined in Eq. 6.5.2, the first-order approximation for the covariance between two spatial averages $\langle F \rangle_i^{(a)}$ and $\langle F \rangle_j^{(b)}$ (see Fig. 4.3.1), takes the form given in Eq. 6.5.7:

$$\begin{aligned}\mathrm{cov}[\langle F \rangle_i^{(a)}, \langle F \rangle_j^{(b)}] \doteq \\ \doteq A_i^{(a)} A_j^{(b)} \mathrm{cov}[H_i^{(a)}, H_j^{(b)}] + B_i^{(a)} B_j^{(b)} \mathrm{cov}[\langle M_v' \rangle_i^{(a)}, \langle M_v' \rangle_j^{(b)}] + \\ + C_i^{(a)} C_j^{(b)} \mathrm{cov}[\langle M_v'' \rangle_i^{(a)}, \langle M_v'' \rangle_j^{(b)}] + D_i^{(a)} D_j^{(b)} \mathrm{cov}[\langle \bar{P}_m \rangle_i^{(a)}, \langle \bar{P}_m \rangle_j^{(b)}] + \\ + C_i^{(a)} D_j^{(b)} \mathrm{cov}[\langle M_v'' \rangle_i^{(a)}, \langle \bar{P}_m \rangle_j^{(b)}] + D_i^{(a)} C_j^{(b)} \mathrm{cov}[\langle \bar{P}_m \rangle_i^{(a)}, \langle M_v'' \rangle_j^{(b)}]\end{aligned} \tag{E.1}$$

where, from Eqns. D.2 and D.3:

$$A_i^{(a)} = E[\langle M_v'' \rangle_i^{(a)}] + \frac{(E[\langle M_v' \rangle_i^{(a)}] - E[\langle M_v'' \rangle_i^{(a)}]) E[\langle \Delta \bar{P} \rangle_i^{(a)}] (1 - \exp(-E[\Delta \bar{P}_i^{(a)}]/E[\langle \Delta \bar{P} \rangle_i^{(a)}]))}{E[\Delta \bar{P}_i^{(a)}]}$$

$$B_i^{(a)} = E[H_i^{(a)}] \left\{ \frac{E[\langle \Delta\bar{P}' \rangle_i^{(a)}](1 - \exp(-E[\Delta\bar{P}_i^{(a)}]/E[\langle \Delta\bar{P}' \rangle_i^{(a)}]))}{E[\Delta\bar{P}_i^{(a)}]} \right\}$$

$$C_i^{(a)} = E[H_i^{(a)}]\left\{1 - \frac{E[\langle \Delta\bar{P}' \rangle_i^{(a)}](1 - \exp(-E[\Delta\bar{P}_i^{(a)}]/E[\langle \Delta\bar{P}' \rangle_i^{(a)}]))}{E[\Delta\bar{P}_i^{(a)}]} \right\}$$

$$D_i^{(a)} = \frac{E[H_i^{(a)}](E[\langle M_v' \rangle_i^{(a)}] - E[\langle M_v'' \rangle_i^{(a)}])}{E[\Delta\bar{P}_i^{(a)}]} \times$$

$$\left\{1 - \exp(-E[\Delta\bar{P}_i^{(a)}]/E[\langle \Delta P \rangle_i^{(a)}])(1 + \frac{E[\Delta\bar{P}_i^{(a)}]}{E[\langle \Delta\bar{P}' \rangle_i^{(a)}]})\right\}$$

(E.2)

and, from Eq. 4.3.1:

$$\mathrm{cov}[\langle M_v' \rangle_i^{(a)}, \langle M_v' \rangle_j^{(b)}] = \frac{1}{n_i^*(a) n_j^*(b)} \sum_{k=1}^{n_i^*(a)} \sum_{\ell=1}^{n_j^*(b)} \mathrm{cov}[M_{v_{ki}}'^{(a)}, M_{v_{\ell j}}'^{(b)}]$$

$$\mathrm{cov}[\langle M_v'' \rangle_i^{(a)}, \langle M_v'' \rangle_j^{(b)}] = \frac{1}{n_i^*(a) n_j^*(b)} \sum_{k=1}^{n_i^*(a)} \sum_{\ell=1}^{n_j^*(b)} \mathrm{cov}[M_{v_{ki}}''^{(a)}, M_{v_{\ell j}}''^{(b)}]$$

$$\text{cov}[\langle \bar{P}_m \rangle_i^{(a)}, \langle \bar{P}_m \rangle_j^{(b)}] = \frac{1}{n_i^{*(a)} n_j^{*(b)}} \sum_{k=1}^{n_i^{*(a)}} \sum_{\ell=1}^{n_j^{*(b)}} \text{cov}[\bar{P}_{m_{ki}}^{(a)}, \bar{P}_{m_{\ell j}}^{(b)}]$$

$$\text{cov}[\langle M''_v \rangle_i^{(a)}, \langle \bar{P}_m \rangle_j^{(b)}] = \frac{1}{n_i^{*(a)} n_j^{*(b)}} \sum_{k=1}^{n_i^{*(a)}} \sum_{\ell=1}^{n_j^{*(b)}} \text{cov}[M''^{(a)}_{v_{ki}}, \bar{P}_{m_{\ell j}}^{(b)}]$$

$$\text{cov}[\langle \bar{P}_m \rangle_i^{(a)}, \langle M''_v \rangle_j^{(b)}] = \frac{1}{n_i^{*(a)} n_j^{*(b)}} \sum_{k=1}^{n_i^{*(a)}} \sum_{\ell=1}^{n_j^{*(b)}} \text{cov}[\bar{P}_{m_{ki}}^{(a)}, M''^{(b)}_{v_{\ell j}}]$$

(E.3)

The expected value factors may be computed with Eq. 4.2.1:

$$E[\langle M'_v \rangle_i^{(a)}] = \frac{1}{n_i^{*(a)}} \sum_{k=1}^{n_i^{*(a)}} E[M'^{(a)}_{v_{ki}}]$$

$$E[\langle M''_v \rangle_i^{(a)}] = \frac{1}{n_i^{*(a)}} \sum_{k=1}^{n_i^{*(a)}} E[M''^{(a)}_{v_{ki}}]$$

$$E[\langle \bar{P}_m \rangle_i^{(a)}] = \frac{1}{n_i^{*(a)}} \sum_{k=1}^{n_i^{*(a)}} E[\bar{P}_{m_{ki}}^{(a)}]$$

$$E[\langle \Delta \bar{P}' \rangle_i^{(a)}] = E[\langle \bar{P}_m \rangle_i^{(a)}] - \bar{p}_{o_i}^{(a)}$$

$$E[\langle \Delta \bar{P}'' \rangle_i^{(a)}] = E[\Delta \bar{P}_i^{(a)}] - E[\langle \Delta \bar{P}' \rangle_i^{(a)}]$$

(E.4)

The covariance factors between pairs of <u>point</u> properties used in Eqs. E.3 may be computed with Eqns. D.2 and D.3:

$$\text{cov}[M'^{(a)}_{v_{ki}}, M'^{(b)}_{v_{\ell j}}] \doteq E_{ki}^{(a)} E_{\ell j}^{(b)} \text{cov}[RR_{ki}^{(a)}, RR_{\ell j}^{(b)}]$$

$$\text{cov}[M''^{(a)}_{v_{ki}}, M''^{(b)}_{v_{\ell j}}] \doteq F_{ki}^{(a)} F_{\ell j}^{(b)} \text{cov}[CR_{ki}^{(a)}, CR_{\ell j}^{(b)}] + G_{ki}^{(a)} G_{\ell j}^{(b)} \text{cov}[\bar{P}^{(a)}_{m_{ki}}, \bar{P}^{(b)}_{m_{\ell j}}]$$

$$\text{cov}[M''^{(a)}_{v_{ki}}, \bar{P}^{(b)}_{m_{\ell j}}] \doteq G_{ki}^{(a)} \text{cov}[\bar{P}^{(a)}_{m_{ki}}, \bar{P}^{(b)}_{m_{\ell j}}]$$

$$\text{cov}[\bar{P}^{(a)}_{m_{ki}}, M''^{(b)}_{v_{\ell j}}] \doteq G_{\ell j}^{(b)} \text{cov}[\bar{P}^{(a)}_{m_{ki}}, \bar{P}^{(b)}_{m_{\ell j}}]$$

(E.5)

in which,

$$E_{ki}^{(a)} = 0.87/(\bar{p}_{o_i}^{(a)} + E[\bar{P}'^{(a)}_{f_{ki}}])$$

$$F_{ki}^{(a)} = 0.87/(E[\bar{P}_{m_{ki}}^{(a)}] + E[\bar{P}''^{(a)}_{f_{ki}}])$$

$$G_{ki}^{(a)} = -0.87\ E[CR_{ki}^{(a)}]/\{E[\bar{P}_{m_{ki}}^{(a)}] + E[\bar{P}''^{(a)}_{f_{ki}}]\}^2 \qquad \text{(E.6)}$$

and,

$$\left.\begin{aligned} E[\bar{P}'^{(a)}_{f_{ki}}] &= \bar{p}_{o_i}^{(a)} + E[\Delta\bar{P}_i^{(a)}] \\ E[\bar{P}''^{(a)}_{f_{ki}}] &= E[\bar{P}_{m_{ki}}^{(a)}] \end{aligned}\right\} \quad E[\Delta\bar{P}_i^{(a)}] \leq E[\bar{P}_{m_{ki}}^{(a)}] - \bar{p}_{o_i}^{(a)}$$

$$\left.\begin{aligned} E[\bar{P}'^{(a)}_{f_{ki}}] &= E[\bar{P}_{m_{ki}}^{(a)}] \\ E[\bar{P}''^{(a)}_{f_{ki}}] &= \bar{p}_{o_i}^{(a)} + E[\Delta\bar{P}_i^{(a)}] \end{aligned}\right\} \quad E[\Delta\bar{P}_i^{(a)}] > E[\bar{P}_{m_{ki}}^{(a)}] - \bar{p}_{o_i}^{(a)} \qquad \text{(E.7)}$$

APPENDIX F: List of Symbols

A - $n \times r$ transformation matrix of applied member loads to vertical foundation loads

B - width of interior footing

C_c - virgin compression index

C_r - recompression index

CR - compression ratio

C_d - cost of damage

C_i - cost of sampling

C_o - initial cost

C_D - $j \times j$ joint displacement covariance matrix

C_L - $r \times r$ covariance matrix of applied member loads

C_Q - $n \times n$ covariance matrix of vertical foundation loads

C_S - $n \times n$ covariance matrix of total settlements

C_U - prior covariance matrix of the soil property U for n_t points

C_ε - $n_s \times n_s$ covariance matrix of error terms due to disturbance and testing errors

C_F^* - 6×6 covariance matrix of joint member forces

C_U^* - prior covariance matrix of the soil property U for n_s points

$C_{U|u}$ - posterior covariance matrix of the soil property U for n_t points

$C_{\langle F \rangle}$ - $kn \times kn$ covariance matrix of pseudo-flexibilities

$\mathrm{cov}[\cdot,\cdot]$ - covariance operator

$\underset{\sim}{d}$ - size j vector of joint displacements

$d_{\cdot}$ - correlation distance operator

$d_{h_{\cdot}}$ - horizontal correlation distance operator

$d_{v_{\cdot}}$ - vertical correlation distance operator

E_d - error component due to sample disturbance

E_t - error component due to testing

E_o - initial void ratio

$E[\cdot]$ - expected value operator

$F^{(i)}$ - (random) soil pseudo-flexibility of the ith sublayer

$f_d^{(i)}$ - $n \times n$ diagonal matrix of (deterministic) pseudo-flexibilities

$\underset{\sim}{f}$ - size j vector of joint forces

H - layer thickness

I - identity matrix

K - $j \times j$ stiffness matrix

k - number of soil sublayers

k^* - 6×6 member stiffness matrix

$\underset{\sim}{\ell}$ - size r vector of applied member loads

M'_v - modulus of volume change in the recompression zone

M''_v - modulus of volume change in the virgin compression zone

$\underset{\sim}{m}_D$ - size j vector of mean joint displacements

$\underset{\sim}{m}_L$ - size r vector of mean applied member loads

$\underset{\sim}{m}_Q$ - size n vector of mean vertical foundation loads

$\underset{\sim}{m}_S$ - size n vector of mean total settlements

$\underset{\sim}{m}_U$ - size n_t vector of prior mean values of the soil property U

$\underset{\sim}{m}^*_F$ - size 6 vector of mean joint member forces

$\underset{\sim}{m}_{U|u}$ - size n_t vector of posterior mean values of the soil property U

$m_{\langle F \rangle_d^{(i)}}$ - $n \times n$ diagonal matrix of mean values of pseudo-flexibilities referred to sublayer i

m_v - modulus of volume change

$m_\cdot$ - mean value operator

n - number of support points

n_p - number of pairs of observations

n_s - number of sample points

n_t - total number of points in a region

n' - number of sampled points inside a region of size n^*

n^* - ratio of layer thickness to specimen thickness

$\bar{P}_f$ - final effective vertical stress

$\bar{P}_m$ - maximum past pressure

$P[\cdot]$ - probability operator

p_d - probability of damage

$\bar{p}_o$ - effective overburden pressure

$\underset{\sim}{Q}$ - size n vector of vertical foundation loads

RR - recompression ratio

$R_\cdot(*)$ - autocorrelation function operator

r_d - sample correlation coefficient

S - (random) total settlement

$s_\cdot^2$ - sample variance operator

$s_\cdot^2(*)$ - sample variance function operator

T - $n \times n$ matrix of load transfer coefficients

U - uncertain value of a soil property

U' - random component of a soil property about a deterministic tread

$\hat{U}$ - field- or laboratory-measured soil property

$\underset{\sim}{u}$ - size n_s vector of observations of the soil property

$\bar{u}$ - sample mean of a soil property

$u_j^{(i)}$ - observation of the soil property at the ith sublayer and the jth boring

$u_j'^{(i)}$ - random component of $u_j^{(i)}$

$u_j^{*(i)}$ - value of $u_j'^{(i)}$ normalized by the sample standard deviation

$V_{\cdot}$ - coefficient of variation operator

$\mathrm{Var}[\cdot]$ - variance operator

$v_{\cdot}$ - sample coefficient of variation operator

W - water content

$\alpha^{(i)}$ - $m \times n$ matrix of stress coefficients referred to sublayer i

$\Gamma_{\cdot}^2$ - factor for transforming a point variance to the variance of a spatial average

$\gamma_{\cdot}(*)$ - covariance function operator

$\Delta\bar{P}$ - effective load-induced vertical stress

Δ_{max} - maximum differential settlement

δ_{all} - allowable differential settlement

Φ - ratio of observed to model-predicted output

$\nu_{\cdot}$ - factor for transforming a point covariance to the covariance between spatial averages

$\rho_{\cdot,\cdot}$ - correlation coefficient operator

$\sigma^2_{\cdot}$ - variance operator

$\sigma^2_{\cdot}(*)$ - variance function operator

$\langle \cdot \rangle$ - spatial average operator

$\doteq$ - approximately

APPENDIX G: List of Figures

Figure		Page
2.4.1	Schematic Representation of a One-dimensional Stochastic Process $\{U(z), z \varepsilon Z\}$	15
2.4.2	Autocorrelation Functions $R_U(h) = \exp(-\|h\|/d_U)$ and $R_U(h) = \exp(-h^2/d_U^2)$	19
2.4.3	Normalized Variance Functions for $R_U(h) = \exp(-\|h\|/d_U)$ and $R_U(h) = \exp(-h^2/d_U^2)$	21
3.2.1	Soil Volume, Borings and Samples	27
3.5.1	W and E_o Values as Functions of Depth	38
3.5.2	RR and CR Values as Functions of Depth	39
3.5.3	$\bar{P}_m$ Values as a Function of Depth	40
3.5.4	Histogram for W Values	41
3.5.5	Histogram for E_o Values	41
3.5.6	Histogram for CR Values	42
3.5.7	Histogram for RR Values	42
3.5.8	Histogram for $\bar{P}_m$ Values	43
3.5.9	Normalized Variance Function for W Values	46
3.5.10	Normalized Variance function for E_o Values	46
3.5.11	Normalized Variance Function for RR and CR Values	47
3.5.12	Normalized Variance Function for $\bar{P}_m$ Values	47
3.5.13	Horizontal Autocorrelation Function for $\bar{P}_m$ Values	48
4.2.1	Γ_U Values for an Autocorrelation Function of the Form $R_U(h) = \exp(-\|h\|/d_U)$ and Specimens 1" Thick	53

4.2.2	Γ_U Values for an Autocorrelation Function of the Form $R_U(h) = \exp(-h^2/d_U^2)$ and Specimens 1" Thick	54
4.3.1	Schematic Representation of Two Spatial Averages $\langle U \rangle_i^{(a)}$ and $\langle U \rangle_j^{(b)}$	56
5.2.1	Soil Profile for Settlement Estimation	62
5.2.2	Definition of the Pseudo-flexibility Parameter f	62
5.2.3	Stress Coefficients for Point Loads and Uniformly Distributed Loads	63
5.2.4	Vertical Stress at a Point Induced by a Number of External Loads	64
5.3.1	Load Transfer Coefficients for a Two-bay One-story Frame	67
5.3.2	Soil-structure Interaction Problem: Three-supports Case	69
5.3.3	Soil-structure Interaction Problem: General Case	70
5.3.4	Algorithm for Solving the Deterministic Soil-structure Interaction Problem	72
5.4.1	e - log $\bar{p}$ Plot for a Cohesive Material	75
5.4.2	Idealized e - log $\bar{p}$ Plot for a Cohesive Material	77
5.4.3	Compressibility Moduli as Functions of Stress	80
5.4.4	Idealized Stress-settlement Characteristic for a Cohesive Soil	81
5.5.1	Example Frame: Spread Footings Foundation	83
5.5.2	Variation with Depth of $\bar{p}_o$ and $\bar{p}_m$ for Example Problem	84
5.5.3	Definition of the Maximum Differential Settlement δ_{max}	85
5.5.4	Settlements as Functions of the Footing Width B Including Stiffness Effect	87

5.5.5	Example Frame: Raft Foundation	88
6.2.1	Spatial Averages of Soil Properties for Settlement Prediction	93
6.5.1	Stress-settlement Characteristic Employed in Estimating the Matrix $C_{\langle F \rangle}$ for a Cohesive Soil	102
6.5.2	Two-bay, One-story Frame Employed in the Sensitivity Analysis	106
6.5.3	Coefficients of Variation: RR, CR and $\bar{P}_m$	108
6.5.4	Coefficients of Variation: $\bar{P}_m$, H and L	109
6.5.5	Horizontal Correlation Distances	110
6.5.6	Model Uncertainty	111
6.6.1	Definition of Δ_{max}	114
6.6.2	Standard Deviations of Settlements as Functions of the Footing Width B, Including Stiffness Effects	116
7.2.1	Footing Optimization Problem: Fixed Amount of Sampling	122
7.4.1	Location of Samples for Case II Example	131
7.4.2	Footing Optimization Problem: Case I and Case II	135

APPENDIX H: List of Tables

Table		Page
2.4.1	Variance Functions for Some Stochastic Processes with Well-known Autocorrelation Functions	20
3.1.1	Coefficients of Variation for Some Properties of Various Types of Soils	26
3.4.1	Coefficients of Variation for Some Soil Properties Due to Experimental Variability	34
3.5.1	Results of Specific Gravity Tests for Bay Mud Samples	36
3.5.2	Soil Properties Analyzed in the Case Study	37
3.5.3	Numerical Summaries for the Soil Properties	43
5.4.1	Mechanisms Causing a Maximum Past Pressure	76
5.5.1	δ_{max} Values for Example Frame	86
5.5.2	Total Settlements for Raft Foundation	89
6.5.1	Values of the Parameters for the Basic Case	105
6.6.1	Values of the Random Soil Parameters for Example Problem	113
6.6.2	First-order Probabilistic Parameters of Δ_{max}: Spread Footings Foundations	117
6.6.3	Standard Deviations of Settlements: Raft Foundation	118
7.3.1	Coefficients of Variation for the Rotation of a Joint	125
7.3.2	Coefficients of Variation for the Bending Moment in a Beam	126
7.4.1	Comparison Between Case I and Case II Results for Δ_{max}	132

7.4.2 Case I and Case II Results for the Rotation of a Joint 133

7.4.3 Case I and Case II Results for the Bending Moment in a Beam 134